QATAR UNIVERSITY

COLLEGE OF HEALTH SCIENCES

PROFILING OF THE DIFFERENTIALLY EXPRESSED GENES OF INFLAMMATION AND ANGIOGENESIS OF HUMAN BRAIN MICROVASCULAR ENDOTHELIAL CELLS EVOKED BY CELL INJURY IN-VITRO TO MIMIC ACUTE ISCHEMIC STROKE-LIKE CONDITIONS

BY

FATIMA ALZAHRA MAHMOUD AL HAMED

A Thesis Submitted to

the College of Health Sciences

in Partial Fulfillment of the Requirements for the Degree of

Masters of Science in Biomedical Sciences

June 2020

© 2020. Fatima Alzahra Al Hamed. All Rights Reserved.

COMMITTEE PAGE

The members of the Committee approve the Thesis of
Fatima Alzahra Mahmoud Al Hamed defended on 10/05/2020.

Nasser Moustafa Ragheb Rizk
Thesis/Dissertation Supervisor

Fatiha Benslimane
Committee Member

Hazem Fathy Ahmed Elewa
Committee Member

Approved:

Hanan Abdul Rahim, Dean, College of Health Science

ABSTRACT

AL HAMED, FATIMA ALZAHRA, M., Masters of Science : June : 2020, Biomedical Sciences

Title: Profiling of the Differentially Expressed Genes of Inflammation and Angiogenesis of Human Brain Microvascular Endothelial Cells Evoked by Cell Injury In-Vitro to Mimic Acute Ischemic Stroke-Like Conditions

Supervisor of Thesis: Nasser M. Rizk.

Ischemic stroke (IS) is a leading cause of disability and death worldwide. IS arises from a blocked artery in the brain that causes a lack of oxygen and nutrient supply to other brain cells, causing cell injury and neuronal death. *In-vitro* Acute ischemic stroke models were developed in the lab, by a method of oxygen-glucose deprivation (OGD), to understand the mechanisms and pathophysiology of brain cell injury in IS. One important cell type of brain is the primary human brain microvascular endothelial cell (PHBMEC), which builds up the blood-brain barrier (BBB), and any disruption of it, could cause injury to other cells in the brain. Acute IS (AIS) injury of PHBMEC is not well characterized in terms of its consequences on cell functions using genomic function profiling. In our study, we aimed to establish a new model of an acute in-vitro ischemic stroke, within a time limit of 2 hrs., with depriving whole nutrients and not just glucose, under hypoxic condition, in a model we created as oxygen nutrients deprivation (OND). Control cells were exposed to normal conditions of glucose (5 mM) and other nutrients with 20% oxygen. In order to establish this model, different methods were used to assess cell injury such as viability, death, and apoptosis, cytoskeleton or F-actin stain, and biochemical

changes. RNA extracted was analyzed using RT-PCR profiling of angiogenesis and inflammatory genes, differentially expressed genes were analyzed by Gene Globe analysis, and signaling pathways were identified using IPA software, Qiagen. Major findings of OND have decreased cell viability, increased cell death, increased F-actin stress fibers that indicated severe cell injury and BBB disruption, and increased acidity. Profiling of the gene expression revealed dysregulation of 20 genes (5 upregulated and 15 down regulated) of both inflammation and angiogenesis. Major signaling pathways identified were HIF1A and NOTCH3. These signaling pathways affected different functions, including cell survival, proliferation, angiogenesis, and cytoskeleton organization. In conclusion, the established OND model could cause severe and acute cell injury that could mimic AIS in humans. Cell injury was evidenced by the results of phenotype changes, differential gene expression, and the signaling pathways identified.

DEDICATION

This work is dedicated to my appreciated parents and lovely siblings.

It is also dedicated to People of Qatar.

All Praise be to Allah.

ACKNOWLEDGMENTS

Special thanks to Dr. Nasser Rizk for his supervision and support with his appreciated following up with me along with the thesis. I learned a lot about how to write in a scientific way and think in a critical way. Thanks a lot to Dr. Fatiha Binslimane, who supervised my lab work and techniques, she facilitated things for me in BRC, and I learned many different experiments. Thanks to Dr. Hazem Alewa, who let me write a review paper about SGLT2 inhibitor and ischemic stroke, to be published inshallah.

Thanks to people who were available in my thesis journey, Ms. Samar Haroon, who helped me in learning the cytoskeleton technique and using the fluorescent microscope. Thanks to Ms. Dana Khamis, who was in the first line to teach me cell culture and sterilizing techniques. Thanks to Dr. Fatiha, who taught me the technique of RNA extraction with good quantity and quality. Thanks to Amina Fadel, who received reagents from companies and facilitates delivering them to me. Thanks to Dr. Balsam Rizeq, whom I had a chance to have several conversations about techniques of apoptosis and Tali machine; thus, I could optimize my procedure. Thanks to Dr. Susu Zughaier from medical college, who I had a chance to have a conversation about cell scraping technique and I could optimize my own technique. Thanks to Ms. Naima Almeer, Ms. Maha Al-Asr, Ms. Mashael Al-Badr, Ms. Muna Almeer, Ms. Maria Smatti, Ms. Fadheela Bakhsh, Ms. Heba El-Khatib, Ms. Sara Fahd, Dr. Sonia Boughattas, Ms. Hend Al Jaber, Ms. Duaa Al-Sadeq, Ms. Hana Adel and Ms. Huda Ahmadi for facilitating things to me in BRC. Thanks to Dr. Farhan Cyprian of medical college, I had a conversation with him about the cell cycle, although not applied to our study. Thanks to Mr. Jilbin Sam of Medical college who facilitated the use of the flow cytometer – Accuri BD.

Thanks to my parents, who supported me along all my years of study throughout my whole life. Their Duaa and prayers were the main support for me; without them, I wouldn’t succeed. Thanks to my brother and sister also who stood by my side. Finally, all praise be to Allah for all these blessings in my life.

TABLE OF CONTENTS

DEDICATION v

ACKNOWLEDGMENTS vi

LIST OF TABLES xiii

LIST OF FIGURES xiv

Chapter 1: Introduction 1

1.1 Background 1

1.2 Hypothesis 2

1.3 Aims 2

Chapter 2: Literature Review 4

2.1 Stroke 4

2.1.1 Definition of stroke 4

2.1.2 Epidemiology 5

2.1.3 Stroke types and causes 6

2.1.3.1 Ischemic stroke 7

2.1.3.2 Hemorrhagic stroke 8

2.1.4 Risk factors for stroke 10

2.1.5 Diagnosis of stroke 10

2.1.6 Stroke complications 13

2.1.7 Stroke prevention 13

2.1.8 Stroke in Qatar 14

2.2 Stroke Biomarkers 15

2.2.1 Definition of biomarker 15

2.2.2 Clinical utility of stroke biomarkers 15

2.2.3 Role of stroke biomarkers in the pathological process 17

2.2.4 Future biomarkers of stroke 17

2.3 Stroke pathophysiology 19

2.3.1 Pathophysiology of ischemic stroke 19

2.3.1.1 Pathogenesis of ischemic stroke caused by Atherosclerosis 26

2.3.1.2 Blood-brain barrier and ischemic stroke 27

2.3.1.2.1 Normal blood-brain barrier 27

2.3.1.2.2 Blood-brain barrier disruption 29

2.3.2 Pathophysiology of hemorrhagic stroke 31

2.4 Ischemic stroke modelling 33

2.4.1 In-vitro ischemic stroke modeling 33

2.4.2 In-vitro modeling using human cells 35

2.4.2.1 OGD conditions in different human cell studies 37

2.4.3 In-vitro modeling using animal cells 39

2.4.3.1 OGD conditions in different animal cell studies 40

Chapter 3: Methodology 43

3.1 Materials 43

3.1.1 Cells 43

3.1.2 Media and reagents used for cell culture 43

3.1.3 Reagents and kits 44

3.1.4 Instruments 45

3.1.5 Lab Supplies 46

3.2 Methods 48

3.2.1 Media preparation 48

3.2.2 Culture of primary human brain microvascular endothelial cell 48

3.2.2.1 Passaging and freezing cells 49

3.2.2.2 Human-like pre-conditioning 50

3.2.2.3 Oxygen Glucose Deprivation (OGD) 50

3.2.3 Viability test analysis 52

3.2.3.1 Live/ Dead stain analysis 53

3.2.3.2 Apoptosis and Death analysis 53

3.2.3.2.1 Detachment protocol 54

3.2.3.2.2 Apoptosis staining 56

3.2.3.3 MTT viability test 58

3.2.4 Actin staining 60

3.2.5 The optimized model for in-vitro ischemic stroke 62

3.2.6 Biochemical Analysis 63

3.2.7 Gene Expression Analysis 63

3.2.7.1 RNA extraction 63

3.2.7.2 c-DNA synthesis 65

3.2.7.3 RT-PCR profiler array 66

3.2.7.4 List of genes in the array analyzed 68

3.2.7.4.1 Inflammatory genes Array 68

3.2.7.4.2 Angiogenesis genes Array 70

3.2.8 Data analysis 72

3.2.8.1 Functional classification of DEGs and their pathways 72

3.2.9 Statistical analysis 73

3.3 Ethical and Biosafety Approvals 73

Chapter 4: Results 74

4.1 Viability test analysis (Apoptosis) 74

4.2 Actin staining 77

4.3 Biochemical analysis 80

4.4 Gene expression analysis 81

4.4.1 Differentially expressed genes (DEGs) 81

4.4.1.1 DEGs of inflammation 83

4.4.1.2 DEGs of Angiogenesis 83

4.5 IPA core canonical pathways 85

4.5.1 HIF and other signaling pathways 85

Chapter 5: Discussion 89

5.1 Establishment an in-vitro acute ischemic stroke model 89

5.1.1 Control condition 89

5.1.2 OGD conditions 90

5.1.3 OND model 92

5.1.3.1 Possible mechanisms of cell injury 93

5.1.3.2 Biochemical analysis 93

5.1.4 Actin staining of different types of OGD and OND 95

5.2 Gene expression of the established OND model 96

5.3 Core signaling pathway of the established OND model 101

Conclusion 104

Limitations And Future Prospective 105

REFERENCES 107

APPENDIX 126

A.1 Experimental work 126

A.1.1 Viability 126

A.1.1.1 Live/Dead staining 126

A.1.1.2 Apoptosis 127

A.1.1.3 MTT test.....129

A.1.1.3.1 Possible interpretation of OND cells reactions in MTT 134

A.1.2 RNA quality and concentration 136

A.2 Data analysis.....137

A.2.1 list of genes 137

A.2.1.1 List of up- and down regulated genes of inflammation 137

A.2.1.2 List of up- and down regulated genes of angiogenesis 139

B.1 Copyrights permission.....143

B.2 iThenticate similarity index report 145

LIST OF TABLES

Table 1. Summary of types and subtypes of stroke. 9

Table 2. Summary of Protein biomarkers related to stroke (prediction, diagnosis, prognosis and therapy). 16

Table 3. OGD conditions by different publications that used human cells. 37

Table 4. OGD conditions in literatures of animal cells. 41

Table 5. Composition of PBS/saline used for dilution of media. 52

Table 6. Inflammatory genes Array. 68

Table 7. Angiogenesis genes Array 70

Table 8. Differentially expressed genes (DEGs) of inflammation. 83

Table 9. Differentially expressed genes (DEGs) of angiogenesis. 84

Table 10. Inflammatory genes function. 98

Table 11. Angiogenic genes functions. 98

Table 12. Aborption of MTT for OND model. 130

Table 13. RNA quality and concertation. 136

Table 14. Significant and insignificant genes of inflammation. 137

Table 15. Significant and insignificant genes of Angiogenesis. 140

LIST OF FIGURES

Figure 1. Ischemic stroke, where an artery blockage causes a lack of blood supply and ischemia. 8

Figure 2. Hemorrhagic stroke, where (a) is Intracerebral hemorrhage and (b) is Subarachnoid hemorrhage. 9

Figure 3. Modified Rankin Scale (MRS). 12

Figure 4. National Institutes of Health Stroke Scale (NIHSS). 12

Figure 5. Mechanism of neuronal death in ischemia. 20

Figure 6. Pathophysiology of ischemic stroke showing the molecular events that occur inside neuronal cells due to ischemia. 21

Figure 7. Signaling pathways for neuronal death or survival. 23

Figure 8. Pathogenesis of Atherosclerosis. 27

Figure 9. Normal blood brain barrier. 28

Figure 10. Blood-brain barrier disruption. 30

Figure 11. Microglial (cerebral resident macrophage) activation and the release of pro-inflammatory molecules after Intracerebral hemorrhage. 32

Figure 12. Optimized *in-vitro* ischemic stroke model (Oxygen Nutrients Deprivation: OND). 62

Figure 13. Apoptosis analysis of OGD type with 2 mM glucose media in PBS with Ca++ and Mg++. 74

Figure 14. Apoptosis analysis of OND model. 76

Figure 15. Actin staining of different types of OGD and OND under 10x power. 78

Figure 16. Actin staining of different types of OGD and OND under 60x power. 79

Figure 17. Biochemical analysis of OND model. 80

Figure 18. Differentially expressed genes of inflammation and angiogenesis. 82

Figure 19. Hypoxia-inducible factor (HIF) singalling pathway. 87

Figure 20. NOTCH3, MYBL2 and SQSTM1 signaling pathway. 88

Figure 21. Live/dead staining. 127

Figure 22. Apoptosis anlaysis with different types of OGD.....128

Figure 23. MTT viability test.....129

Figure 24. MTT control with triton.....131

Figure 25. MTT of OND with triton.....132

Figure 26. MTT of OND with PBS/media.....133

Figure 27. Copyright permision 1.....143

Figure 28. Copyright permission 2 143

Figure 29. Copyright permission 3 144

Figure 30. Copyright permission 4 144

Figure 31. iThenticate Report. 145

Chapter 1: Introduction

1.1 Background

Ischemic stroke is an incidental condition where the patient has a blocked artery in the brain due to thrombus formation. The blocked artery causes a lack of oxygen and nutrient supply to brain cells surrounding the blockage, leading to ischemia, severe cell injury, and neuronal death. This condition makes the patients under very high risk of permanent disability or death if not transferred to the hospital within a tight window from stroke symptoms onset (The Internet Strokecenter, 2018b).

Furthermore, stroke is characterized by severe cell injury, and therefore understanding the pathophysiology of cellular changes after exposure to severe stress caused by interruption of nutrients and oxygen is an essential part that could help in the management of such severe disorder.

There are no prior signs that can make the patient care about his condition. Therefore, finding biomarkers that can predict stroke can help in the prevention of stroke and protection of patients from its occurrence by taking the right therapy. Moreover, stroke is a progressive disorder where the patient's condition can sometimes deteriorate quickly. It will be helpful to determine biomarkers for prognosis so the physician can expect the health condition and take the right action ahead of time. Additionally, investigating stroke biomarkers may help in identifying an alternative therapy that can function better than the currently available therapeutics (Jickling & Sharp, 2015).

Most studies were performed using human or animal models for stroke. Few studies were performed using *in-vitro* stroke model of cell culture. Therefore, in this

study, primary human brain microvascular endothelial cell (PHBMEC) were used as *in-vitro* model for stroke.

Microvascular endothelial cells are the cells that line the blood vessels in the brain. They have important functions in delivering the oxygen and nutrients to other brain cells surrounding the blood vessel. They have a significant function as they form the BBB, which excludes harmful components from reaching the brain cells. The occurrence of stroke disrupts the function of these cells, leading to endothelial dysfunction, which is the first barrier protection of brain cells including neurons (Camós & Mallolas, 2010).

In this study, microvascular endothelial cells were exposed to severe hypoxia and nutrients deprivation to elucidate their response under this mimicry condition of ischemic stroke. This study was carried out with an aim to evaluate the expression levels of 168 genes related to the angiogenesis and inflammatory pathways of endothelial cell biology in vitro using PHBMEC, trying for identifying the genes whose expression might be changed and their impact on functional pathways under this pathological condition of cell injury.

1.2 Hypothesis

Exposure of cultured human brain microvascular endothelial cells to severe injury by hypoxia and nutrients deprivation can cause gene expression profile changes indicative of endothelial dysfunction. Identification of the dysregulated genes and functional pathways using bioinformatic tools could be implemented to explore the pathophysiological changes of acute severe stroke-like condition *in vitro*.

1.3 Aims

1- Establishing an *in-vitro* cell injury as a model to mimic stroke conditions using human brain microvascular endothelial cells and evaluate its effects on cellular

function such as:

a. Cell viability: the number of live/dead, apoptosis, and necrosis.
b. Biochemical changes: the impact of stress on glucose, lactate, and pH changes.
c. Changes in cytoskeleton organization/ actin filaments.

2- Analyzing the gene expression profile of inflammation and angiogenesis panels as an indicative of endothelial function of the *in-vitro* cell injury as a model to mimic stroke-like conditions.

a. Exploring the functional changes of the dysregulated genes using bioinformatics tools such as the pathway enrichment analysis, and identifying the core signaling pathways affecting gene regulation.
b. Correlating phenotype/biological changes with genotype/differentially expressed genes of inflammation and angiogenesis.

Chapter 2: Literature Review

2.1 Stroke

Stroke is a cerebrovascular accident characterized by the sudden death of brain cells that results from an interruption of the blood supply to the central nervous system. The interruption of the blood flow in the brain vessels causes lack of oxygen and nutrients supply to brain cells, thus cell death increases. Neuronal death in the brain affects the function of peripheral neurons in the body (The Internet Strokecenter, 2018b).

2.1.1 Definition of stroke

World Health Organization (WHO) defined a stroke as "rapidly developed clinical signs of focal (or global) disturbance of cerebral function, lasting more than 24 hours or leading to death, with no apparent cause other than of vascular origin" (Aho et al., 1980). This definition is applied to the well-known types of stroke, which are namely: cerebral infarction (ischemic stroke), intracranial hemorrhage, and subarachnoid hemorrhage. However, this definition is not applied to the transient ischemic attack, which was described by Fisher C.M. as "it may last from a few seconds up to several hours, the most common duration being a few seconds up to 5 or 10 minutes" (Fisher, 1958).

The American Heart Association/American Stroke Association (AHA/ASA) provided an update of stroke definition for the 21st century (Sacco et al., 2013). They defined stroke generally, then according to its types. Central Nervous System infarction is defined as "brain, spinal cord, or retinal cell death attributable to ischemia," and its symptoms persist for more than 24 hours or until death. Ischemic stroke is defined as "An episode of neurological dysfunction caused by focal cerebral, spinal, or retinal infarction." A stroke that is caused by Intracerebral Hemorrhage

(ICH) is defined as “Rapidly developing clinical signs of neurological dysfunction attributable to a focal collection of blood within the brain parenchyma or ventricular system that is not caused by trauma.” A stroke that is caused by Subarachnoid Hemorrhage (SAH) is defined as “Rapidly developing signs of neurological dysfunction and/or headache because of bleeding into the subarachnoid space (the space between the arachnoid membrane and the pia mater of the brain or spinal cord), which is not caused by trauma” (Sacco et al., 2013).

2.1.2 Epidemiology

Johnson, W. et al. (2016) reported that according to WHO, stroke is the second leading cause of death and the third leading cause of disability worldwide (WHO, 2010). The incidence of stroke in the last decades has been recorded to occur more in low- and middle-income countries than in high-income countries. Furthermore, the age of stroke patients of low- and middle-income countries was 15 years younger than in high-income countries (Johnson, Onuma, Owolabi, & Sachdev, 2016). In general, around 82% of cases stroke occurs in individuals aged more than 65 years old (R.-L. Chen, Balami, Esiri, Chen, & Buchan, 2010). WHO statistics revealed that 15 million strokes occur worldwide each year. Among this number of patients, 5 million get permanent disability, and 5 million dies (WHO, 2010).

A systematic review of stroke epidemiology in the Middle East countries investigated published articles from the year 1980 to 2015 and reported the incidence to be 22.7-250/100,000 population/year, whereas the prevalence was reported to be 508-777/100,000 population/year. The mean age of patients was in the 60s to 70s years old, with 75% of the higher female to male ratio. Hypertension and diabetes were reported to be the main risk factors (El-Hajj, Salameh, Rachidi, & Hosseini, 2016).

2.1.3 Stroke types and causes

Stroke types are determined according to their sources. As explained in previous paragraphs, stroke can be initiated mainly due to ischemia or hemorrhage. Stroke that is due to ischemia can persist for a long time more than 24 hours and called an ischemic stroke. This type is the most common in stroke, accounting for 88% of all cases. Ischemic stroke can show temporary symptoms for a short time from seconds to a few hours, and this type is called a transient ischemic attack (TIA). Stroke that is due to hemorrhage is called hemorrhagic stroke, and it accounts for 12% (The Internet Strokecenter, 2018b) and (National Institute of Health, 2018). Stroke evolves into different stages. It starts as an acute stroke from day 1 to day 7 of stroke onset, then subacute stage from week 1 to month 1, then chronic stage for a period over one month (The Internet Strokecenter, 2018a). Patients who had an initial stroke will have a higher risk of having another or recurrent stroke. Kocaman, G. et al. (2015) performed a hospital-based study in Turkey and reported that 18% of patients who had ischemic stroke experienced a recurrent stroke (KOCAMAN, Dürüyen, Kocer, & Asil, 2015). Oza, R., K. Rundell, and M. Garcellano (2017) reported that recurrent stroke account for 25% of all strokes reported annually in the United States (Oza, Rundell, & Garcellano, 2017).

2.1.3.1 Ischemic stroke

Ischemic stroke and TIA are caused by an obstruction in an artery that supplies blood that carries oxygen and nutrient to the brain. Lack of blood supply causes damage and death to brain cells. Figure 1 represents ischemic stroke. The reasons for that obstruction can happen due to atherosclerosis and build-up of cholesterol plaque that blocks the blood flow due to thrombus formation in the artery. The thrombus can be initiated originally in the brain, which is called small vessel or lacunar stroke, and this is considered as a subtype of ischemic stroke. In another subtype of ischemic stroke, the thrombus can be initiated in the heart and it can be transported by the blood to brain site in a case which is called a cardio-embolic stroke. Abnormal heart conditions, such as arterial fibrillation, are the leading cause of embolic stroke. A third subtype, a thrombus, is initiated in a large artery that supplies the brain, and this is called a large artery atherosclerotic stroke (The Internet Strokecenter, 2018b), (National Institute of Health, 2018) and (Adams Jr et al., 1993). Zafar, A. et al. (2016) performed a study about stroke subtypes in the King Fahad hospital in Saudi Arabia from the year 2008 till 2015. It was recorded that the most frequent subtype was small vessel disease accounting for 32%, followed by cardioembolic stroke (22%) and large artery atherosclerosis (15%) (Zafar, Al-Khamis, Al-Bakr, Alsulaiman, & Msmar, 2016).

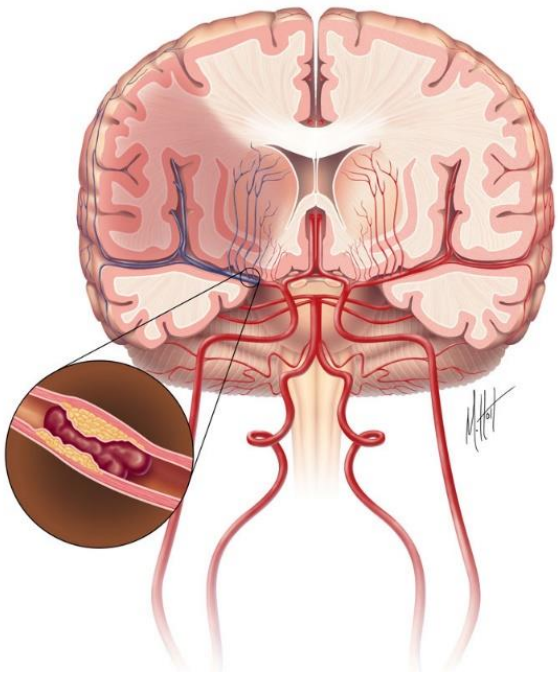

Figure 1. Ischemic stroke, where an artery blockage causes a lack of blood supply and ischemia.
This Figure was adopted from The Internet Stroke center that is supported by the National Institutes of Health (The Internet Strokecenter, 2018b).

2.1.3.2 Hemorrhagic stroke

Hemorrhagic stroke is caused by an artery rupture, causing blood leakage inside the brain. The bleeding could be within the brain structure known as Intracerebral Hemorrhage (ICH) or surrounding the brain, known as Subarachnoid Hemorrhage (SAH). Figure 2 represents hemorrhagic stroke. This leads to swelling inside the brain, or the swelling causes a high pressure that causes damage to the brain cells. The possible reasons for bleeding are hypertension, aneurysm, or arterio-venous malformation. The most common cause of ICH is hypertension, whereas SAH is mostly caused by a cerebral aneurysm (The Internet Strokecenter, 2018b) and (National Institute of Health, 2018). A summary presented in Table 1, indicating different types of stroke.

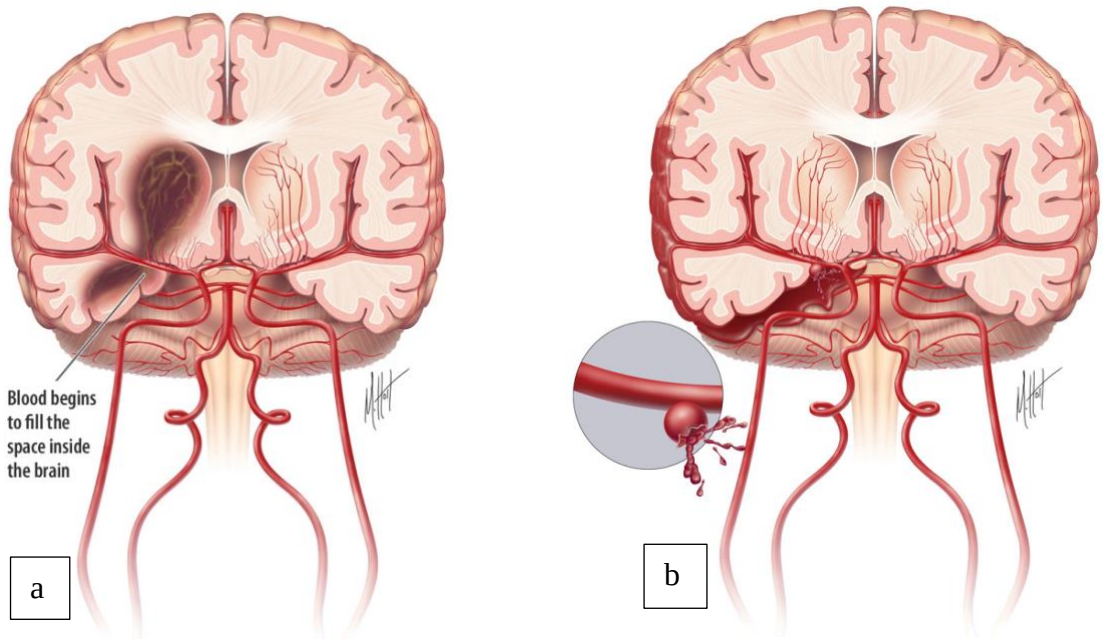

Figure 2. Hemorrhagic stroke, where (a) is Intracerebral hemorrhage and (b) is Subarachnoid hemorrhage.
This Figure was adopted from The Internet Stroke center that is supported by the National Institutes of Health (The Internet Strokecenter, 2018b).

Table 1. Summary of types and subtypes of stroke.

Types of strokes	**Ischemic stroke**	**Hemorrhagic stroke**
Cause of stroke	Artery occlusion and lack of blood supply leading to ischemia and tissue damage	Artery rupture and bleeding leading to tissue damage
Subtypes of stroke	1-Small vessel/lacunar stroke 2-Cardioembolic stroke 3-Large artery atherosclerosis	1-Intracerebral hemorrhage 2-Subarachnoid hemorrhage

2.1.4 Risk factors for stroke

The risk factors for stroke are multifactorial and dissected to modifiable and non-modifiable risk factors. Advanced age is a non-modifiable risk factor, and it was reported that the stroke risk increased by age greater than 65 years old (Thrift et al., 2017). Other modifiable risk factors are reported by different studies. Zafar, A. et al. (2016) did a cross-sectional study in the King Fahd hospital in Saudi Arabia to report risk factors among ischemic stroke patients. Hypertension was on the top of risk factors accounting for 78% of total patients. Diabetes mellitus was the second top risk factor contributing to around 63%, followed by hyperlipidemia as 55% and ischemic heart disease in around 24% of patients (Zafar et al., 2016). Recurrent stroke risk factors were reported in a study done in Turkey by KOCAMAN, G. et al. (2015). Hypertension was on top of risk factors accounting for 88% observed in patients, followed by diabetes mellitus (43%), ischemic heart disease (36%), hyperlipidemia (30%), atrial fibrillation (11%), and smoking (14%) (KOCAMAN et al., 2015).

2.1.5 Diagnosis of stroke

Many people are not aware of stroke symptoms, and stroke patients are at risk of delayed treatment, especially that stroke is painless. A hospital-based study in Qatar was published in 2008 reported that only 18% of patients arrived at the hospital within 3 hours of stroke onset (Khan et al., 2008).

Since stroke is painless and most people are not aware of it, significant warning signs of stroke were created in one acronym: FAST, which refers to Face drooping, Arm weakness, Speech difficulty, and Time to call emergency, respectively. Additional symptoms that can be present in stroke patients are trouble seeing, speaking and walking, loss of balance, and sudden weakness or numbness of

one side of the body. Very few cases of stroke can have a possibility to have severe headache where hemorrhage caused severe pressure on the skull.

Stroke severity can be determined clinically by different scales, such as the Modified Rankin Scale (MRS) and the National Institutes of Health Stroke Scale (NIHSS), (Musuka, Wilton, Traboulsi, & Hill, 2015) and (Christensen, 2014). MRS has a scale from 0 to 6 as represented in Figure 3, where MRS = 0 means no symptoms at all, MRS = 1 – 5 identifies the severity of stroke where 1 = no significant disability, 2 = slight disability, 3 = moderate disability, 4 = moderately severe disability, and 5 = severe disability. MRS = 6 means dead (Christensen, 2014). Figure 3 represents the MRS scale.

MRS = 0	MRS = 1	MRS = 2	MRS = 3	MRS = 4	MRS = 5	MRS = 6
No symptoms	The severity of stroke from less to most severe disability					Dead

Figure 3. Modified Rankin Scale (MRS).
This figure is designed by the present author © Fatima Alzahra Al Hamed, using the information presented by (Christensen, 2014).

NIHSS has a scale from 0 to 42 represented in Figure 4, where NIHSS = 0 has no signs on examination, NIHSS = 1-5 indicates a minor stroke, NIHSS = 6-10 indicates moderate disabling stroke, NIHSS = 11-20 indicates moderate to severe disabling stroke and NIHSS greater than 20 indicates severe and life-threatening stroke (Musuka et al., 2015). Figure 4 represents the NIHSS scale.

NIHSS = 0	NIHSS = 1-5	NIHSS = 6-10	NIHSS = 11-20	NIHSS > 20
No signs	Minor stroke	Moderate stroke	Severe stroke	Life-threatening

Figure 4. National Institutes of Health Stroke Scale (NIHSS).
This figure is designed by the present author © Fatima Alzahra Al Hamed, using the information presented by (Musuka, Wilton, Traboulsi, & Hill, 2015).

2.1.6 Stroke complications

Stroke patients, in case of delayed, ineffective, or absent treatment, can get permanent disability or die soon. Stroke is considered a leading cause of death and disability worldwide (Johnson et al., 2016). Functional disability occurred as a result of the dysfunction of the nervous motor system (S Pandya et al., 2011). Additional complications that worsen stroke include hemorrhagic transformation and cerebral edema and stroke recurrence which is increased in the presence of diabetes, hypertension, atherosclerosis or other risk factors of stroke (S Pandya et al., 2011). Other complications of stroke are myocardial infarction, congestive heart failure, pneumonia or chest infection, urinary tract infection, deep vein thrombosis, pulmonary embolism, osteopenia and hip fractures, fatigue, depression, and fever (Langhorne et al., 2000).

2.1.7 Stroke prevention

The first line of defense against stroke is treating its risk factors. Anti-hypertensive therapy has shown a 30-40% reduction in stroke incidence (R.-L. Chen et al., 2010). Anti-coagulant therapy to patients with arterial fibrillation led to a 68% reduction in stroke risk (R.-L. Chen et al., 2010). Statin, which is a medication to reduce cholesterol in the blood, proved to reduce the risk by around 20% in patients (R.-L. Chen et al., 2010). Controlling glucose level and intensive diabetes therapy has proved to reduce the risk of cardiovascular diseases (CVD) by 42% and the events of CVD, including stroke by 57% (Lachin, Orchard, Nathan, & Group, 2014).

2.1.8 Stroke in Qatar

The population in Qatar is multi-diverse, and different people from different ethnic groups around the world come to work and live in Qatar. This multi-ethnicity contributes to different diseases epidemiology.

Hamad, A. et al. (2001) studied patient records in Hamad General Hospital for the full year of 1997. The mean age of patients was around 57-60 years old. A considerable number of patients (18%) were younger than 45 years old (Hamad et al., 2001). Mushlin, et al. (2012) reported that half of the stroke patients were younger than 55 years old (Mushlin et al., 2012).

Khan, F.Y., et al. (2008) reported that male patients were dominant, accounting for 73% of stroke patients, which reflects Qatar's population of labor force where males outweigh females. The mean age of women was higher than men as reported to be around 61 vs. 56 years old, respectively. Native Qatari accounted for 37.4% of patients, while the majority (62.6%) were non-Qatari representing different nationalities. Major nationalities were Asian (Indian, Pakistani, Bengali, Philippine), and the rest were from Arabs (Egyptian, Palestinians) and other nationalities (Khan et al., 2008).

Khan, F.Y. (2007) investigated the risk factors in young stroke patients aged from 17-44 years old. There were five major risk factors reported with the following percentages: hypertension (40%), diabetes mellitus (32.5%), hypercholesterolemia (27.5%), smoking (27.5%), and alcohol intake (22.5%) (Khan, 2007). Mushlin, et al. (2012) reported that patients who had a history of diabetes, hypertension, or dyslipidemia had increased risk of stroke incidence illustrated by hazard ratio (5.12, 3.56, 2.45 respectively) (Mushlin et al., 2012).

2.2 Stroke Biomarkers

2.2.1 Definition of biomarker

The biomarker was defined by the National Institute of Health (NIH) as “a characteristic that is objectively measured and evaluated as an indicator of normal biological processes, pathogenic processes, or pharmacologic responses to a therapeutic intervention.”(Group et al., 2001).

2.2.2 Clinical utility of stroke biomarkers

Currently, there are no biomarkers that can be used clinically in stroke diagnosis, prediction, or prognosis. However, clinical research studies revealed several biomarkers related to stroke diagnosis, prediction, or prognosis, but they are still under investigation and not yet being applied to clinical field. Table 2 reperesnt biomarkers of stroke that are still under investigation with their reference. It is crucial sometimes to differentiate stroke from other neurological diseases, especially when there are mild symptoms or when neuroimaging, such as CT scan and MRI, is not available. Determining the etiology of stroke is also challenging. Therefore, biomarkers can help in improving the diagnosis, differentiating different types of strokes, and determining the cause of stroke. Biomarkers can be applied as well as a prognostic tool to determine the recurrence of stroke and treatment efficiency (Jickling & Sharp, 2015).

Stroke is a heterogeneous disease, identification of several biomarker arranged in panels can provide key insights about different pathophysiological processes of stroke, such as atherosclerosis, thrombus formation, oxidative stress, inflammation, endothelial injury, and cerebral ischemia. Some studies reported panels of biomarkers that can be used to increase the sensitivity and specificity of ischemic stroke diagnosis. However, none of these panels were approved sufficiently to be used clinically. (Jickling & Sharp, 2015).

Table 2. Summary of Protein biomarkers related to stroke (prediction, diagnosis, prognosis and therapy).

Biomarkers for Prediction
(VEGF, CRP, TNFR-2, Homocysteine)(Shoamanesh et al., 2016)
Extracellular Vesicles (Agouni et al., 2019)
Biomarkers for Diagnosis
Ischemic Stroke
(CRP, Homocysteine, P-Selectin)(Hasan, McColgan, Bentley, Edwards, & Sharma, 2012)
A Panel Of (S100b, MMP-9, BNGF, MCP-1, And vWF)(Reynolds et al., 2003)
(NT - Pro BNP, Endostatin)(Bustamante et al., 2017)
P-Selectin (Kalmarova et al., 2018), (R. Zhang, Chopp, Zhang, Jiang, & Powers, 1998), E-Selectin (R. Zhang et al., 1998)
Hemorrhagic Stroke (Intracerebral Hemorrhage)
GFAP(Hasan et al., 2012), (Foerch et al., 2011), (Katsanos et al., 2017)
MMP-9, D-dimer, S-100b, and BNF(Laskowitz et al., 2009)
Cardioembolic Stroke
A Panel Of (D-Dimer And NT Pro-BNP)(Montaner et al., 2008)
All strokes
MMP-9, D-dimer, S-100b, and BNF(Laskowitz et al., 2009)
Biomarkers for Prognosis
Poor Prognosis Within 48 Hours
Glutamate (Hasan et al., 2012), Glucose (Hasan et al., 2012)
Infection Within A Week
IL-6 (Kwan et al., 2013), L-Arginine (AMDA/SDMA) (Molnar et al., 2016)
Hemorrhagic transformation
MMP-9 (Turner & Sharp, 2016)
In-Hospital Death
D-Dimer (Hasan et al., 2012), Glucose (Hasan et al., 2012)
Poor Outcome Within 2 Weeks
CRP (Geng et al., 2016)
Poor Outcome at Day 30 (Disability/Death)
D-Dimer (Hasan et al., 2012), CRP (Hasan et al., 2012), Adiponectin (Marousi et al., 2010), NSE (Zaheer et al., 2013), MDA (Lorente et al., 2015), Copeptin (Katan et al., 2009)
Poor Outcome At 3 Months (Disability/Death)
IL-6 (Whiteley et al., 2012), NT Pro-BNP (Whiteley et al., 2012), E-Selectin (Richard et al., 2015), Omentin-1 (T. Xu, Zuo, Wang, Gao, & Ke, 2018), D-Dimer (X.-y. Yang et al., 2014), MMP-9 (Zhong et al., 2017),(Zhong et al., 2018)
Progressive ischemic stroke
P-Selectin(Q. Wang, Zhao, & Bai, 2013)
Mortality Within 1-2 Years
IL-6 (Shaafi et al., 2014),(Kwan et al., 2013)
Good outcome and recovery
MMP-2 (Lagente & Boichot, 2008), (Kurzepa, Kurzepa, Golab, Czerska, & Bielewicz, 2014)
Biomarkers for Therapy
Blood-Brain Barrier Dysfunction and Risk of Hemorrhagic Transformation
Occludin (Pan et al., 2017), S100b (Foerch et al., 2007), MMP-9 (Castellanos et al., 2003)
Improved Outcome
IL-1ra (Emsley et al., 2005), Anti-ICAM-1 (Bowes MP, 1993)

2.2.3 Role of stroke biomarkers in the pathological process

As indicated previously, research studies reported several circulating biomarkers are elevated in stroke and reflect the different pathological processes. These pathological processes are systemic inflammation such as CRP, TNF-α, TNFR-2, IL-6, MMP-9, and MCP-1 , endothelial dysfunction such as VEGF, homocysteine, and P-selectin , cerebral and neuronal damage such as GFAP, S100B, glutamate, occludin, copeptin, NSE, and BNGF , thrombosis such as D-dimer, fibrinogen, and vWF , and cardiac complications such as NT pro-BNP biomarker (Maas & Furie, 2009), (Katan & Elkind, 2018), (Miao & Liao, 2014), and (Simats, García-Berrocoso, & Montaner, 2016).

2.2.4 Future biomarkers of stroke

MicroRNA (miRNA) is a small non-coding RNA that regulates gene expression in post-transcribed messenger RNAs (mRNA). Several studies reported the dysregulation of various miRNAs during ischemic stroke.

Jickling, G.C. et al. (2014) reported two miRNAs to be up-regulated (miR-363 and miR-487b) in ischemic stroke patients vs. vascular risk factors controls. Furthermore, 6 miRNAs were downregulated (let-7i, miR-122, miR-148a, miR-19a, miR-320d, miR-4429) (Jickling et al., 2014). These biomarkers were known to regulate several pathways of ischemic pathogenesis, such as NFkB, JNK, and p38-MAPK. Some examples are: miR-363 and miR-487b regulate MAP2K4 pathways, Let-7i and miR-19a regulate TLR pathway, miR-122 regulates growth factor receptor (GFR), miR-320d regulates PI3K, interleukin-1 receptor-associated kinase (IRAK) and AKT, let-7i and miR-122 regulate AKT. Thus, miRNAs can be promising biomarkers for the diagnosis or prognosis of ischemic stroke (Jickling et al., 2014).

Tiedt, et al. (2017) reported that miR-125a, miR-125b, and miR-143 are significantly increased in acute ischemic stroke patients compared to healthy controls (AUC: 0.93) and transient ischemic attack patients (AUC: 0.66). The levels of these miRNAs were similar in different subtypes of ischemic strokes, such as large vessel stroke and cardioembolic stroke. However, the levels of these miRNAs did not have any correlation with the infarct size. Such data indicate that these miRNAs are potential promising biomarkers to diagnose acute ischemic stroke (Tiedt et al., 2017).

Khoshnam, S.E. et al. (2017) reported several miRNAs that are involved in stroke pathogenesis and act on different gene targets that have a potential therapeutic future. Some examples are: miR-101 that targets Cycloxygenase-2 (COX-2) gene is downregulated in the ischemic stroke which enhances ROS production, miRNA-107 suppresses Glutamate transporter-1 (GLT-1) gene which leads to glutamate accumulation and miRNA-181c, which targets TLR4 and inhibit NF-kB activation and expression of pro-inflammatory genes, is downregulated in ischemic stroke (Khoshnam, Winlow, Farbood, Moghaddam, & Farzaneh, 2017).

2.3 Stroke pathophysiology

2.3.1 Pathophysiology of ischemic stroke

Interruption of blood flow or ischemia causes a lack of oxygen and glucose supply to neuronal cells. This causes neuronal depolarization where glutamate receptor is activated, and glutamate, which is an excitatory neurotransmitter, is released in an uncontrollable fashion. Glutamate leads to the activation of kainite receptors (N-methyl-D-Aspartate (NMDA) and α-amino-3-hydroxy-5-methyl-4-propionate (Marousi et al.), which results in the influx of calcium and sodium into the cell. The increase in intracellular calcium and sodium causes electrolyte imbalance and release of potassium extracellularly, which eventually leading to edema and water accumulation. High intracellular calcium leads to activation of a wide variety of cellular components including enzymes, lipase, protease, and endonuclease, which consequently leads to the release of free radicals: Nitric Oxide Synthase (NOS), and Reactive Oxygen Species (ROS). These intracellular changes cause break down of proteins and lipids, resulting in cellular membrane damage and **degradation** of the **cytoskeleton**. Free radical production causes nuclear and mitochondrial damage where the inflammatory cascade is triggered, leading to cell death and the release of inflammatory mediators. Mitochondrial damage results in the release of caspases, which triggers the apoptosis pathway, which leads to cell death (Deb, Sharma, & Hassan, 2010), (Brott & Bogousslavsky, 2000) and *(Bonaventura et al., 2016)*. Figure 5 represents the mechanism of neuronal death in ischemia and Figure 6 represents pathophysiology and molecular events that occur in neuronal cells due to ischemia.

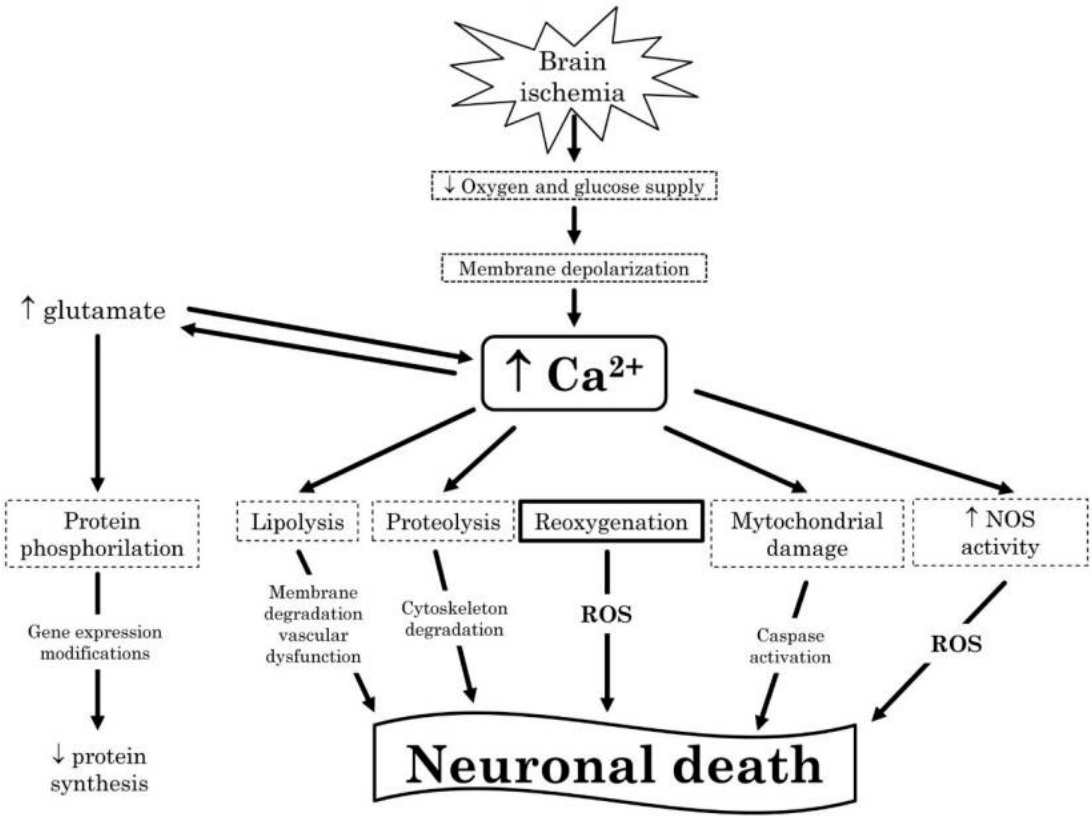

Figure 5. Mechanism of neuronal death in ischemia.
This figure was designed by Bonaventura, A. et al. (2016), *(Bonaventura et al., 2016)*. Permitted from https://creativecommons.org/licenses/by/4.0/. Copyrights' permission is in the Appendix.

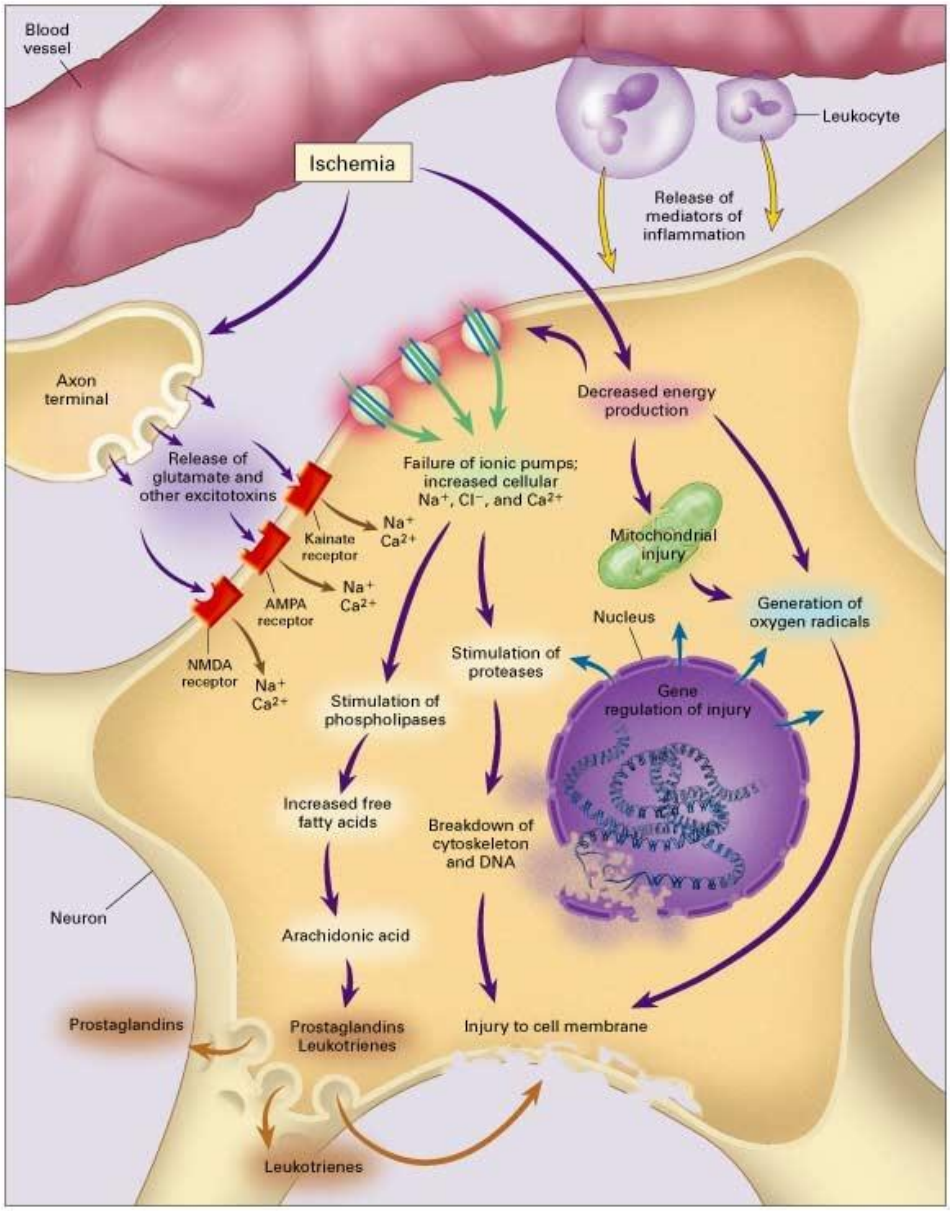

Figure 6. Pathophysiology of ischemic stroke showing the molecular events that occur inside neuronal cells due to ischemia.
This figure was designed by Brott, T. and J. Bogousslavsky (2000). Adopted from (scientific reference citation), Copyright Massachusetts Medical Society (Brott & Bogousslavsky, 2000). Copyright permission is in the Appendix.

ROS activates different contrasting pathways that lead to either neuronal death or survival through gene expression modifications. Neuronal death is induced through the activation of p-53, mitogen-activated protein kinases (MAPK), extracellular signal-regulated kinase (ERK), and signal transducer and activator of transcription (STAT). MAPK includes p-38 and c-Jun N-terminal kinases (JNK), which respond to stress stimuli. Neuronal protection or survival is induced through **activation** of nuclear factor kappa-light-chain-enhancer of activated B cells (NFκB), heat shock transcription factor 1 (HSF1), **hypoxia-inducible factor 1** (HIF1) and protein kinase C (PKC). NFκB is mediated through phosphoinositide 3- kinase (PI3k) and Akt signaling pathway. NFκB regulates inflammation and is expressed by activated microglia, glial cells, endothelial cells, and several immune cells, lymphocytes, macrophages, and monocytes. It regulates expression of tumor necrosis factor (TNF-α), Interleukin-1β (IL-1β), Interleukin-6 (IL-6), Intercellular adhesion molecule-1 (ICAM-1), cyclooxygenase-2 (COX-2), and iNOS. The activation of MAPK and activation factor-1 NFκB leads to activation of a transcription factor called activation factor-1 (AP-1), which regulates gene expression (Hess, Angel, & Schorpp-Kistner, 2004) (Woodruff et al., 2011) & (Bonaventura et al., 2016). Figure 7 represents the signaling pathways of neuronal death or survival.

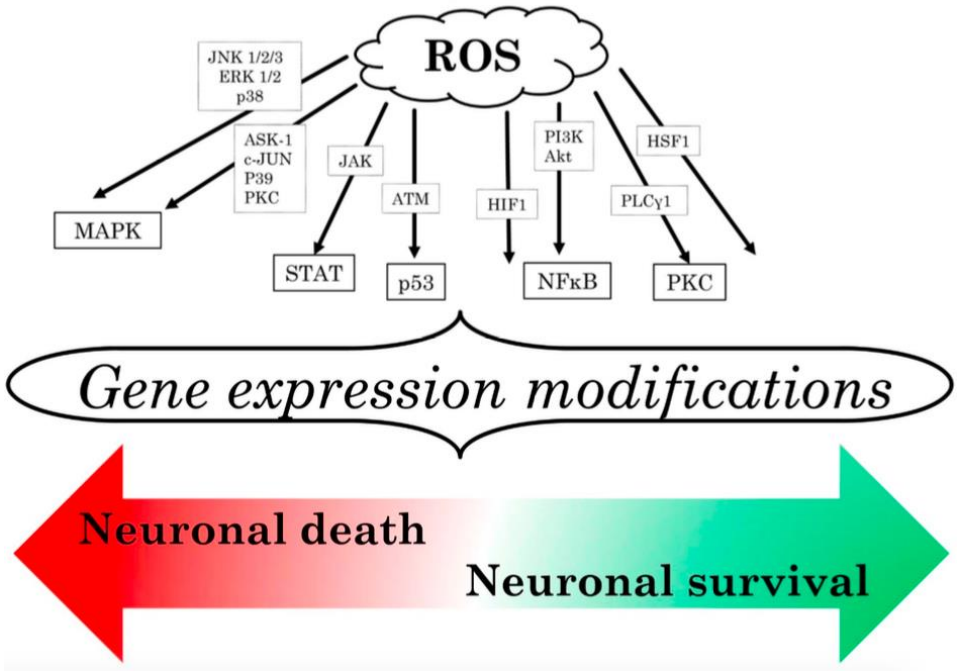

Figure 7. Signaling pathways for neuronal death or survival.
This figure was designed by Bonaventura, A. et al. (2016), *(Bonaventura et al., 2016)*. Permitted from https://creativecommons.org/licenses/by/4.0/. Copyrights' permission is in the Appendix.

The inflammatory cascade includes both glial and endothelial cells, which trigger the recruitment of leukocytes. The soluble mediators that are released due to recruitment help in the disruption of the BBB. Though therapy of ischemic stroke helps in the restoration of blood flow, however, it can lead to exacerbation of tissue injury leading to what is known as 'reperfusion injury.' Reperfusion and returning of blood supply or re-oxygenation lead to an increase in ROS production, which causes damage and death to neuronal cells as well. Reperfusion also can lead to the transformation of stroke from ischemia to hemorrhage, where it is called hemorrhagic transformation (Deb et al., 2010), (Woodruff et al., 2011) and (Bonaventura et al., 2016).

Inflammation is a defense mechanism where leukocytes migrate from the bloodstream to the targeted tissue to destroy agents that cause injury. IL-6 is an inflammatory cytokine that is released from different types of cells such as macrophage, T and B lymphocytes, and fibroblasts. IL-6 acts mainly on the differentiation of B cells and stimulate the production of acute-phase proteins such as C-reactive protein (CRP) (Vaillant & Qurie, 2018). IL-6 activates immune cells through acting on gp130 cell receptor and induce different signaling pathways; JAK, MAPK, and STAT3 pathways (Gabay, 2006; Hirano, 2010). Gabay, C. has cited that the interaction of IL-6 with its soluble receptor (IL-6Rα) plays a role in activating endothelial cells to recruit leukocytes by inducing the production of IL-8 and monocyte chemoattractant protein-1 (MCP-1) and the expression of adhesion molecules (Gabay, 2006).

Matrix Metalloproteinase-9 and -2 (MMP-9 and MMP-2) are known to be elevated in stroke. They belong to calcium- and zinc-dependent endopeptidase family. They are known as gelatinase due to their function of breaking down gelatin in the extracellular matrix (ECM). MMP-9 is referred to as gelatinase B, and MMP-2 as gelatinase A. MMP-9 is usually expressed at a very low level; however, its expression increases when ECM remodeling is needed. MMP-2 is usually expressed in high levels in normal circumstances, and it doesn’t respond to inflammatory stimuli like MMP-9 (Harrington, Stefanec, Newton, & Rounds, 2006).

At nuclear level, MMP-9 is activated by nuclear factor (NF-kB), activator protein-1 (AP-1), serum amyloid A-activating factor (SAF-1), polyomavirus enhancer A-binding protein-3 (PEA3), specificity protein-1 (SP-1) and E-26 (Ets) transcription factor. MMP-2 gene promoter acts as a housekeeping promoter that contains only activator protein-2 (AP-2), which makes it expressed in a normal situation. MMP-2

can get also activated by the activation of other types of MMPs (Harrington et al., 2006).

.

Furthermore, P-selectin and E-selectin are known to be elevated in stroke. Selectins are cell-surface glycoproteins that belong to the adhesion molecules family. They initiate the adhesion of leukocytes to endothelial cells of the blood vessel's lumen, where the attachment facilitates the migration of leukocytes from the bloodstream to the target tissue of injury or inflammation. E-selectin is expressed on the surface of endothelial cells, P-selectin that is expressed by both platelets and endothelial cells (Tedder, Steeber, Chen, & Engel, 1995). E-, P- and L-selectins interact with P-selectin glycoprotein ligand-1 (PSGL-1) that is expressed in different leukocytes, such as neutrophils, monocytes, and lymphocytes. These selectins have different roles in pathologic pathways such as inflammation, atherosclerosis, and coagulation. The interaction between the selectins that are expressed on endothelial cells (E- and P-selectins) with the ligand (PSGL-1) on leukocyte facilitates rolling and firm attachment of leukocytes to endothelial cells then diapedesis of leukocytes to inflamed or atherosclerotic tissue. The interaction of P-selectin on platelets with PSGL-1 on leukocytes play a role in coagulation (Ley, 2003). In **normal conditions**, **cerebral endothelial** cells **don't recruit leukocytes** much **as other organs** do, such as skeletal muscles or intestinal mesentery. However, during ischemia or any inflammatory condition in the brain, the expression of E- and P-selectins is upregulated on the surface of cerebral endothelium leading to the recruitment of a large number of leukocytes (Yilmaz & Granger, 2008). The P-selectin expression is upregulated in response to inflammatory cytokines (IL-1, IL-4, IL-13, TNF-α) or to thrombin and reactive oxygen species (Woltmann, McNulty, Dewson, Symon, &

Wardlaw, 2000) and (Blann, Nadar, & Lip, 2003). E-selectin increased expression is a response of the released TNF-α. It was reported that increased soluble E-selectin in the blood is due to increased endothelial cells apoptosis (Harrington et al., 2006).

2.3.1.1 Pathogenesis of ischemic stroke caused by Atherosclerosis

Atherosclerosis is one of the primary causes of stroke. It is a disease of arteries that causes a condition of chronic inflammation due to the formation of atherosclerotic plaque. It could lead to an acute medical case if the thrombus blocked a blood vessel in the brain (Lusis, 2000). The inflammatory process that is occurring in the wall of the atherosclerotic artery is quite complicated, and many factors are contributing to the process. These factors are the adhesion molecules that are expressed by the endothelial cells, Vascular Cellular Adhesion Molecule-1 (VCAM-1), and Inter-cellular adhesion Molecule-1 (ICAM-1), which causes the recruitment of leukocytes. Low density lipoprotein (LDL) molecules migrate inside the wall where macrophages ingest them and becoming foam cells. Foam cells produce metalloproteinase and several inflammatory cytokines that trigger smooth muscle immigration from the media and the dysregulation of the wall matrix, including collagen and elastin, which consequently causes luminal stenosis and formation of the fibrous cap. Activated foam cells produce a C-Reactive protein (CRP) that contributes to circulatory inflammation and to the recruitment of platelets, which leads to thrombus formation and artery occlusion (Esenwa & Elkind, 2016) & (Linton et al., 2015). Figure 8 represents the pathogenesis of atherosclerosis in ischemic stroke.

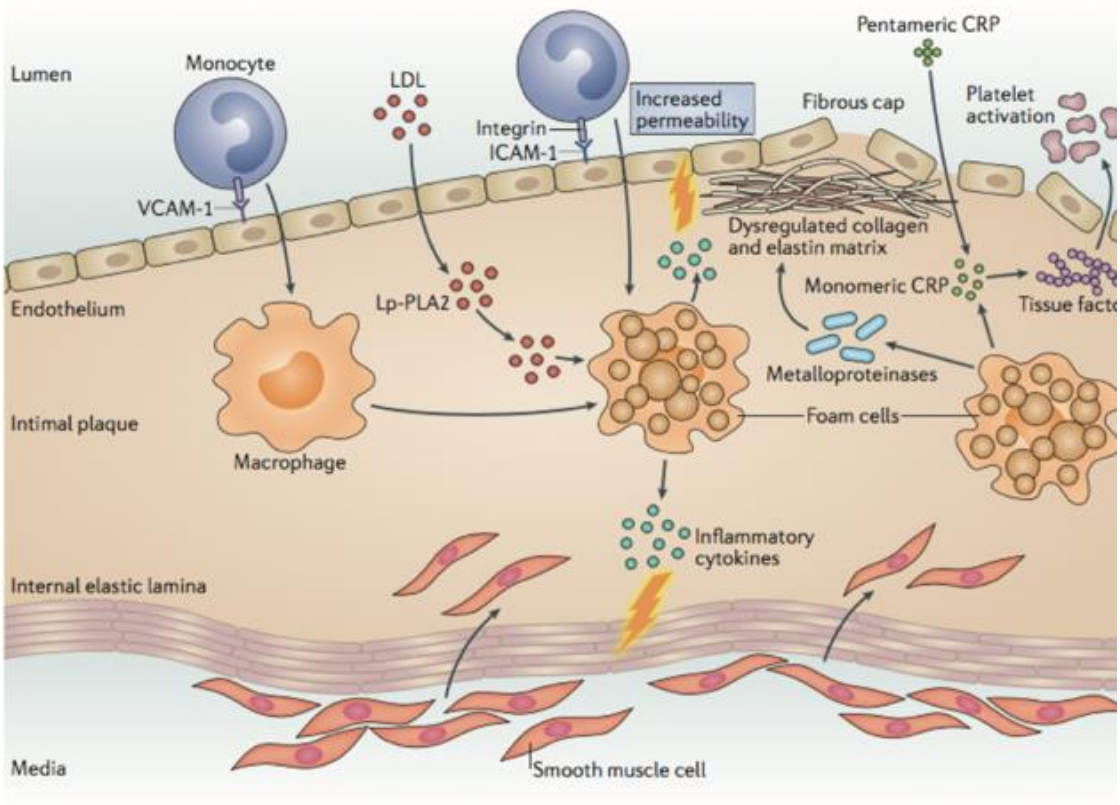

Figure 8. Pathogenesis of Atherosclerosis.
This figure is designed by Esenwa, C.C., and M.S. Elkind (2016), i (Esenwa & Elkind, 2016). Copyrights' permission is in the Appendix.

2.3.1.2 Blood-brain barrier and ischemic stroke

2.3.1.2.1 Normal blood-brain barrier

The blood-brain barrier is constructed of highly resistant endothelial cells that line the brain blood vessel. They are linked to each other by several types of tight and adherence junctions, which make them lack fenestration. Tight junction markers are occludin and claudin-5 and junction adhesion molecule (JAM) (Jiang et al., 2018). Adherence junction markers are cadherins. Tight and adherence junctions are connected to the **actin cytoskeleton** through zonula occludens, cingulin, and catenin proteins. This feature regulates the movement of molecules from the blood to the

brain through either by paracellular/transcellular diffusion, transcytosis, nutrient or ion-transporter. Figure 9 illustrates the normal blood brain barrier. Furthermore, brain endothelial cells consist of a double fold of mitochondria than the peripheral vessels' endothelium, and a low number of pinocytic vesicles that limit endocytosis and transcytosis. These characteristics of the blood brain barrier keep brain cells protected from being damaged from any particles in the blood (Jiang et al., 2018).

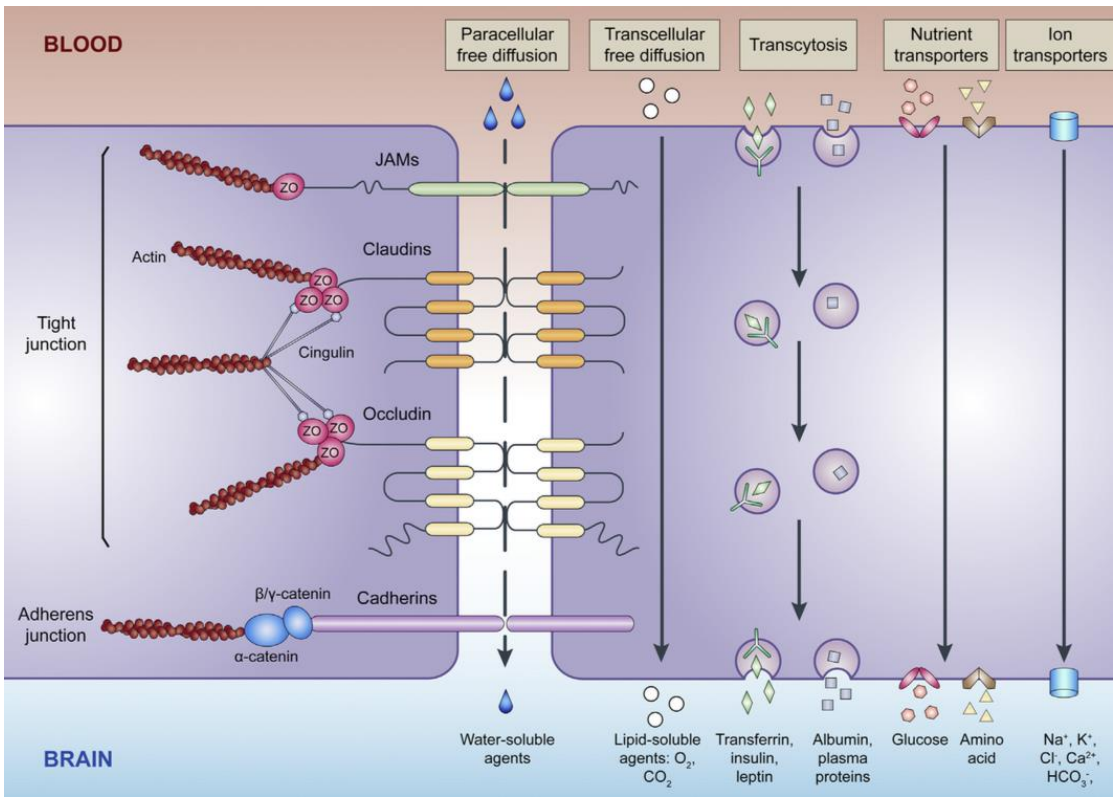

Figure 9. Normal blood brain barrier.
This figure is designed by (Jiang et al., 2018). Copyrights' permission is in the Appendix.

2.3.1.2.2 Blood-brain barrier disruption

Ischemic stroke causes BBB dysfunction in several ways, including impaired cellular ion transporters, which induces edema, degradation of extracellular matrix (ECM) surrounding blood vessel, and disruption of tight and adherence junction. Tight and adherence junctions can get disrupted through protein phosphorylation, translocation, or degradation. Phosphorylation can cause dissociation of tight junctions which increases BBB permeability. Phosphorylation is induced through different factors, including; VEGF, Rho-associated protein kinase/ (ROCK), cyclic-AMP/ PKA, and by the released inflammatory biomarkers TNF-α and IL-6 (Jiang et al., 2018).

Ischemia enhances the **polymerization** of **actin filaments** and the formation of **stress fiber,** which causes a cellular tension that causes the tight junctions to be translocated intracellularly. Chemokine MCP-1 enhances the internalization of tight junctions into the cell through endocytosis. Translocation facilitates the degradation of tight junctions, either extracellularly or intracellularly. Subsequent to stroke, zinc accumulation leads to activation of MMP-9 and MMP-2 extracellularly, which degrade tight junctions. Furthermore, ubiquitination produces protostomes and lysosomes which degrade those junctions. BBB disruption increases permeability from blood to the brain, which leads to the infiltration of peripheral immune cells and the accumulation of fluids in the ischemic area. This will lead to neurovascular damage. Figure 10 illustrates the BBB disruption (Jiang et al., 2018).

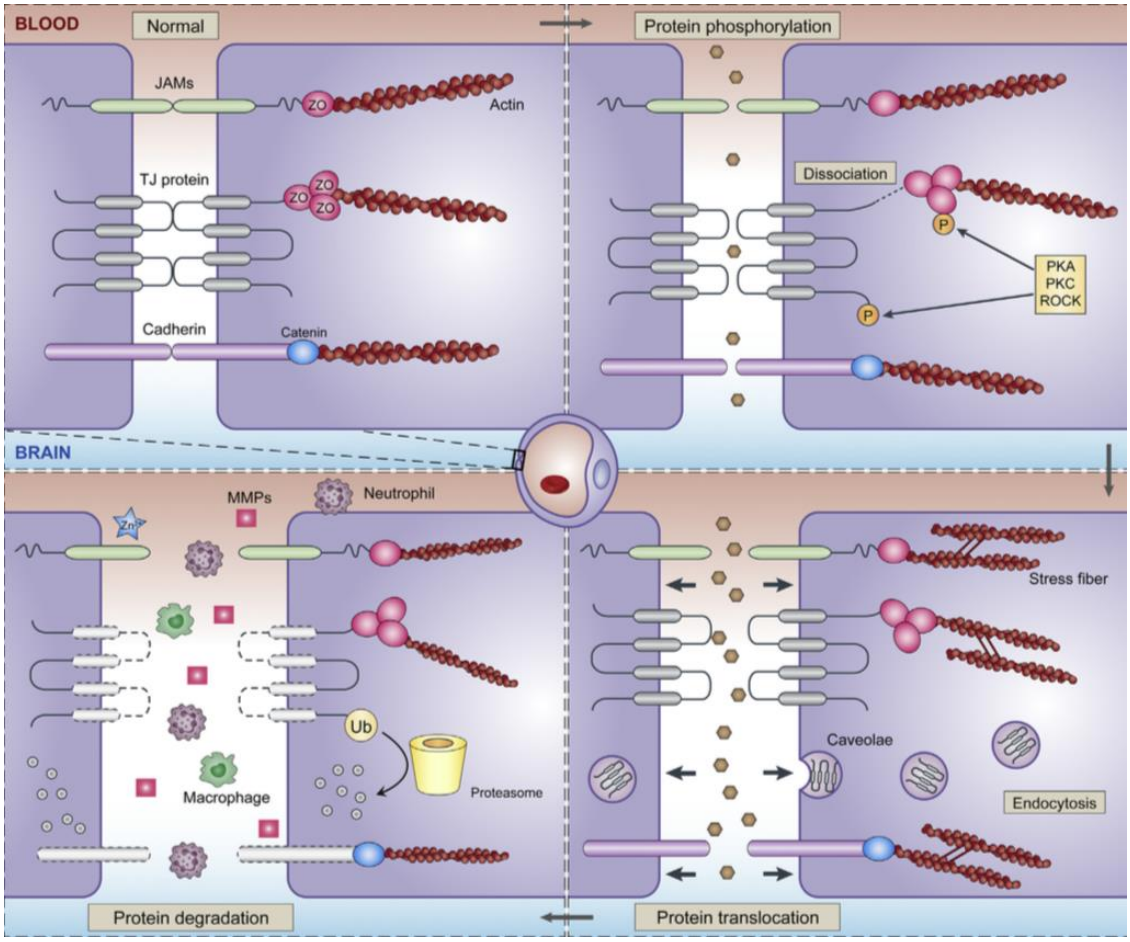

Figure 10. Blood-brain barrier disruption.
This figure is designed by (Jiang et al., 2018). Copyrights' permission is in the Appendix.

Microglia contribute to this pathophysiology through releasing inflammatory cytokines; IL-1 and IL-6, which enhance endothelial cells to express leukocyte adhesion molecules; ICAM-1, P-selectin, and E-selectin. This leads to further recruiting, accumulation, and transmigration of peripheral leukocytes. Brain endothelial cells play a key role in protecting the neurons from ischemia by creating new blood vessels through **angiogenesis**. The blood vessel dilates, and the ECM gets degraded by MMP-9 and MMP-2. Endothelial cells **proliferate**, **migrate**, and

assemble to form new cord and then differentiate to meet local needs (Jiang et al., 2018).

2.3.2 Pathophysiology of hemorrhagic stroke

An intracerebral hemorrhage causes primary and secondary brain damage. In primary damage, bleeding and blood accumulation leads to the formulation of a mass inside the brain, which is called a hematoma. Hematoma causes mechanical damage to brain cells due to the enhancement of hydrostatic pressure, which causes BBB damage and plasma release, followed by edema formation. Edema causes an increase in intracranial pressure, which eventually causes neuronal injury. In the secondary damage, hemostatic or coagulative factors get activated as a part of the physiological response to bleeding. Thrombin gets activated, and it contributes to BBB damage and edema formation. Erythrocytes get lysed, and hemoglobin is released, which is converted to heme and iron by heme oxygenase-1 (HO-1) enzyme. Heme and iron are toxic components that contribute to neuronal damage (Mracsko & Veltkamp, 2014).

Damaged neurons and components of a blood clot (Fibrin, thrombin, and heme) trigger activation of inflammatory and oxidative stress pathways and the recruitment of innate and adaptive immune cells. Microglia, which is a type of macrophages that are residents in the brain, get activated through toll-like receptor-4 (TLR-4) that is expressed on its surface, leading to activation of NF-kB, proteinase-activated receptor-1 (PAR-1) and MAPK signaling pathway. Activation of these pathways leads to upregulation of pro-inflammatory genes and the release of inflammatory cytokines, chemokines and oxidation molecules (TNF-α, IL-1β, IL-6, CXCL-2, CCL-2, nitric oxide (NO) synthase, and ROS) and other protective molecules such as IL-10 and CXC3R-1 that facilitates recovery. CXCL-2 has a chemotactic activity that attracts neutrophils. CCL-2 is a monocyte chemoattractant

protein-1 (MCP-1). IL-1β recruits T cells which produce gamma interferon (IFN-γ). This immune cell migration leads to further damage to BBB and exacerbation the inflammation inside the brain (Mracsko & Veltkamp, 2014).

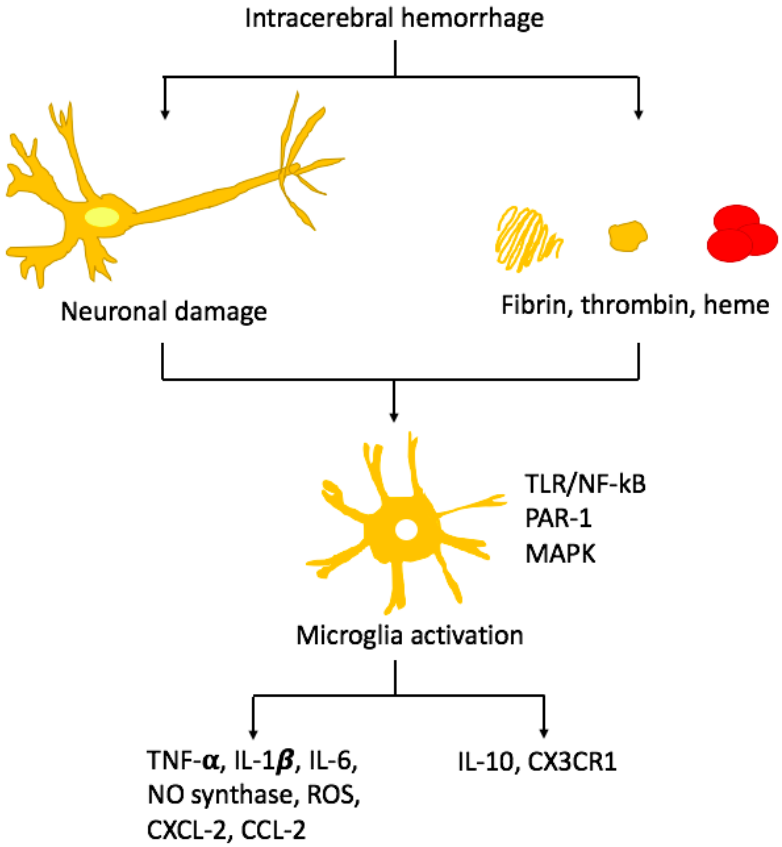

Figure 11. Microglial (cerebral resident macrophage) activation and the release of pro-inflammatory molecules after Intracerebral hemorrhage.
This figure is designed by the present author © Fatima Alzahra Al Hamed, using the information presented by Mracsko, E., and R. Veltkamp in the review article (Mracsko & Veltkamp, 2014).

2.4 Ischemic stroke modelling

In vivo stroke modelling using rats or mice have been used mostly in stroke research. However, few studies used in vitro cell culture modelling. It was reported that there are 10% differences in the genome between rodents and humans. It was illustrated that the expression of cytokines and chemokines could be different, which affects the binding of ligands to receptors. For example, MCP-5, CCL-6, and CCL-9 are expressed in mice but not humans. On the other hand, IL-8, MCP-4, CXCL-7, CCL-18, CCL-24, and CCL-26 are expressed in humans but not mice (Holloway & Gavins, 2016). These micro-differences play a critical role in the failure of human clinical trials even though successfully tested in animals. One example is TGN1412, in a clinical trial where CD28 superagonist antibody was tested in 6 healthy volunteers after safe use in animals. Although of a very small dose that was given to the volunteers, they suffered from a life-threatening condition and had a multiorgan failure. The reasons for these adverse results in humans were addressed, and it was discovered that the drug acted on different receptors in humans than those in animal models. A very important step that was missing before testing this drug in humans was the testing of the drug in an in-vitro human cell culture model. Using a human model of cell culture can reflect a real reaction of what can happen in the human body (Attarwala, 2010).

2.4.1 In-vitro ischemic stroke modeling

Ischemic stroke is caused by a blood clot that blocks a small blood vessel in the brain, causing a lack of oxygen and blood supply to that ischemic area. The in-vitro ischemic stroke model is performed by removing oxygen and glucose from cellular culture through different ways such as enzymatic, chemical, or physiological approaches. Enzymatic is performed using a glucose oxidase/catalase system.

Chemicals can be used to induce ischemic conditions such as antimycin, sodium azide, or rotenone. Physiological ischemic induction is based on performing oxygen and glucose deprivation (OGD) through replacing oxygen with nitrogen gas and normal glucose with glucose-free medium with maintaining a balanced salt solution (BSS) (Holloway & Gavins, 2016). The **aim** of **exposing** the **OGD** model to a **BSS** is not to promote growth but to **maintain** the **viability** of cells (Camós & Mallolas, 2010).

OGD duration can be performed to several hours from 1 up to 24 hours based on the experimental protocol. An option can be added, which is to return the culture to normal conditions as normoxia and normoglycemia to reflect the reperfusion effect as if it is in the brain. *In-vitro* stroke model can be made using either human cells or animal sources. The model of a human source can be a brain slice obtained from a cadaver or just primary cells extracted from that brain. Cells of human sources are usually difficult to obtain compared to animal sources. In contrast to primary human cells, immortalized human cell lines are readily available, and they can produce high throughput; however, cell lines don't reflect the physiological characteristics as primary cells do, such as blood-brain barrier cell adhesion molecules and enzymes. Human brain cells can be generated as well from stem cells, either embryonic or induced pluripotent stem cells (Holloway & Gavins, 2016).

Cell culture can be in a single culture of a monolayer of cells or co-culture of two different cell types or a 3-D cell culture system (Holloway & Gavins, 2016). Different brain cells can be cultured in the laboratory. They can be neurons, astrocytes, microglial cells, or microvascular endothelial cells. Different cell types can be cultured together to study ischemic stroke pathophysiology (Camós & Mallolas, 2010).

A blood-brain barrier model can be created as well using a co-culture system to study the consequences of ischemic injury. The BBB endothelial cells have unique characteristics that distinguish them from normal peripheral capillary's endothelium. The cerebral endothelial cells have a high number of mitochondria and a low number of transcytosis and endocytosis vesicles. They also lack fenestration and have complex tight junctions, which make them continuous and more resistant than peripheral endothelial cells. Some studies used the co-culture of endothelial cells with astrocyte or endothelial cells with neurons to study the BBB model. Furthermore, some studies used a combination of human cells and animal cells to create BBB (Camós & Mallolas, 2010).

2.4.2 In-vitro modeling using human cells

Zhang, W., et al. (1999) performed an OGD experiment on human cerebral endothelial cells (HCEC) and human fetal astrocytes (HFAS) separately. Cells were exposed to OGD for 4 hours and to reperfusion for 4, 16, and 24 hours. Cells were harvested, and the mRNA expression of IL-8 and MCP-1 was assessed by RT-PCR. Culture media were collected, and the levels of IL-8 and MCP-1 were assessed as well. ICAM-1 expression was assessed by immunohistochemistry, and its level was quantified by ELISA. Furthermore, the grade of neutrophil adhesion was assessed by fluorescence microscopy. Ischemia followed by reperfusion upregulated the gene expression to of IL-8 and MCP-1 as intracellularly or as proteins released in culture media (W. Zhang et al., 1999).

Furthermore, the surface expression of ICAM-1 was upregulated, and neutrophils adhesion was increased following ischemia/reperfusion condition. MCP-1 was expressed as 30 times higher in HFAS than in HCEC. In the same study, cells were exposed to IL-1β without ischemia/reperfusion, and the same results of

upregulation of ICAM-1 and neutrophil adhesion were found. In contrast to ischemia, IL-1β induced expression of MCP-1 and IL-8 in HCEC, as around 20 and 50 times, respectively, more than HFAS (W. Zhang et al., 1999).

Xiang, W. et al. (2017) reported that let-7 micro-RNA family's expression decreases in ischemic stroke patients. However, its expression increases after they receive the therapy of tissue plasminogen activator. Following their discovery, they did an ischemic in vitro model for human brain endothelial cells to investigate the role of let-7 miRNA. Let-7 miRNAs were decreased significantly after 6 hours of OGD. It was reported that high levels of let-7i increased cell survival, decreased their death, and their permeability significantly after OGD compared to controls. Furthermore, let-7i decreased expression of inflammatory biomarkers such as MMP-9 and inducible nitric oxide synthase (Katsanos et al.) through lowering TLR-4 expression. Moreover, silencing TLR-4 inhibited the effect of let-7i, which suggests that TLR-4 is the main target for let-7i (Xiang et al., 2017).

Zhang, Y., T.S. Park, and J.M. Gidday (2007) reported that exposing human brain endothelium to hypoxia of 2% Oxygen before performing OGD of anoxia (0% O_2) led to the release of p-survivin through PI3 kinase/Akt pathway. P-survivin protected cells from apoptosis and increased cell viability (Yunhong Zhang, Park, & Gidday, 2007).

Li, W. et al. (2016) performed a diabetic stroke model of human brain endothelial cell culture. The diabetic factor used was methylglyoxal, which is a product of glucose metabolism that gets elevated in diabetic patients and was proved to cause vascular damage. Methylglyoxal was reported to increase cell apoptosis after OGD, including caspase 3 and 8 expressions, ROS release, and NF-kB activation through Fas and FasL expression. The authors tested isorhamnetin, which was

reported to have a protective effect in hypertensive rats on the diabetic stroke model. Isorhamnetin proved to have a protective effect against the damage caused by both OGD and methylglyoxal. It showed an anti-oxidative, anti-inflammatory, and anti-apoptotic effect in diabetic stroke model (Li et al., 2016).

2.4.2.1 OGD conditions in different human cell studies

Different studies performed OGD experiments in different ways. Most studies used glucose-free media, or glucose-free balanced salt solutions such as Krebs, PBS, HBSS, or Earls solution in performing the OGD condition. Oxygen was absent or very low (0.05 – 1%). The duration of OGD ranged from 1-24 hrs.

Regarding the control condition, it was noticed that most studies used cells grown in growth media, which is known to have high glucose concentration ranging from 2 g/L (10 mM) to 4.5 g/L (25 mM). Few studies used the glucose concentration 0.9 - 1 g/L (5 - 5.5 mM), which reflects the normal level of the human being. Table 3 illustrates the details of each study.

Table 3. OGD conditions by different publications that used human cells.

Reference	Type of cells	Control condition	OGD condition
(W. Zhang et al., 1999)	Human brain microvascular endothelial cells and human fetal brain astrocytes	Krebs buffer supplemented with 5 mM glucose Normoxia (20% O2) Duration: 4 hrs.	Glucose-free Krebs solution containing in mM (119 NaCl, 4.7 KCl, 1.2 KH_2PO_4, 25 $NaHCO_3$, **2.5 $CaCl_2$**, **1 $MgCl_2$**) Hypoxia (95% N2, 5% CO2) Duration: 4 hrs.
(Allen, Srivastava, & Bayraktutan, 2010)	Human brain astrocyte and microvascular endothelial cells	5 mM glucose (No further details) Normoxia (75% N2, 20% O2, 5% CO2) Duration: 4/ 20 hrs.	No Details mentioned about the media Hypoxia (94.95% N2, 5% CO2, 0.05 O2) Duration: 4/ 20 hrs.
(Liao et al., 2016)	HUVEC	Growth media: high glucose DMEM (containing: 4.5 g/L = **25 mM**) Normoxia (95% air, 5% CO2)	Earls balanced salt solution Duration: 4 hrs.

Reference	Type of cells	Control condition	OGD condition
(Shi et al., 2016)	Primary Human brain microvascular endothelial cells	Growth media: EGM-2 MV Normoxia (95% air, 5% CO2)	Glucose-free media Hypoxia (95% Argon, 5% CO2) Duration: 1 hr.
(Niego et al., 2017)	Primary Human brain microvascular endothelial cells	Growth media: Brain endothelial cell growth media 2 Normoxia (20% O2, 5% CO2)	Glucose- and Serum-free DMEM/F12 media Hypoxia (95% N2, 5% CO2)
(Zhu et al., 2010)	Primary human brain astrocytes, and microvascular endothelial cells	Growth media: Astrocyte-conditioned media	Glucose-free Krebs solution Hypoxia (<1% O2)
(Li et al., 2016)	Primary Human brain microvascular endothelial cells	Growth media: RPMI-1640 Normoxia (5% CO2)	Glucose-free RPMI-1640 Hypoxia (95% N2, 5% CO2) Duration: 3 hrs.
(Abdulkadir, Alwjwaj, Othman, Rakkar, & Bayraktutan, 2020)	Human brain astrocytes, pericytes and microvascular endothelial cells	Growth media: Relevant specialized media Normoxia (75% N2, 20% O2, 5% CO2)	Glucose-free DMEM Hypoxia (94.95% N2, 5% CO2, 0.05% O2) Duration: 4 hrs.
(Xin & Jiang, 2017)	Primary Human brain microvascular endothelial cells	Growth media: CSC media include glucose and serum Normoxia (5% CO2, humidity>95%)	Glucose- and serum-free media Hypoxia (95% N2, 5% CO2, <1% O2) Duration: 4 hrs.
(Xiang et al., 2017)	Human brain microvascular endothelial cells	Growth media: complete media for endothelial cells Normoxia (5% CO2)	Glucose-free DMEM Hypoxia (94% N2, 5% CO2, 1% O2) Duration: 6 hrs.
(Cowan & Easton, 2010)	Human brain endothelial cell line hCMED/D3	Growth media: Complete EGM-2MV media Normoxia (5% CO2)	Glucose-free PBS Glucose-free DMEM Hypoxia (95% N2, 5% CO2)
(Slevin et al., 2009)	Primary Human brain microvascular endothelial cells	Not explained	Glucose-free media Anoxia (95% N2, 5% CO2) Duration: 24 hrs.
(S. Guo, Stins, Ning, & Lo, 2010)	Human brain microvascular endothelial cell line	Not explained	Glucose-free DMEM Hypoxia (90% N2, 5% H2, 5% CO2) Duration: 6 hrs.
(X. Yang, He, Li, & Xu, 2017)	HUVEC	Growth media: (M199)	Glucose-free balanced salt solution Hypoxia (95% N2, 5% CO2) Duration: 3 hrs.
(Yunhong Zhang et al., 2007)	Human brain microvascular endothelial cells	Not explained	Serum-free HBSS Hypoxia (95% N2, 5% CO2) Duration: 8 hrs.

Reference	Type of cells	Control condition	OGD condition
(Stanimirovic, Shapiro, Wong, Hutchison, & Durkin, 1997)	Human brain microvascular endothelial cells	Growth media (M199)	Glucose-free Krebs solution containing in mM: (119 NaCl, 4.7 KCl, 1.2 KH_2PO_4, 25 $NaHCO_3$, **2.5 $CaCl_2$**, **1 $MgCl_2$**) Hypoxia (95% N2, 5% CO2)

2.4.3 In-vitro modeling using animal cells

Song, J. et al. (2014) studied the effect of melatonin on the ischemic stroke model of murine brain endothelial cells. Melatonin is a sleeping hormone that is produced by pineal glands, and it proved in other studied to play a protective role against brain injury and apoptosis after hypoxia. In the study of Song, J. et al., cells were exposed to melatonin of different concentrations (1-100 nM) for 24 hours, then cells were washed with PBS, and media was replaced by glucose-free media and cells were incubated in the anoxic chamber for 6 hours. Cells were transferred to normal growth conditions for 18 hours to represent reperfusion injury. Melatonin reversed the cell injury caused by OGD as represented by increasing cell viability, decreasing cytotoxicity and apoptosis, decreasing ROS production, **increasing tight junctions (claudin-5) expression which preserve BBB from permeability, decreasing VEGF expression which plays a role in permeability**, activating Akt and deactivating JNK which protect against inflammation and apoptosis, and downregulating Bax protein which has a role in mitochondrial apoptosis (Song et al., 2014).

Liao, L.-X. et al. (2016) investigated the effect of 2,4,5-trihydroxybenzaldehyde (Shalia et al.) on the ischemic model of Bend.3 mouse brain cell line. THBA is a plant extract that proved to have an anti-oxidative effect. In this study, THBA increased cell viability after OGD, decreased apoptosis, decreased lactate dehydrogenase release, decreased the level of active cleaved caspase-3 and

PARP, and increase Bcl-2 transcription, which protects against apoptosis. Furthermore, THBA downregulated miR-34a, which plays a role in the degradation of Bcl-2. Therefore, it was suggested that THBA increase Bcl-2 through targeting miR-34a, thus protecting mitochondrial membrane potential and increasing cell survival (Liao et al., 2016).

2.4.3.1 OGD conditions in different animal cell studies

Most studies used glucose-free media, or glucose-free balanced salt solutions, PBS, or HBSS as an OGD condition. One study used a low level of glucose that was below the normal condition of a human being (0.2 g/L / 1.11 mM), which was another way to do OGD (Gong, Li, Zou, Tian, & Xu, 2019). Another study used a DMEM media that is featured by low glucose. However, this type of media has glucose concentration as (1 g/L / 5.5 mM), which does not reflect the real type of OGD (Milner et al., 2008). Oxygen level was absent or very low (0.02 – 2%). The duration of OGD here ranged from 1-18 hrs. Similar to human studies, few studies used control cells exposed to the normal level of glucose 0.9 - 1 g/L (5 – 5.5 mM), which reflects the normal human being. Most studies used cells grown in growth media, which is known to have high glucose concentration ranging from 2 g/L (10 mM) to 4.5 g/L (25 mM). Table 4 illustrates the details of each study.

Table 4. OGD conditions in literatures of animal cells.

Reference	Type of cells	Control condition	OGD condition
(Kaneko, Tajiri, Shojo, & Borlongan, 2014)	Primary rat neural cells	Glucose (5 mM) buffer containing in mM (5 glucose, 116 NaCl, 5.4 KCl, 0.8 $MgSO_4$, 1 NaH_2PO_4, 26.2 $NaHCO_3$, 0.01 glycine, 1.8 $CaCl_2$, with pH 7.4) Normoxia (5% CO2)	Glucose-free buffer containing in mM (116 NaCl, 5.4 KCl, 0.8 $MgSO_4$, 1 NaH_2PO_4, 26.2 $NaHCO_3$, 0.01 glycine, 1.8 $CaCl_2$, with pH 7.4) Hypoxia (95% N2, 5% CO2) Duration: 1.5 hrs.
(Jessick et al., 2013)	Primary rat neuronal cells	Growth media: Neurobasal A media Normoxia	PBS solution containing in mM (1.73 NaCl, 2.7 KCl, 10 mM Na_2HPO_4, 1.7 KH_2PO_4, 0.5 **$CaCl_2$, 1 $MgCl_2$** with pH 7.4) Hypoxia (85% N2, 5% H2, 10% CO2) Duration: 2 hrs.
(Yuan Zhang et al., 2016)	Mouse brain microvascular endothelial cells (bEND.3 cells)	Growth media: DMEM Normoxia (95% air, 5% CO2)	Glucose-free DMEM Hypoxia (95% N2, 5% CO2) Duration: 1, 3, 6 hrs.
(Tornabene, Helms, Pedersen, & Brodin, 2019)	Bovine brain microvascular endothelial cells and rat astrocytes	Growth media: Differentiation media (DM-TES) with **25 mM** glucose Normoxia (90% room air, 10% CO2)	Glucose-free DM-TES Hypoxia (89% N2, 10% CO2, 1% O2) Duration: 4 hrs.
(S.-L. Chen et al., 2017)	Murine brain microvascular endothelial cells (bEND.3 cells)	Growth media: DMEM Normoxia (5% CO2)	Glucose-free balanced salt solution (BSS) Hypoxia (0.1% O2) Duration: 6 hrs.
(Milner et al., 2008)	Mouse Primary brain endothelial cells and astrocytes	Growth media: high glucose DMEM (4.5 g/L = **25 mM**) Normoxia (5% CO2) Duration: 18 hrs.	Low glucose DMEM (1 g/L = **5.5 mM**) Hypoxia (95% N2, 5% CO2) Duration: 18 hrs.
(Song et al., 2014)	Murine brain microvascular endothelial cells (bEND.3 cells)	Culture media: DMEM Normoxia (5% CO2)	Glucose-free balanced salt solution Hypoxia (0.1% O2) Duration: 6 hrs.
(Yin et al., 2010)	Mouse brain endothelial cells	Culture media: DMEM Normoxia	Glucose-free HBSS Hypoxia (95% N2, 5% CO2) Duration: 4, 15 hrs.
(Liu, Song, Liu, Zhang, & Zuo, 2003)	PC12 rat adrenal medulla cell	Growth media: high glucose DMEM (4.5 g/L = 25 mM) Normoxia (90% air, 10% CO2)	Glucose-free DMEM Hypoxia
(J. Xu et al., 2000)	Bovine brain endothelial cells	Normoglycemic with no further details	Glucose-free HBSS Hypoxia (85% N2, 10% H2, 5% CO2, 0.02-0.2% O2) Duration: 1-8 hrs.

Reference	Type of cells	Control condition	OGD condition
(Alluri et al., 2014)	Primary rat brain microvascular endothelial cells	Growth media: complete DMEM Normoxia (95% room air, 5% CO2)	Glucose-free DMEM Hypoxia (95% N2, 5% CO2)
(Sun et al., 2019)	Mouse brain endothelial cell line (bEND.3 cells)	Growth media: high glucose DMEM (4.5 g/L = 25 mM) Normoxia: normal atmosphere Duration: 24 hrs.	Glucose-free DMEM Hypoxia (95% N2, 5% CO2) Duration: 6 hrs.
(Song et al., 2014)	Murine brain endothelial cells (bEND.3 cells)	Culture media: DMEM Normoxia (5% CO2)	Glucose-free balanced salt solution Hypoxia (0.1% O2) Duration: 6 hrs.
(Gong et al., 2019)	Rat microvascular endothelial cells	Growth media: M131 media Normoxia (95% air, 5% CO2)	Low glucose media (**0.2 g/L** = **1.11 mM**) Hypoxia (95% N2, 5% CO2) Duration: 4 hrs.
(Narasimhan, Liu, Song, Massengale, & Chan, 2009)	Mouse brain endothelial cells	Growth media: M199 Endothelial cell medium Normoxia: (95% air, 5% CO2)	Glucose-free buffered salt solution Anaerobic Duration: 8 hrs.

Chapter 3: Methodology

3.1 Materials

3.1.1 Cells

Primary Human Brain Microvascular Endothelial Cell of passage 3 – cell system with catalog number ACBRI 376 - was used in this research.

3.1.2 Media and reagents used for cell culture

The following reagents with their catalogue number were provided from Cell System, USA. Complete Classic Media (that contains 2.84 g/L (15.76 mM) glucose, with different amino acids, vitamins, and inorganic salts such as Ca++ and Mg++) with Serum and Culture Boost with catalogue number (4Z0-500). Complete Medium formulated at Normal Blood Glucose (that contains 0.901 g/L (5 mM glucose, with different amino acids, vitamins, and inorganic salts such as Ca++ and Mg++) with Serum and Culture Boost with catalogue number (4N0-500). Culture boost (Growth factors) with a catalogue number (4CB-500). Bac-off (Antibiotic) with catalogue number (4Z0-642). Attachment factor with catalogue number (4Z0-201). Cell freezing medium with catalogue number (4Z0-705). Passage Reagent Group (PRG) which contains 3 reagents: PRG-1: (EDTA-dPBS Solution) , PRG-2: (Trypsin 0.06% /EDTA-dPBS Solution), PRG-3: (Trypsin Inhibitor-dPBS Solution) with catalogue number (4Z0-800).

Other reagents were provided by other companies. Penicillin streptomycin (Antibiotic: Pen Strep) was provided by Gibco, USA with catalogue number (15140-122). Trypsin 10X (2.5%) solution (that was EDTA-free) was provided from sigma with catalogue number (59427C). Fetal Bovine Serum (FBS) was provided from ATCC with catalogue number (0523). EDTA 0.5 M pH 8.0 was provided from Thermo fisher scientific, Invitrogen, Lithuania, with catalogue number (AM9260G).

RPMI Medium 1640 (1X) with L-glutamine (that contains (2 g/L or 11.11 mM) glucose, with different amino acids, vitamins and inorganic salts such as Ca++ and Mg++) was provided from Gibco with catalogue number (21875-034).

Dulbecco's Phosphate Buffered Saline (DPBS: 1X) with $CaCl_2$ and $MgCl_2$ was provided by Gibco with catalogue number (14040-117). PBS (without $CaCl_2$, or $MgCl_2$) was provided from Gibco, USA with catalogue number (10010023). Normal physiological Saline for hospital use (NaCl 0.9% w/v intravenous infusion B.P.) was provided locally by Qatar Pharma or Kuwait Saudi Pharmaceutical Industries Co.

3.1.3 Reagents and kits

Trypan Blue stain (0.4%) was provided by Gibco – Life Technologies – with catalogue number (15250-061). Live/Dead (Viability/Cytotoxicity) stain kit that contains: Ethidium Homodimer-1, and Calcein – AM stains was provided by ThermoFischer Scientific - Life Technologies, USA with catalogue number (L3224). Tali Apoptosis kit that contains: Annexin V Alexa Flour 488 (Annx V): 20X, Propidium Iodide (PI): 100 μg/mL, and Annexin Binding Buffer (ABB): 1X, was provided from Thermo fisher scientific – Invitrogen, USA with catalogue number (A10788). Tali cellular analysis slides were provided from Thermo fisher scientific, Invitrogen with catalogue number (T10794). Vybrant TM MTT cell proliferation assay kit was provided from Thermo fisher scientific, Invitrogen with catalogue number (V13154). DMSO (Dimethyl sulfoxide), anhydrous was provided from Thermo fisher scientific, Invitrogen, USA, with catalogue number (D12345). Triton – 10% in H_2O was provided from Sigma with catalogue number (93443).

Paraformaldehyde (PFA) powder was provided from Sigma-Aldrich, Germany, with catalogue number (P6148). Paraformaldehyde (4%) solution in PBS was provided from Santa Cruz Biotechnology with catalogue number (sc-281692).

Dapi stain was provided from Sigma-Aldrich with catalogue number (D9542-10MG). AlexaTM Flour 488 Phalloidin (F-actin stain) was provided by Thermo fisher scientific, Life technologies, USA with catalogue number (A12379). Bovine Serum Albumin (BSA) was provided from Thermo fisher scientific, Invitrogen, USA, with catalogue number (15561020). ProLong Diamond Antifade Mountant – (Gel mount) was provided from Molecular Probes by life technologies – Fischer scientific - USA, with catalogue number (P36961).

TRizol Reagent – RNA lysis solution - was provided from Life Technologies, USA, with catalogue number (15596018). Chloroform was provided from Sigma-Aldrich with catalogue number (650498-1L). Isopropyl Alcohol was provided from VWR with catalogue number (UN1219). Absolute Ethanol was provided from Honeywell, Research Lab, scharlab with catalogue number (32221, 0671A, ET00052500). Nuclease-free water was provided from Qiagen with catalogue number (129114). Diethyl PyroCarbonate was provided from Sigma with catalogue number (D5758). Superscript IV Vilo Reverse transcription master mix - cDNA synthesis was provided by Thermofischer, Lithuania, with catalogue number (11756050).

RT2 SYBR Green ROX qPCR Master Mix – for RT profiler PCR array was provided from Qiagen, USA with catalogue number (330523). Human Inflammatory cytokines and receptors - RT_2 Profiler PCR array was provided from Qiagen, USA with catalogue number (PAHS-011ZA-12). Human Angiogenesis - RT_2 Profiler PCR array was provided from Qiagen, USA, with catalogue number (PAHS-024ZA-12).

3.1.4 Instruments

Hypoxia Chamber for cells was used (BioSpherix, USA with catalogue numbers ProOx 110, ProCO2 120). Tali image-based cytometer (Invitrogen, USA catalogue number (T10791). Olympus Fluorescence microscope with ZEN program

(Olympus with, USA). Microplate reader – for MTT assay – was provided from BioTek, USA, with catalogue number (EPOCH2). Nanodrop Lite Spectrophotometer model (ND-LITE)from Thermo-Fischer Scientific, a USA model. Pro-flex PCR – for cDNA synthesis using IV Vilo from Applied Biosystem, Thermo-Fischer Scientific, USA.. Real Time PCR system 7500 – for microarray from Applied Biosystems - Life Technologies, USA.

pH meter (Orion Star A111) from Thermo-Fischer Scientific, USA. Dry bath (FB15103) from Thermo-Fischer Scientific with the catalogue number. Universal 320 R Centrifuge for 15 mL conical tubes from Hettich, USA. MicroCL 17 R Centrifuge for Eppendorf tubes (ThermoFischer Scientific, USA). MiniSpin (Eppendorf, Germany). Centrifuge 5810R for RT-Profiler PCR arrays (Eppendorf, Germany).

3.1.5 Lab Supplies

T-75 cm^2 flasks were provided by VWR /Thermo-Scientific, with catalogue number (734-2314 /156472). T-25 cm^2 flasks were provided by Falcon, with catalogue number (353082-353109). Cell culture dishes (surface area: 21 cm^2 – diameter: 60 mm) were provided by Sigma with catalogue number (SIAL0166). 6-well plate was provided by Sigma, USA, with catalogue number (SIAL0516). 96-well plate was provided by Thermo-Scientific with catalogue number (167425). Cell scraper was provided by BD Falcon, catalogue number (353085). Hemocytometer (Glasstic slide 10 with Grids, combination coverslip-microscope slides) was provided by Kova, USA, catalogue number (87144).

50 mL conical tubes were provided by VWR/Falcon with catalogue number (89039-656/ 352070). 15 mL conical tubes were provided by Corning/Falcon with catalogue number (430052/ 352099). Cryogenic tubes were provided by Nalgene with catalogue number (5000-0020). Eppendorf or Microcentrifuge tubes were provided by

VWR with catalogue number (20170-038). Polystyrene round bottom tubes with volume of 5 mL were provided by BD Falcon with catalogue number (352054). PCR 8-well tube strips without caps were provided by VWR with catalogue number (20170-002).

Electronic Pipette was provided by CAPP with catalogue number (M10-1). 2 mL serological pipette was provided from Falcon with catalogue number (356507). 5 mL Serological pipette was provided from Thermo-Scientific with catalogue number (170355). 10 mL Serological pipette was provided from Thermo-Scientific with catalogue number (170356). Filter tips of 10 μL volume with filter was provided from VWR with catalogue number (732-1486). Filter tips of 200 μL volume was provided from Thermo-Scientific with catalogue number (Art 200 S*2069-HR). Filter tips of 1000 μL volume was provided from Thermo-Scientific with catalogue number (Art 1000 REACH S*2079-HR).

3.2 Methods

3.2.1 Media preparation

Complete Classic Media (C.M) which contains 2.84 g/L (15.76 mM) glucose and Complete Normal Glucose (N.G) Media, which contains 0.901 g/L (5 mM) were prepared according to the manufacture's protocol provided. The bottle of 500 mL of media (either C.M or N.G) was activated by growth factors of 10 mL culture boost and an antibiotic added as 1 mL bac-off or 5 mL pen-strep. The media (C.M or N.G) was aliquoted into around 12 conical tubes of 50 mL and frozen in -20°C until time of use. Once needed, the aliquoted conical tube was thawed and kept in the fridge at 4°C for a 1-month maximum.

3.2.2 Culture of primary human brain microvascular endothelial cell

The vial of Primary human brain Microvascular Endothelial Cell (PHBMEC) was grown in T-75 cm^2 flask. The vial started in passage 4. An amount of 5 mL of attachment factor was applied into a sterile T-75 cm^2 flask for 10 seconds, and then it was aspirated back to its bottle to be reused. An amount of 14 mL of warm, classic media was dispensed into the flask and then incubated in a normal CO_2 incubator at 37°C (5% CO_2, 20% O_2 with Humidity 85%-95%). The frozen vial was thawed quickly, and the cell suspension was added to 14 mL chilled classic media in a conical tube. It was centrifuged at 900 rcf, 4°C, for 10 min. The supernatant was discarded, and 60-100 mL of warm culture boost was added over the pellet, the tube was flicked by the finger, then 1 mL of classic media was added and pipetted up and down to break down the cell pellet. The cell suspension was added to the prepared flask, and it was a slide on the surface as east-west-north-south, to ensure equal distribution of the

cells over the flask surface. It was incubated for 24 – 48 hours until having 80-90% of confluency. The media was changed after 24 hours or every other day.

3.2.2.1 Passaging and freezing cells

Once T-75 cm^2 is confluent by 80-90%, cells were prepared for passage or freezing. Cells were grown to passage numbers of 5, 6, and 7, where each cell passage was frozen in a separate vial. T-75 cm^2 or T-25 cm^2 was prepared, as indicated in the previous section, with regard that T-25 cm^2 needs 4 mL classic media. T-75 cm^2 flask was split into a 1:4 ratio. The freezing medium was chilled on ice. The old media of confluent T-75 cm^2 was discarded, and the flask was washed by 5 mL warm PRG-1 or by saline and then discarded. 5 mL of warm PRG-2 or 1X (0.25%) trypsin was added to the flask, and then it was observed under the microscope until cells detached. Trypsin was inhibited by 5 mL of chilled PRG-3 or by 20-30% of Fetal Bovine Serum (FBS) diluted in saline. The suspension was pipetted up and down over the surface, and then it was collected in a conical tube labelled with freezing. Part of the suspension, around 2 mL, was aspirated and collected in another conical tube labelled with the passage. They were centrifuged at 900 rcf, 4°C, for 10 min. The cells for passage number were resuspended by media, as indicated in the previous section, and then dispensed in the prepared flask. For freezing, the supernatant was discarded, and the cell pellet was resuspended with 3 mL of freezing medium and collected in 3 cryogenic vials. The vials were stored in a frosty container at -80°C for 24 hours to freeze it gradually, then transferred to a labelled box in -80°C freezer.

Cell count was performed before culturing or sub-culturing PHBMEC using trypan blue. A volume of 10 µl cell suspension was mixed with 10 µl of trypan blue, and 10 µl of this mixture was loaded onto to hemocytometer and counted under a

microscope. Cells were counted in all 9 squares, and the below formula was used to retrieve the total number of cells:

{Total no. of cells counted x 2(dilution factor) ×10,000} / 9 (no. of squares)

3.2.2.2 Human-like pre-conditioning

Cells were passaged from T-25 cm^2 flask into 2 or more Petri dishes. The seeding density for each dish was around 170,000 – 180,000 cells. The cells were cultured under normal conditions 5% CO_2, 20% O_2, and in normal glucose media for 17-24 hours prior to the experiment. Around 1-2 mL of warm attachment factor was applied to a Petri dish for 10 seconds. 2 mL of warm Normal glucose media was added to each petri dish and kept in the incubator with 37°C. Cells were passaged as indicated earlier, and the cell pellet was activated by 60-70 mL of culture boost. The cell pellet was resuspended with 2 mL or more of warm normal glucose media. Cells were counted prior to transfer them to the dishes. Around 0.5-1 mL was applied to each petri dish based on the counting, then they were incubated for 17-18 hours until reaching 60-80% confluency.

3.2.2.3 Oxygen Glucose Deprivation (OGD)

Once the PHBMEC reached 60-80% confluency, petri dishes were divided into two groups; Control and OGD. Passages of 6, 7, and 8 were used. Prior to the experiment, petri-dish was washed by saline or PBS to remove any traces of old media or dead cells, then new fresh media was added and were incubated for at 37°C for 2-3 hours.

Control group was incubated in complete medium formulated at normal blood glucose from cell system (4N0-500) that contains (0.901 g/L (5 mM) of glucose, with growth factors and different nutrients such as amino acids, vitamins, and inorganic salts such as Ca++ and Mg++), and under the normal level of oxygen (20%).

OGD group was cultured in conditions with partial/complete deprivation of nutrients, glucose, and growth factors and constantly in the presence of low oxygen tension (1.0%) by the Biospherix chamber for time duration of 2 hours. Details about OGD experiments that were performed are illustrated as follow:

1- Partial deprivation of glucose and nutrients using 2 mM glucose media, prepared by dilution of normal glucose (N.G) media (5 mM) from cell system (4N0-500) by either PBS/saline as a ratio of 0.4 (20 mL of N.G media to total 50 mL PBS/saline) as illustrated as follow:
    a. 2 mM glucose media diluted in PBS **with** Ca++ and Mg++
    b. 2 mM glucose media diluted in PBS **without** Ca++ and Mg++
    c. 2 mM glucose media diluted in normal Saline (without Ca++, Mg++ and no buffer system)
2- Partial deprivation by absence of glucose and other nutrients (growth factors, different nutrients such as amino acids, vitamins), cells were incubated in:
    a. PBS **with** Ca++ or Mg++
    b. PBS **without** Ca++ and Mg++
3- Partial deprivation by the absence of Growth factors only using:
    a. RPMI media (that **lacks** growth factors, **but** contains (2 g/L or 11.11 mM) glucose, with different amino acids, vitamins and inorganic salts such as Ca++ and Mg++)
4- **Complete deprivation** with an absence of glucose, growth factors, different nutrients such as amino acids, vitamins, and different inorganic salts such as Ca++ and Mg++). This model was abbreviated as (Oxygen Nutrients Deprivation: OND) and was incubated in:
    a. Normal isotonic saline, without Ca++, Mg++ or buffer system

Since different types of PBS/saline were used, and cells react differently to them, compositions of PBS/saline are illustrated in Table 5.

Table 5. Composition of PBS/saline used for dilution of media.

Reagents	Catalogue number	Composition	Concentration
PBS (**without** CaCl2, or MgCl2)	Gibco: 10010023	Potassium Phosphate monobasic (KH2PO4)	1.54 mM
		Sodium Chloride (NaCl)	**155.2 mM**
		Sodium Phosphate dibasic (Na2HPO4-7H2O)	2.71 mM
Dulbecco's Phosphate Buffered Saline (DPBS: 1X) **with CaCl2 and MgCl2**	Gibco: 14040-117	**Calcium** Chloride (**CaCl2**) (anhyd.)	0.9 mM
		Magnesium Chloride (**MgCl2**-6H2O)	0.49 mM
		Potassium Chloride (KCl)	2.67 mM
		Potassium Phosphate monobasic (KH2PO4)	1.47 mM
		Sodium Chloride (NaCl)	**137.9 mM**
		Sodium Phosphate dibasic (Na2HPO4-7H2O)	8.05 mM
Normal saline (Physiological Intravenous infusion)	Provided locally by Qatar Pharma or Kuwait Saudi Pharmaceutical Industries Co.	Sodium Chloride (NaCl)	**154 mM**

3.2.3 Viability test analysis

The aim was to investigate the severity of cell injury by different types of OGD and OND that can be illustrated by a marked increase of death. Different techniques were applied in order to figure out which one would be the best for our model.

3.2.3.1 Live/ Dead stain analysis

Control and OGD experiment were performed as mentioned earlier in section 3.2.2.2 and 3.2.2.3. Here, the OGD condition was selected to be as a partial deprivation (2 mM glucose media). It was prepared by dilution of normal glucose (N.G) media (5 mM) by PBS with Ca++ and Mg++ as a ratio of 0.4 (20 mL of N.G with 30 mL PBS = total 50 mL). After incubation of **3 hours**, cells were washed by PBS, then 1-2 mM of Live/dead stain (from ThermoFischer Scientific - Life Technologies, USA with catalogue number: L3224) was added and incubated at room temperature for 20-30 min. The stain was prepared by diluting Calcein-AM and Ethidium Homodimer-1 as (5 μL and 40 μL) in total 10 mL of PBS. The stain preparation was optimized for this type of cell using methanol fixed cells as dead cells. The final concentration optimized was 2 μM for Calcein and 8 μM for Ethidium Homodimer-1. Finally, the stained cells were analyzed by Olympus Fluorescence microscope (IX73). Live/dead stain wasn't applicable to be used for optimization for this type of experiment. Thus, different viability techniques were followed as explained in the next section. The results of this section are illustrated in the Appendix with a justification for the reason not to use this in the optimization procedure.

3.2.3.2 Apoptosis and Death analysis

The aim here was to implement different models of OGD to investigate which one would cause severe injury within 2 hrs., to mimic acute ischemic stroke. Control and OGD were performed as mentioned earlier in sections 3.2.2.2 and 3.2.2.3. Control was incubated in 5 mM glucose media, in normoxia (20%) for 2 hrs. OGD experiment was performed in different conditions as illustrated as follow:

- OGD 1: 2 mM glucose media in PBS **with** Ca++ and Mg++, hypoxia for 2 hrs.
- OGD 2: 2 mM glucose media in PBS **without** Ca++ or Mg++, hypoxia for 2 hrs.
- OGD 3: 2 mM glucose media in **saline**, hypoxia for 2 hrs.
- OGD 4: PBS **with** Ca++ and Mg++, hypoxia for 2 hrs.
- OGD 5: PBS **without** Ca++ or Mg++, hypoxia for 2 hrs.
- OGD 6: RPMI media **without** growth factors, hypoxia for 2 hrs.
- **OND** model: Saline, hypoxia for 2 hrs.

3.2.3.2.1 Detachment protocol

After incubation of 2 hours, control and OGD cells were washed by PBS/saline. All types of OGD cells were detached by standard 1X (0.25%) trypsin **(that was EDTA-free)** except for the OND model that was incubated in saline, which did not respond to trypsin and was detached by cell scraper. Cells of OND in saline tend to attach firmly to the plate and not affected by trypsin, which in contrast, trypsin, caused detachment of the control cells.

For trypsinization protocol for OGD models, old media was collected in a conical tube, cells were washed by 2 mL of warm PBS/saline, and it was collected in the same tube, then 2 mL of warm trypsin diluted in saline as 1X (0.25%) concentration was added to the cells, and they were observed under the microscope until cells become rounded, then 2 mL of chilled 20-30% FBS diluted in saline was added. The suspension was pipetted up and down to collect cells over the surface, and then it was collected in the same tube. Cells were centrifuged for 10 min., with 900 rcf speed at 4°C. After centrifugation, the supernatant was discarded, and the apoptosis test was performed on the cell pellet.

For scraping protocol of OND model, old media was collected in a conical tube, 2 mL of warm media/saline was added, cells were scraped gently by passing it once over the plate, it was observed under the microscope to ensure detachment, then 2 mL of chilled 20-30% FBS was added, the suspension was pipetted up and down over the surface to collect the cells, then it was collected in the conical tube. Cells were centrifuged for 10 min., with 900 rcf speed at 4°C. After centrifugation, the supernatant was discarded, and the apoptosis test was performed on the cell pellet.

3.2.3.2.1.1 Understanding the mechanism beyond the firm attachment of cells under OND model

Since it was noticed that cells cultured in saline **were not responding well** to trypsin, different concentrations of trypsin (1X and 2X) with EDTA of 10 mM were used to investigate whether cells would respond to trypsin and EDTA together. A concentration of 10 mM EDTA was prepared by diluting 200 mL of 0.5 Molar EDTA in a total of 10 mL Saline. Different concentrations of trypsin as 1X (0.25%) and 2X (0.5%) were prepared by diluting 1 and 2 mL of 10X trypsin in a total of 10 mL Saline.

After incubation of cells in saline for 2 hrs., cells were washed by warm saline (37^{0}C) and warm EDTA-trypsin, that was prepared, was applied onto the cells to observe if detachment would happen. Observations were that few cells tend to detach under 10 mM EDTA – **1X** trypsin, but not 10 mM EDTA – 2X trypsin after a long time of incubation reaching 15 min. This raised a question that EDTA could help in detachment but not trypsin itself. As with the increase in trypsin concentration (2X) and with the same EDTA level (10 mM), cells tend to be resistant as the same reaction to previous 1X trypsin (that was EDTA-free) that was used. It was concluded that although few cells tend to detach by the model of 10 mM EDTA – **1X** trypsin,

still this technique was not applicable to be used as most of the cells did not detach, and different concentrations of EDTA-trypsin must be applied to figure out which one could help in complete detachment of the cells.

Furthermore, the question was raised about whether the absence of glucose factor only would make this firm attachment of the cells. Therefore, 18 mg of glucose powder was dissolved in 50 mL saline as a concentration of 2 mM, and cells were cultured under this condition for 2 hrs., then trypsinization technique was applied. However, cells were still firmly attached with glucose factor only. It was concluded that absence glucose alone doesn't play a role in firm attachment and there are other factors such as; Ca++ or Mg++ or buffer system, that their absence plays a role in firm attachment of the cells.

Thus, it was concluded that some changes happened in the cell membrane of the OND model that made them not responding to trypsin and these changes must be investigated in another study to figure out the reason behind it. Finally, and in order to facilitate the ongoing project, cell scraper was used as a detachment procedure for the OND model in order to assess cell viability.

3.2.3.2.2 Apoptosis staining

Apoptosis was used as an optimization procedure for different types of OGD and OND. Tali® Apoptosis Kit - Annexin V Alexa Fluor® 488 & Propidium Iodide (Life Technologies USA A10788) was used in this analysis with the modification of the manufacturer's protocol. The assay for apoptosis was performed using the Tali® Image Cytometer (Life Technologies USA). Apoptosis kit was validated by testing it on DMSO treated cells (a frozen vial of cells that was thawed and used) to investigate if viability results are reliable.

Reagents were prepared ahead of time. They were vortexed very well, then Annexin Binding buffer (ABB) was aliquoted as 1000 μL in each 3 Eppendorf tubes. Annexin V (AnxV) stain was diluted as 50 μL per 1000 μL ABB in one tube. The Propidium Iodide (PI) stain was diluted as 10 μL per 1 tube. The third tube was kept as a buffer only to be used for unstained control or for the wash.

After centrifugation using either trypsinization or scraping technique, the supernatant was discarded, and the cell pellet was resuspended by 100 μL of (Annx V) stain solution for both control and OGD tubes. One extra tube was prepared as unstained control and was resuspended with ABB buffer only. Cells of trypsinization technique were pipetted up and down while cells of scraping technique were vortexed to break down cells aggregates and facilitate making the suspension.

The cell suspension was transferred to labelled Eppendorf tubes and incubated in the dark for 20 min., at room temperature (RT). Cells of control and OGD were centrifuged at 200 rcf for 2 min., at RT. The supernatant was discarded, and the cell pellet was resuspended with 100 μL of (PI) stain solution. Cells were incubated in the dark for 5 min., at RT. Cells were centrifuged at 200 rcf for 2 min., at RT. The supernatant was discarded, and the cell pellet was resuspended with 100 μL of ABB buffer. Cells were washed 3 times by centrifugation and resuspension with 100 μL of ABB buffer.

It was analyzed by Tali-cytometer using Tali slides. An amount of 25 μL of unstained control was applied to the slide and analyzed by choosing the maximum number of fields as 20. Cells were gated to include only the size of 5-21 μm of cells, and the Relative Fluorescent Unit (RFU) was managed to exclude the false signal of both Annx V and PI stain. A prepared Tali slide for control and OGD is analyzed by Tali using the unstained control as a negative control.

3.2.3.3 MTT viability test

MTT was performed as an extra experiment in order to confirm the results of apoptosis for the OND model. However, the results of MTT concluded that this technique wasn't applicable to be used for this model (OND) as cells resembled nonresponsive to this type of stain. Cells kept intact and not absorbing MTT, although they were alive and still attached, refer to the Appendix for pictures of cells under microscope after MTT incubation. Although an optimization was performed to enhance cells of OND to absorb MTT, yet cells tend not to respond. Therefore, this was a second issue, along with trypsinization, that to be considered for investigation in future studies in order to understand the mechanism beyond it. For further details, and for possible interpretation of such result, refer to the Appendix.

The procedure of OND was followed, as explained previously, but few modifications using a 96-well plate. Three different passages (P7-P9) of frozen vials were thawed, cultured in 3 flasks of T-25 cm^2 with classic media for 17-24 hours. Once they became confluent, they were passaged to 2 plates of 96-well with a cell density of 6,400 cells per well. Cells were counted manually using a hemocytometer and trypan blue. Three wells were used for each passage. Cells were cultured in normal glucose and normoxia conditions for 17-18 hours. Negative control was prepared as (media + No cells). After incubation, cells were prepared for the experiment as media was changed for control with new fresh N.G media and for OND with saline solution. Control was incubated in Normoxia (20% O_2) and OND in Hypoxia (1% O_2) for 2 hrs. at 37^oC.

MTT assay (provided from Thermo fisher scientific, Invitrogen with catalogue number: V13154) was performed by the manufacturer's protocol. MTT stock solution was prepared by dissolving 5 mg of MTT in 1 mL of PBS. After 2 hrs. incubation, old

media was discarded, and new fresh media/saline was replaced as 100 μL per well. MTT was added as 10 μL per well. Each plate was returned back to the incubator and incubated for 4 hrs. 85 μL of the old media was discarded, and 50 μL of DMSO was added to each well. It was incubated again for 10 min. Absorbance was read at 540 nm by Plate reader: EPOCH12 – BioTek.

Cells incubated in Saline tend not to absorb the MTT component. Therefore, optimization was tried to figure out if absorption would increase, pictures are displayed in the Appendix. After 2 hrs. incubation in saline, and during MTT incubation, cells were incubated in different conditions. For example, old media was discarded and then replaced by Saline with 0.01% / 0.001% triton. Triton concentrations of 0.01% / 0.001% were prepared by diluting 10 μL / 5 μL of triton 10% in 10 mL saline/N.G media. Triton was applied to the control plate as well. The results of this section are illustrated in the Appendix as it wasn't applicable to be used for confirmation of OND model. Further optimization was conducted by incubating OND cells in PBS/2 mM glucose media, results are illustrated in the Appendix. Although viability measurements were not applicable, the way for calculating them should be as following:

1- Control and OND absorbance were subtracted from negative control absorbance (which contains media + no cells).
2- Viability of Control with N.G and Normoxia was set to be as 100%.
    a. Viability of Control with Triton was calculated as {absorbance of control-triton/absorbance of control-no triton} * 100
3- Viability of OND was calculated as {absorbance of OND/absorbance of control} * 100
    a. Viability of OND with Saline-Triton was calculated based on

Control with Triton

b. Viability of other types of OGD was calculated based on control with N.G and No Triton.

3.2.4 Actin staining

The aim of actin staining was to figure out the stress caused by different types of OGD and OND models on the cells. Actin staining was used by different studies to assess cytoskeleton changes as it could indicate blood-brain barrier disruption (Shi et al., 2016), (Abdulkadir et al., 2020) and (Jessick et al., 2013). Actin staining was also a confirmation method for the results of the apoptosis procedure.

The procedure of OGD and OND was followed as in section 3.2.2.2 and 3.2.2.3. but with minor modification. After cells were grown in classic media for 24 hours, they were passaged to petri-dish prepared earlier with autoclaved coverslips. The cell density applied was 118,000-120,000. It was cultured with normal glucose for 17-18 hrs. at 37$_o$C. Then, control was cultured in (Normoglycemia + Normoxia), and OGD were cultured in (partial/complete deprivation of glucose and nutrients with Hypoxia 1%) for 2 hrs at 37$_o$C as following:

- OGD group 1: 2 mM glucose media in PBS with Ca++ and Mg++, and hypoxia for 2 hrs.
- OGD group 2: 2 mM glucose media in PBS without Ca++ or Mg++, and hypoxia for 2 hrs.
- OGD group 3: 2 mM glucose media in saline, and hypoxia for 2 hrs.
- OGD group 4: PBS with Ca++ or Mg++, and hypoxia for 2 hrs.
- OND model: saline, and hypoxia for 2 hrs.

OGD incubation under PBS **without** Ca++ or Mg++, and under RPMI media **without** growth factors, were excluded from actin staining for the following reasons:

1- PBS without Ca++ or Mg++: cells tend to die and detach within 2 hrs. of incubation; thus, actin staining wasn't applicable for completely dead cells.

2- RPMI media: although it lacks growth factors, it doesn't represent true glucose deprivation, as it contains a high level of glucose (2 g/L or 11.11 mM), and it was only used for apoptosis as a preliminary data to investigate the absence of growth factors.

Cells were washed with saline/PBS then fixed with 4% Para-formaldehyde (PFA) for 15 min. (4% PFA was prepared by dissolving 4 grams of PFA in 80 mL PBS in a container that was put on a pre-warmed heating plate at 60$_o$C while adding drops of NaOH until the solution is clear). The pH was adjusted to 7.00 by adding HCL drops, then PBS is added until the total volume reaches 100 mL). After fixation, cells were washed twice by PBS, then permeabilized by 0.1% Triton and 1% BSA for 30 min. (It was prepared by diluting 100 µL Triton and 100 µL of Bovine serum Albumin in 10 mL PBS). After permeabilization, cells were washed twice, then stained by 2.5% Alexa-488 (F-actin stain, Thermo-scientific, A12379) and incubated overnight – entire weekend – in Fridge - 4$_o$C. (The stain was prepared by diluting a ratio of 2.5 µL of the stain in 100 µL of PBS).

After overnight incubation, cells were washed twice then stained by 0.002 mg/mL Dapi for 2 min. and washed again. (Dapi was prepared by diluting 20 µL of the stain in 10 mL of distilled water). Microscopic slides were prepared with gel mount, and the coverslip of cells was applied to it. It was analyzed under a microscope on 10x and 60x oil immersion with Green Fluorescent Protein (GFP) and Dapi filters. Images were combined using ImageJ software.

3.2.5 The optimized model for *in-vitro* ischemic stroke

Oxygen Nutrients Deprivation (OND) model which had complete deprivation of glucose, nutrients, growth factors and ionic molecules (Ca++/Mg++), was selected as the optimized model for this research. The model was selected as it caused severe cell injury based on the number of live/dead cell and based on actin filaments staining (refer to results sections for comparison to other OGD models). This mimic model conditions of severe acute severe stroke, whereas complete interruption of blood supply posing the cells on severe stress and may causes irreversible cell injury. Figure 12 illustrates the optimized model that was used for biochemical analysis and gene expression.

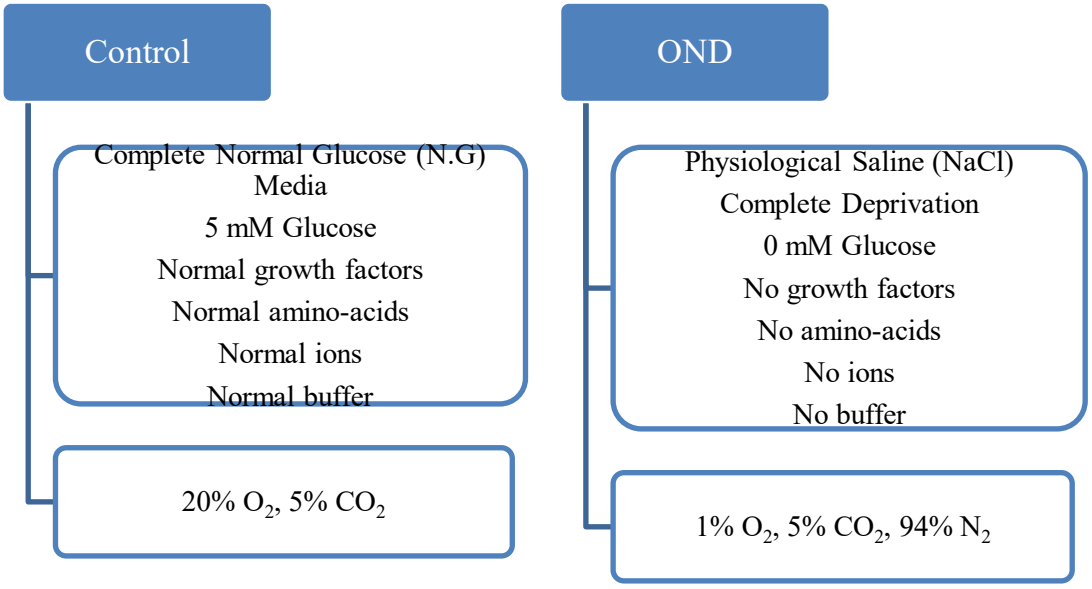

Figure 12. Optimized *in-vitro* ischemic stroke model (Oxygen Nutrients Deprivation: OND).

3.2.6 Biochemical Analysis

The Conditional Media (CM) was collected **after** the incubation. The CM was centrifuged, and the supernatant was collected and aliquoted in several tubes for further analysis. Glucose and lactic acid were measured using the following technique: photometric, electro-chemiluminescence, using Roche-Hitachi Cobas 8000 instrument in Clinical pathology labs at HMC. pH measurement was assessed using a pH meter (Thermo-Fischer Scientific - Orion Star A111) at Biomedical Research Center (BRC).

3.2.7 Gene Expression Analysis

3.2.7.1 RNA extraction

Total RNA was extracted from treated PHBMEC using TRIZOL® reagent. A total of 4 samples were prepared for both control and OND. The 4 samples were of the passage number 6,7, 8, and 9. After incubation, petri-dish of control and OGD groups were placed on ice. The old media was discarded, and dishes were washed by ice-cold saline. An amount of 1 mL of ice-cold Trizol was added per dish, and cells were lysed gently using a cell scraper. Cells were collected in an autoclaved Eppendorf tubes and stored in -80°C over-night or until the day of use. On the day of use, cells in Trizol were thawed at RT, and then they were vortexed to homogenize them properly. An amount of 200 μL of chloroform was added to each Eppendorf, and then they were shaken vigorously for 15 seconds. Eppendorf tubes were left on RT for 5 min, then centrifuged at maximum speed, 4°C for 15 min. The upper aqueous layer, which contains the RNA, was collected carefully in another autoclaved Eppendorf tube, and caution was taken to not touch the whitish layer, as it contains the DNA. An amount of 500 μL of ice-cold isopropyl alcohol was added over the

collected aqueous layer. If whitish thread appeared, then we proceeded in the protocol. If not, then the mixture was kept at -80°C over-night.

The next day, the mixture was centrifuged at maximum speed, 4°C for 15 min. The supernatant was poured into a waste container, and the Eppendorf was kept upside down on a paper tissue for a few seconds to allow getting rid of all the liquid. An amount of 1 mL of absolute ice-cold ethanol was added to RNA pellet; it was vortexed and centrifuged at max speed, 4°C for 10 min. The supernatant was poured into a waste container, and the Eppendorf was kept upside down on a paper tissue for a few seconds. An amount of 1 mL of absolute ice-cold ethanol was added again for a second wash and centrifuged at max speed, 4°C for 10 min. The supernatant was poured, and the RNA pellet was let to air-dry for 1 hour. During this time, Rnase-free water was heated to 60°C on a dry bath to facilitate resuspension of RNA. Once RNA was dried, 20 μL of RNase-free water was added to RNA pellet; RNA could appear as transparent, which means it was pure RNA. The Eppendorf of RNA was vortexed and was put on ice immediately. Then, it was centrifuged for 10 seconds at 4°C to precipitate the solution down.

RNA concentration and yield were measured using a nanodrop, and RNase-free water was used as a blank. The extracted RNA was stored at -80°C until the day of use. RNase-free water was prepared by adding a proportion of 1 μL of Diethyl Pyrocarbonate (DEPC) to 1 mL distilled water. The mixture was incubated at 37°C incubator overnight. DEPC inactivate RNase enzymes at 37°C. After incubation, the RNase-free water must be autoclaved to deactivate DEPC, and it was ready to use once it cooled down.

3.2.7.2 c-DNA synthesis

RNA dilution was prepared from a stock solution to facilitate the calculation of the volume needed for cDNA synthesis. The final concentration was determined to be 100 ng/μL and the final volume was determined to be 30 μL. The initial volume was calculated according to the formula:

Concertation (initial) x volume (initial) = Concertation (final) x volume (final)

Rnase-free water was added according to the calculation:

The final volume (30 μL) – initial volume

For cDNA synthesis, small Eppendorf strips were used to perform the reaction.

Superscript IV VILO Master Mix (5X) that contain dNTPS and Reverse transcriptase enzyme was used as the following proportion of a total of 25 μL:

1- 5 μL Master mix
2- 5 μL of RNA sample (which had 100 ng/μL, so total was 500 ng of RNA)
3- 15 μL of RNase-free water

The above mixture was considered as one cDNA synthesis reaction. We made a total of 3 reactions, and the total volume was 75 μL of cDNA.

The mixture was loaded into ProFlex PCR – Applied Biosystem, to do the reaction by the following program:

1- Anneal primers: 10 min. at 25°C
2- Reverse transcribe RNA: 10 min. at 50°C
3- Inactivate enzyme: 5 min. at 85°C
4- Sample volume: 75 mL
5- Cycles: 1 cycle only

Once finished, the machine stored it at 4°C, and then it was transferred to -20°C for up to a week, or -80°C for long term storage.

3.2.7.3 RT-PCR profiler array

Two types of arrays were used: inflammatory cytokines and angiogenesis. A total of 4 inflammatory arrays and 4 angiogenesis arrays were used for different samples of control and OND. Therefore, cDNA was diluted as 145 μL of RNase-free was added for each 75 μL of the cDNA sample. An amount of 102 μL of cDNA was used per RT-PCR profiler array. RT-SYBR Green ROX qPCR Master Mix was used for RT-PCR profiler array. In 5 mL Polystyrene round bottom tube, the following PCR mixture was prepared:

1- Master mix: 1350 μL
2- RNase-free water: 1248 μL
3- cDNA: 102 μL

The mixture was vortexed and using an electronic pipette, μL mL of cDNA mixture was added to each well of RT-PCR array. Then, it was centrifuged at 1000 rpm, 25°C for 1 min. to precipitate the mixture down before analysis.

The plate was applied to the 7500 Real Time PCR system as the following program:

The Experimental setup includes:

1- 7500 (96 wells)
2- Quantification-standard curve
3- SYBER green Reagents
4- 2 hours to complete the run

Plate setup:

1- Target 1
2- Sample 1

3- Highlight the entire plate

Run method:

1- Reaction volume: 25 μL

2- Holding stage 95°C for 10 min.

3- Cycling stage:

   a. Number of cycles: 40

   b. Temperature: 95°C for 15 sec., 60°C for 1 min.

4- Melting curve: 60°C-95°C.

Once setup is ready, click run and wait a few minutes for initial priming. Once the PCR run finished, the file can be exported as excel.

3.2.7.4 List of genes in the array analyzed

3.2.7.4.1 Inflammatory genes Array

Total genes studied were 84, included in the position from A1-G12. Details are in Table 6.

Table 6. Inflammatory genes Array.

Position	Symbol	Gene Name
A01	AIMP1	Aminoacyl tRNA synthetase complex-interacting multifunctional protein 1
A02	BMP2	Bone morphogenetic protein 2
A03	C5	Complement component 5
A04	CCL1	Chemokine (C-C motif) ligand 1
A05	CCL11	Chemokine (C-C motif) ligand 11
A06	CCL13	Chemokine (C-C motif) ligand 13
A07	CCL15	Chemokine (C-C motif) ligand 15
A08	CCL16	Chemokine (C-C motif) ligand 16
A09	CCL17	Chemokine (C-C motif) ligand 17
A10	CCL2	Chemokine (C-C motif) ligand 2
A11	CCL20	Chemokine (C-C motif) ligand 20
A12	CCL22	Chemokine (C-C motif) ligand 22
B01	CCL23	Chemokine (C-C motif) ligand 23
B02	CCL24	Chemokine (C-C motif) ligand 24
B03	CCL26	Chemokine (C-C motif) ligand 26
B04	CCL3	Chemokine (C-C motif) ligand 3
B05	CCL4	Chemokine (C-C motif) ligand 4
B06	CCL5	Chemokine (C-C motif) ligand 5
B07	CCL7	Chemokine (C-C motif) ligand 7
B08	CCL8	Chemokine (C-C motif) ligand 8
B09	CCR1	Chemokine (C-C motif) receptor 1
B10	CCR2	Chemokine (C-C motif) receptor 2
B11	CCR3	Chemokine (C-C motif) receptor 3
B12	CCR4	Chemokine (C-C motif) receptor 4
C01	CCR5	Chemokine (C-C motif) receptor 5
C02	CCR6	Chemokine (C-C motif) receptor 6
C03	CCR8	Chemokine (C-C motif) receptor 8
C04	CD40LG	CD40 ligand
C05	CSF1	Colony-stimulating factor 1 (macrophage)
C06	CSF2	Colony-stimulating factor 2 (granulocyte-macrophage)
C07	CSF3	Colony-stimulating factor 3 (granulocyte)
C08	CX3CL1	Chemokine (C-X3-C motif) ligand 1
C09	CX3CR1	Chemokine (C-X3-C motif) receptor 1
C10	CXCL1	Chemokine (C-X-C motif) ligand 1 (melanoma growth stimulating activity, alpha)
C11	CXCL10	Chemokine (C-X-C motif) ligand 10
C12	CXCL11	Chemokine (C-X-C motif) ligand 11

Position	Symbol	Gene Name
D01	CXCL12	Chemokine (C-X-C motif) ligand 12
D02	CXCL13	Chemokine (C-X-C motif) ligand 13
D03	CXCL2	Chemokine (C-X-C motif) ligand 2
D04	CXCL3	Chemokine (C-X-C motif) ligand 3
D05	CXCL5	Chemokine (C-X-C motif) ligand 5
D06	CXCL6	Chemokine (C-X-C motif) ligand 6 (granulocyte chemotactic protein 2)
D07	CXCL9	Chemokine (C-X-C motif) ligand 9
D08	CXCR1	Chemokine (C-X-C motif) receptor 1
D09	CXCR2	Chemokine (C-X-C motif) receptor 2
D10	FASLG	Fas ligand (TNF superfamily, member 6)
D11	IFNA2	Interferon, alpha 2
D12	IFNG	Interferon, gamma
E01	IL10RA	Interleukin 10 receptor, alpha
E02	IL10RB	Interleukin 10 receptor, beta
E03	IL13	Interleukin 13
E04	IL15	Interleukin 15
E05	IL16	Interleukin 16
E06	IL17A	Interleukin 17A
E07	IL17C	Interleukin 17C
E08	IL17F	Interleukin 17F
E09	IL1A	Interleukin 1, alpha
E10	IL1B	Interleukin 1, beta
E11	IL1R1	Interleukin 1 receptor, type I
E12	IL1RN	Interleukin 1 receptor antagonist
F01	IL21	Interleukin 21
F02	IL27	Interleukin 27
F03	IL3	Interleukin 3 (colony-stimulating factor, multiple)
F04	IL33	Interleukin 33
F05	IL5	Interleukin 5 (colony-stimulating factor, eosinophil)
F06	IL5RA	Interleukin 5 receptor, alpha
F07	IL7	Interleukin 7
F08	CXCL8	Interleukin 8
F09	IL9	Interleukin 9
F10	IL9R	Interleukin 9 receptor
F11	LTA	Lymphotoxin alpha (TNF superfamily, member 1)
F12	LTB	Lymphotoxin beta (TNF superfamily, member 3)
G01	MIF	Macrophage migration inhibitory factor (glycosylation-inhibiting factor)
G02	NAMPT	Nicotinamide phosphoribosyltransferase
G03	OSM	Oncostatin M
G04	SPP1	Secreted phosphoprotein 1
G05	TNF	Tumor necrosis factor
G06	TNFRSF11B	Tumor necrosis factor receptor superfamily, member 11b
G07	TNFSF10	Tumor necrosis factor (ligand) superfamily, member 10
G08	TNFSF11	Tumor necrosis factor (ligand) superfamily, member 11
G09	TNFSF13	Tumor necrosis factor (ligand) superfamily, member 13
G10	TNFSF13B	Tumor necrosis factor (ligand) superfamily, member 13b
G11	TNFSF4	Tumor necrosis factor (ligand) superfamily, member 4
G12	VEGFA	Vascular endothelial growth factor A

3.2.7.4.2 Angiogenesis genes Array

Total genes studied were 84, included in the position from A1-G12. Details are in Table 7.

Table 7. Angiogenesis genes Array

Position	Symbol	Description
A01	AKT1	V-akt murine thymoma viral oncogene homolog 1
A02	ANG	Angiogenin, ribonuclease, RNase A family, 5
A03	ANGPT1	Angiopoietin 1
A04	ANGPT2	Angiopoietin 2
A05	ANGPTL4	Angiopoietin-like 4
A06	ANPEP	Alanyl (membrane) aminopeptidase
A07	ADGRB1	Brain-specific angiogenesis inhibitor 1
A08	CCL11	Chemokine (C-C motif) ligand 11
A09	CCL2	Chemokine (C-C motif) ligand 2
A10	CDH5	Cadherin 5, type 2 (vascular endothelium)
A11	COL18A1	Collagen, type XVIII, alpha 1
A12	COL4A3	Collagen, type IV, alpha 3 (Goodpasture antigen)
B01	CTGF	Connective tissue growth factor
B02	CXCL1	Chemokine (C-X-C motif) ligand 1 (melanoma growth stimulating activity, alpha)
B03	CXCL10	Chemokine (C-X-C motif) ligand 10
B04	CXCL5	Chemokine (C-X-C motif) ligand 5
B05	CXCL6	Chemokine (C-X-C motif) ligand 6 (granulocyte chemotactic protein 2)
B06	CXCL9	Chemokine (C-X-C motif) ligand 9
B07	EDN1	Endothelin 1
B08	EFNA1	Ephrin-A1
B09	EFNB2	Ephrin-B2
B10	EGF	Epidermal growth factor
B11	ENG	Endoglin
B12	EPHB4	EPH receptor B4
C01	ERBB2	V-erb-b2 erythroblastic leukemia viral oncogene homolog 2, neuro/glioblastoma derived oncogene homolog (avian)
C02	F3	Coagulation factor III (thromboplastin, tissue factor)
C03	FGF1	Fibroblast growth factor 1 (acidic)
C04	FGF2	Fibroblast growth factor 2 (basic)
C05	FGFR3	Fibroblast growth factor receptor 3
C06	FIGF	C-fos induced growth factor (vascular endothelial growth factor D)
C07	FLT1	Fms-related tyrosine kinase 1 (vascular endothelial growth factor/vascular permeability factor receptor)
C08	FN1	Fibronectin 1
C09	HGF	Hepatocyte growth factor (hepapoietin A; scatter factor)
C10	HIF1A	Hypoxia-inducible factor 1, alpha subunit (basic helix-loop-helix transcription factor)
C11	HPSE	Heparanase
C12	ID1	Inhibitor of DNA binding 1, dominant negative helix-loop-helix protein
D01	IFNA1	Interferon, alpha 1
D02	IFNG	Interferon, gamma
D03	IGF1	Insulin-like growth factor 1 (somatomedin C)
D04	IL1B	Interleukin 1, beta

Position	Symbol	Description
D05	IL6	Interleukin 6 (interferon, beta 2)
D06	CXCL8	Interleukin 8
D07	ITGAV	Integrin, alpha V (vitronectin receptor, alpha polypeptide, antigen CD51)
D08	ITGB3	Integrin, beta 3 (platelet glycoprotein IIIa, antigen CD61)
D09	JAG1	Jagged 1
D10	KDR	Kinase insert domain receptor (a type III receptor tyrosine kinase)
D11	LECT1	Leukocyte cell derived chemotaxin 1
D12	LEP	Leptin
E01	MDK	Midkine (neurite growth-promoting factor 2)
E02	MMP14	Matrix metallopeptidase 14 (membrane-inserted)
E03	MMP2	Matrix metallopeptidase 2 (gelatinase A, 72kDa gelatinase, 72kDa type IV collagenase)
E04	MMP9	Matrix metallopeptidase 9 (gelatinase B, 92kDa gelatinase, 92kDa type IV collagenase)
E05	NOS3	Nitric oxide synthase 3 (endothelial cell)
E06	NOTCH4	Notch 4
E07	NRP1	Neuropilin 1
E08	NRP2	Neuropilin 2
E09	PDGFA	Platelet-derived growth factor-alpha polypeptide
E10	PECAM1	Platelet/endothelial cell adhesion molecule
E11	PF4	Platelet factor 4
E12	PGF	Placental growth factor
F01	PLAU	Plasminogen activator, urokinase
F02	PLG	Plasminogen
F03	PROK2	Prokineticin 2
F04	PTGS1	Prostaglandin-endoperoxide synthase 1 (prostaglandin G/H synthase and cyclooxygenase)
F05	S1PR1	Sphingosine-1-phosphate receptor 1
F06	SERPINE1	Serpin peptidase inhibitor, clade E (nexin, plasminogen activator inhibitor type 1), member 1
F07	SERPINF1	Serpin peptidase inhibitor, clade F (alpha-2 antiplasmin, pigment epithelium derived factor), member 1
F08	SPHK1	Sphingosine kinase 1
F09	TEK	TEK tyrosine kinase, endothelial
F10	TGFA	Transforming growth factor, alpha
F11	TGFB1	Transforming growth factor, beta 1
F12	TGFB2	Transforming growth factor, beta 2
G01	TGFBR1	Transforming growth factor, beta receptor 1
G02	THBS1	Thrombospondin 1
G03	THBS2	Thrombospondin 2
G04	TIE1	Tyrosine kinase with immunoglobulin-like and EGF-like domains 1
G05	TIMP1	TIMP metallopeptidase inhibitor 1
G06	TIMP2	TIMP metallopeptidase inhibitor 2
G07	TIMP3	TIMP metallopeptidase inhibitor 3
G08	TNF	Tumor necrosis factor
G09	TYMP	Thymidine phosphorylase
G10	VEGFA	Vascular endothelial growth factor A
G11	VEGFB	Vascular endothelial growth factor B
G12	VEGFC	Vascular endothelial growth factor C

3.2.8 Data analysis

Differentially expressed genes were generated using Gene Globe analysis software available on the Qiagen website. The threshold for significance in expression change was set at FC of ≤ -1.4 for down-regulated and up-regulated genes, and a Student's t-test of the replicate 2**(-Delta CT)** values for each gene in the control group and treatment groups using globe analysis by Qiagen. The options selected on Gene Globe were as following:

1- Choosing the right catalogue number based on the study, either inflammatory or angiogenesis.
2- CT value was set to 40
3- Fold regulation was set to 1.4
4- P-value= 0.05
5- Normalization was done based on geometric mean for five housekeeping genes: Actin-beta, B2M, GAPDH, HPRT1, RPLPO.

3.2.8.1 Functional classification of DEGs and their pathways

Pathways and interaction network analysis were performed using Ingenuity Pathway Analysis (IPA®) by uploading the DEG's of the data set. Studying gene functions at a particular set was performed using (https://www.uniprot.org).

3.2.9 Statistical analysis

Statistical analyses were conducted using Microsoft Excel 2013 (Microsoft Corp., Redmond, WA). For in vitro studies, at least 3 to 4 biological replicates (of passage 6, 7, 8, and 9) were prepared for each treatment group along with at least three technical replicates. The results are presented as the mean of three different experiments with a standard deviation of the mean. Group differences were evaluated by student's t-test. For all analysis, a two-tailed $P < 0.05$ will be considered sufficient to reject the null hypothesis. Bonferroni correction was performed to adjust for multiple comparisons of gene expressions using RT-PCR array, by dividing the P value (0.05) by the number of genes tested

3.3 Ethical and Biosafety Approvals

This research has granted the approval of the Institutional Biosafety Committee of Qatar University. The approval number is QU-IBC-2018-076.

Chapter 4: Results

4.1 Viability test analysis (Apoptosis)

Viability was assessed on PHBMECs using apoptosis staining. The aim was to model an *in-vitro* ischemic stroke that resembles severe cell injury illustrated by marked increase in cell death within a timeline of 2 hrs.

Figure 13 represents the OGD type with 2 mM glucose media in PBS with Ca++ and Mg++. Results represent no significant difference between control and OGD as *p-value* was higher than 0.05. This concluded that this type of OGD didn't produce serious injury as cells could survive in this low level of glucose and other nutrients.

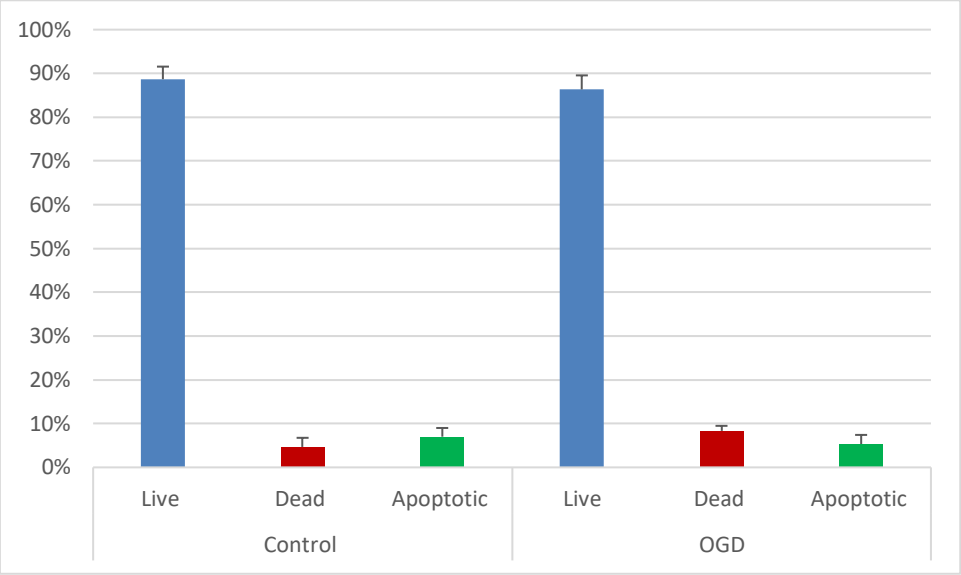

Figure 13. Apoptosis analysis of OGD type with 2 mM glucose media in PBS with Ca++ and Mg++.
Control was exposed to 5 mM glucose media. OGD exposed cells were incubated in 2 mM glucose media diluted in PBS with Ca++ and Mg++. The experiments were performed in triplicates. Control represented with high viability (89% ± 0.029), low dead (5% ± 0.021) and apoptotic cells (7% ± 0.02). OGD represents high viability (86% ± 0.032) with no significance with control (*p-value* > 0.05). Furthermore, there was no significant difference between dead (8% ± 0.012) and apoptotic cells (5% ± 0.021) between OGD and control (*p-value* > 0.05). Two tailed T-test was used by Excel to measure mean, standard deviation, and *p-value*.

Since the first type of OGD (2 mM glucose media in PBS without Ca++ or Mg++) showed no difference with control, we aimed to perform a pilot study with different composition of diluted media/PBS/saline to figure out which OGD model would present the most severe cell injury by marked increase of death. Since the pilot study we performed didn't have triplicates data, results are shown in the Appendix. Although other types of OGD were performed once, results were confirmed by actin staining which will be explained by the next section. Refer to the Appendix for details about viability for other types of OGD.

The results of a pilot study gave an indication about viability represented by different types of OGD. Other OGD types had high viability similar to control. Therefore, we tried to do complete deprivation of all nutrients in the OND model to investigate whether viability would decrease. OND model lacks all type of nutrients: glucose, growth factors, different amino acids, vitamins and different inorganic salts such as Ca++ and Mg++. Viability in the OND model was significantly very low (around 45%) compared to control (around 70%). Dead cells of OND were significantly very high (around 42%) compared to control (around 10%). On the other hand, the OND model showed a low level of apoptotic cells (around 10%) compared to control (around 20%). The results here showed that scraper in some way decreased viability of cells as illustrated by control. Although the viability of control decreased, the OND model still shows very low viability with significant p-values as illustrated in figure 14.

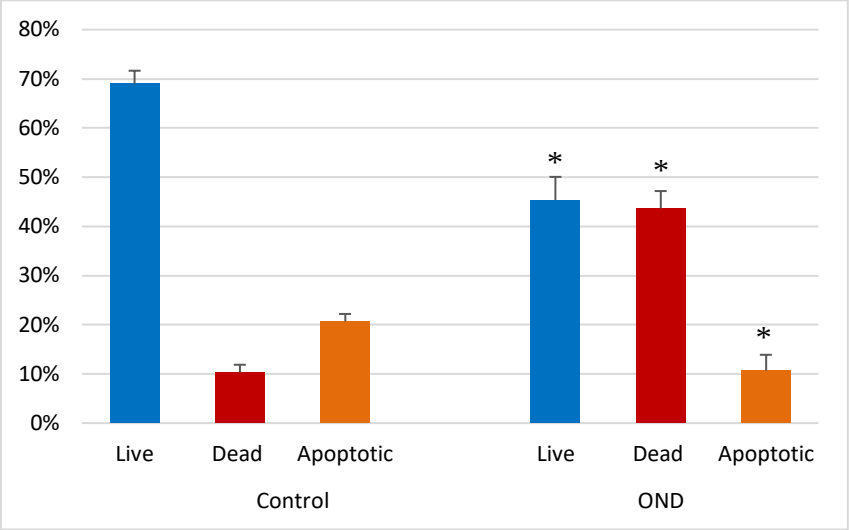

Figure 14. Apoptosis analysis of OND model.
Control was exposed to 5 mM glucose media. OND was exposed to saline. The experiments were performed in triplicates. Control represents high viability (69% ± 0.026), and very low cell death (10% ± 0.015), and apoptotic cells (20% ± 0.015). OND represents a low level of viable cells around 45% ± 0.047 with *p-value* (<0.01) compared to control. Moreover, OND model had a high level of dead cells around 42% ± 0.035 with *p-value* (<0.001) compared to control. On the other hand, OND model had a low level of apoptotic cells around 10% ± 0.035 with *p-value* (<0.05) compared to control. Two tailed T-test was used by Excel to measure mean, standard deviation, and *p-value*.

4.2 Actin staining

Cytoskeleton filaments were assessed in PHBMECs using actin stain. The aim of this experiment is to study the effect of low oxygen, low/absent glucose, and different types of PBS/saline with different ion composition on cell shape and mobility assessed by cytoskeleton filament changes.

Actin staining was performed on PHBMECs exposed to the normal condition of the human brain (control) and other conditions of OGD and OND that cause cell injury and mimic the ischemic stroke model. Control cells were cultured in 5 mM glucose media, normoxia, at 37$_o$C for 2 hrs. Different types of OGD conditions were performed as follows:

- OGD group 1: 2 mM glucose media in PBS with Ca++ and Mg++, and hypoxia for 2 hrs.
- OGD group 2: 2 mM glucose media in PBS without Ca++ or Mg++, and hypoxia for 2 hrs.
- OGD group 3: 2 mM glucose media in saline, and hypoxia for 2 hrs.
- OGD group 4: PBS with Ca++ or Mg++, and hypoxia for 2 hrs.
- OND model: saline, and hypoxia for 2 hrs.

The results displayed in figure 15 and 16 indicated a major change in the cell shape of OND compared to control or even other types of OGD. Different OGD types had a slight change in shape with the presence of few stress fibers, which could mimic chronic ischemic stroke. However, OND exposed cells showed condensation of actin stress actin fiber around the nucleus that results in apparent contraction of the cells. The actin changes in OND model could indicate severe cell injury that mimics an acute ischemic stroke. Figures 15 and 16 show actin filaments staining under a fluorescent microscope, where 10x illustrated in figure 15 and 60x illustrated in figure 16.

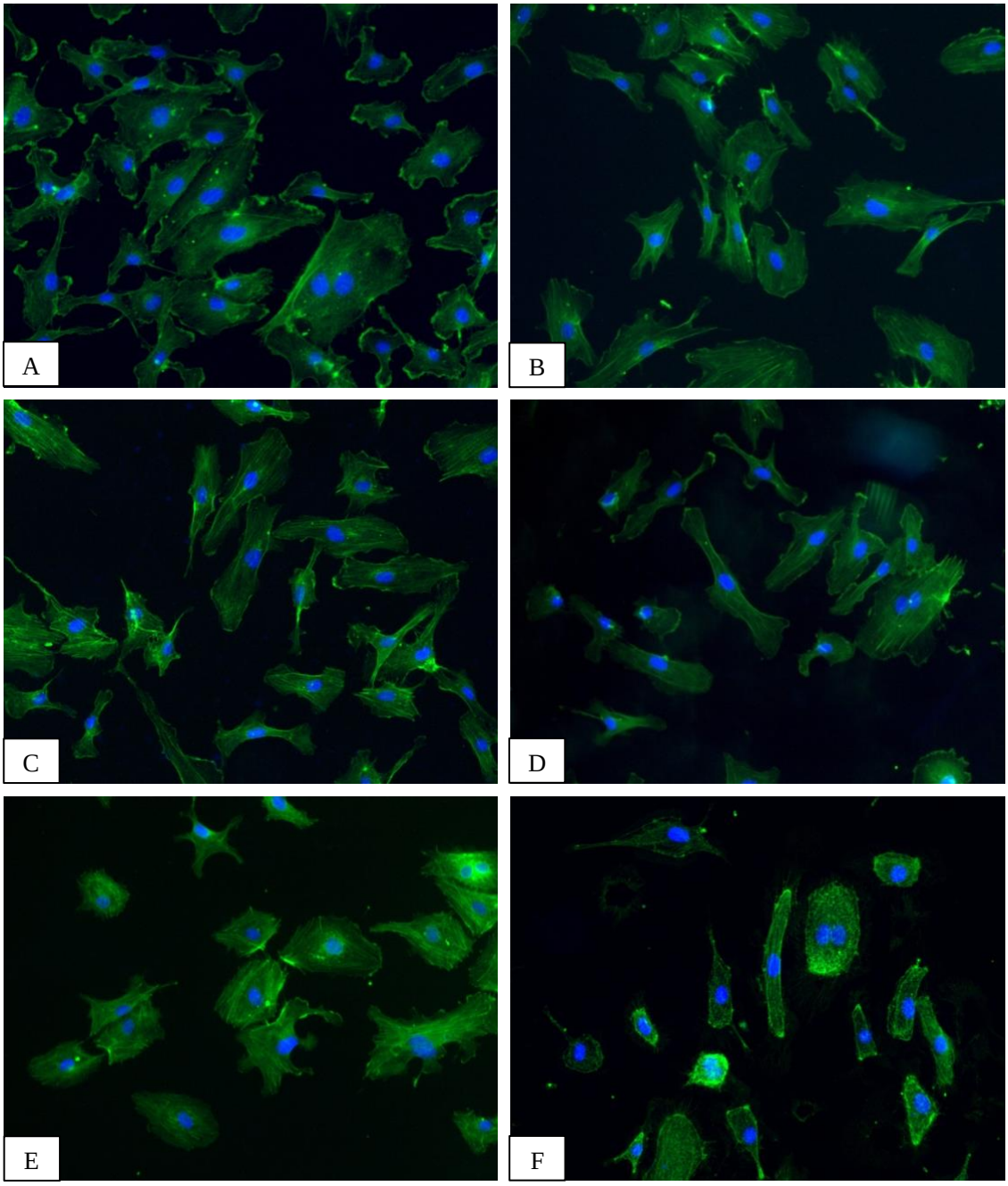

Figure 15. Actin staining of different types of OGD and OND under 10x power.
Figures 15 (under 10x) and Figure 16 (under 60x) presented in next page; both represent actin staining of PHBMECs under a fluorescent microscope. **A. Control**: the actin filaments in control cells are diffused through the cell representing normal cell shape with no thick stress fibers or contraction in the cells. **B. OGD- group 1:** cells were exposed to 2 mM glucose media in PBS with Ca++ and Mg++. **C. OGD-group 2:** cells were exposed to 2 mM glucose media in PBS without Ca++ or Mg++. **D. OGD-group 3:** cells were exposed to 2 mM glucose media in saline. **E. OGD-group 4:** cells were exposed to PBS with Ca++ and Mg++. The actin filaments in **OGD 1-4** exposed cells started to change slightly. It represents thick stress fibers with a slight contraction of cells that had an impact on the shape of the cell. **F. OND:** cells were exposed to saline for 2 hrs. in hypoxia. **The actin filaments** in OND-exposed cells had a major change compared to control or OGD. Stress fibers altered the cell shape to the greatest impact, where cells had a massive contraction. Cells were present with irregular shapes that are mostly having the fibers condensed around the nucleus comparing to control.

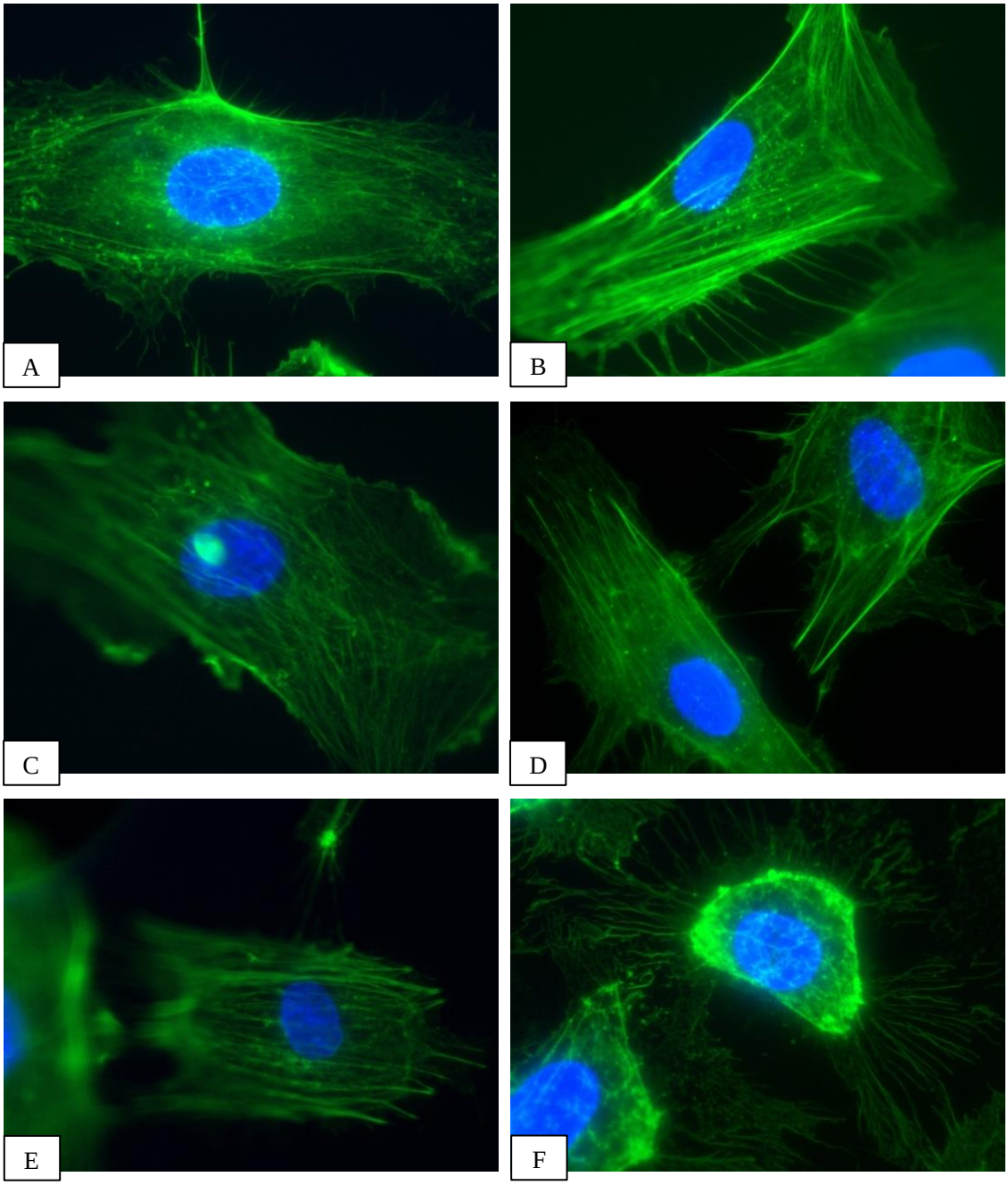

Figure 16. Actin staining of different types of OGD and OND under 60x power.

4.3 Biochemical analysis

The aim was to assess whether exposure of complete deprivation of glucose and other nutrients with oxygen could (OND) cause biochemical changes of PHBMECs. Biochemical measurements performed were glucose, lactic acid, and pH. The pH of OND model was significantly decreased (around 6) compared to control (around 7.5). Glucose and lactic acid were nearly absent from OND model (less than zero). Figure 17 illustrates pH, glucose, and lactic acid readings that were taken after incubation as a mean ± standard deviation with a significant *p-value*.

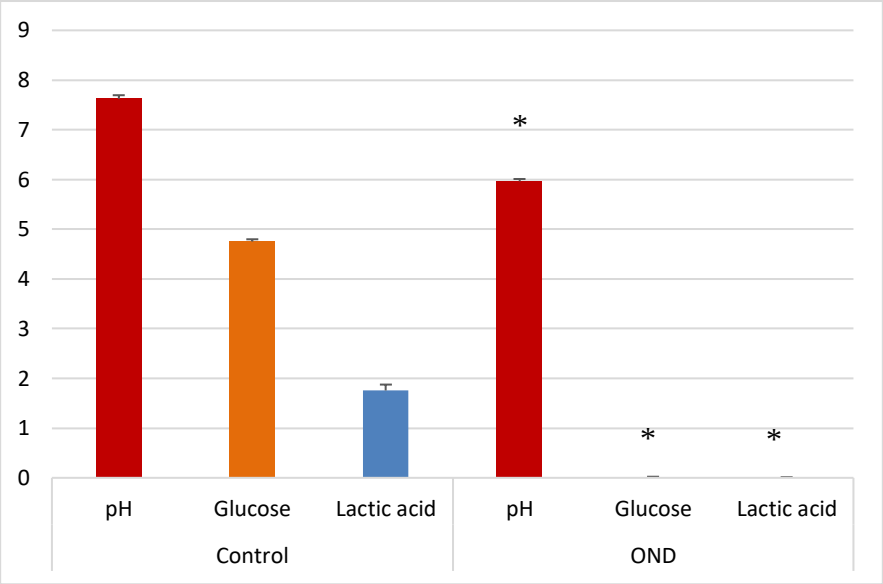

Figure 17. Biochemical analysis of OND model.
Control represented normal pH value as (7.62 ± 0.072) while OND represented with a significant low pH as (5.96 ± 0.047) and with a significant *p-value* (<0.0001). Glucose and lactic acid in control were represented as (4.75 ± 0.045) and (1.76 ± 0.119), respectively. On the other hand, since saline lacks glucose or lactate, the measurement after incubation represented with nearly zero levels as (0.017 ± 0.006) for glucose and (0.0067 ± 0.006) for lactic acid. Significant *p-values* for glucose and lactic acid were <0.0001 and <0.01, respectively. Data are presented as mean and SD. * p-value significant versus control. Two tailed *p-value* is significant <0.05.

4.4 Gene expression analysis

4.4.1 Differentially expressed genes (DEGs)

Two sets of gene arrays related to the endothelial function (inflammation and angiogenesis) were investigated through RT-PCR on the control and OND model. Differentially expressed genes (DEGs) were analyzed using the globe gene of Qiagen (https://www.qiagen.com) with a cut off value of 1.4 for fold regulation, a Student's t-test of the replicate 2**(-Delta Delta CT)** method, and *p-value* for multiple corrections of (p=0.05). Fold regulation is another expression of fold change as if fold change was less than 1, it indicates down regulation, and if it was higher than 1, it indicates up-regulation. The fold regulation expression is the negative inverse of fold change. The results demonstrated that out of 84 genes of inflammatory array analyzed, 2 genes were significantly upregulated, which were (IL-8/CXCL8 and TNFSF4), and 1 gene was significantly downregulated, which was (CCL2). On the other hand, out of 84 genes of angiogenesis array analyzed, 3 genes were significantly upregulated which were (CXCL1 and IL-8/CXCL8) and S1PR1) and 14 genes were significantly down regulated which were (ANGPTL4, CCL2, CTGF/CCN2, EDN1, EFNB2, EPHB4, FLT1, ID1, JAG1, PDGFA, PGF, SERPINE1, SPHK1, and VEGFA). There were two genes repeated between the two gene arrays which were IL-8/CXCL8 and CCL2 and they have the same regulation. Thus, total differentially expressed genes were 18. Total upregulated genes were IL-8/CXCL8, TNFSF4, CXCL1 and S1PR1, and total down regulated genes were CCL2, ANGPTL4, CTGF/CCN2, EDN1, EFNB2, EPHB4, FLT1, ID1, JAG1, PDGFA, PGF, SERPINE1, SPHK1, and VEGFA. Figure 18 displays the differentially expressed genes of both inflammation and angiogenesis.

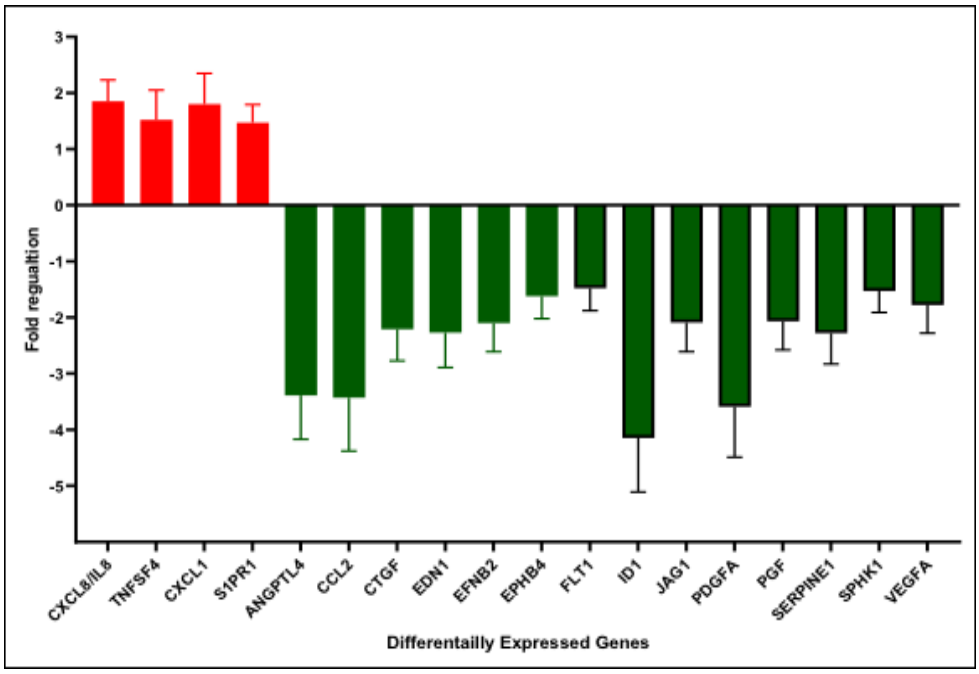

Figure 18. Differentially expressed genes of inflammation and angiogenesis.
Up-regulated genes are displayed in red bars and the down-regulated genes are displayed in green bars. The X-axis displays DEG, while Y-axis displays the fold regulations of such changes. Fold regulation cut off value is ± 1.4. Data are displayed as mean ± standard deviation. Data were analyzed based on 4 different samples from cell passage 6, 7, 8, and 9 for each inflammatory and angiogenesis array. Student's t-test of the replicate $2^{(-\text{Delta Delta CT})}$ method with significant *p-value* as < 0.05. Bonferroni correction was performed to adjust for multiple comparisons of gene expressions

Figure 18 displays total 18 dysregulated genes. A total 4 genes were upregulated and 14 genes were down regulated. CXCL8/IL8, TNFSF4, CXCL1, and S1PR1 were significantly upregulated with mean and standard deviation values (1.85 ± 0.38), (1.52 ± 0.53), (1.8 ± 0.55), (1.47 ± 0.32) and (1.47 ± 0.32) respectively. Other genes were significantly down regulated; ANGPTL4 (-3.39 ± 0.78), CCL2 (-3.43 ± 0.95), CTGF/CCN2 (-2.21 ± 0.56), EDN1 (-2.27 ± 0.62), EFNB2 (-2.1 ± 0.51), EPHB4 (-1.62 ± 0.4), FLT1 (-1.48 ± 0.4), ID1 (-4.15 ± 0.96), JAG1 (-2.09 ± 0.52), PDGFA (-3.59 ± 0.9),

PGF (-2.07 ± 0.51), SERPINE1 (-2.28 ± 0.55), SPHK1 (-1.53 ± 0.38), and VEGFA (-1.78 ± 0.5).

4.4.1.1 DEGs of inflammation

Differentially expressed genes of inflammation are illustrated in Table 9 with their gene name, fold regulation and significant *p-value*. Other details of genes with insignificant p-value are illustrated in the Appendix.

Table 8. Differentially expressed genes (DEGs) of inflammation.

Gene Symbol	Gene Name	Fold regulation	p-value
CXCL8/IL8	Interleukin 8	+1.85	0.037547
TNFSF4	Tumor necrosis factor (ligand) superfamily, member 4	+1.52	0.003728
CCL2	Chemokine (C-C motif) ligand 2	-3.6	0.023179

4.4.1.2 DEGs of Angiogenesis

Differentially expressed genes of angiogenesis are illustrated in Table 10 with their gene name, fold regulation and significant *p-value*. Other details of genes with insignificant p-value are illustrated in the Appendix.

Table 9. Differentially expressed genes (DEGs) of angiogenesis.

Gene Symbol	**Gene Name**	**Fold regulation**	**p-value**
CXCL1	Chemokine (C-X-C motif) ligand 1 (melanoma growth stimulating activity, alpha) – cytokine	+1.8	0.01771
CXCL8/IL8	Interleukin 8	+1.8	0.045896
S1PR1	Sphingosine-1-phosphate receptor 1	+1.47	0.013039
ANGPTL4	Angiopoietin-like 4	-3.39	0.000056
CCL2	Chemokine (C-C motif) ligand 2	-3.43	0.006638
CTGF/CCN2	Connective tissue growth factor	-2.21	0.021852
EDN1	Endothelin 1	-2.27	0.000004
EFNB2	Ephrin-B2	-2.1	0.015109
EPHB4	EPH receptor B4	-1.62	0.005298
FLT1	Fms-related tyrosine kinase 1 (vascular endothelial growth factor (VEGF)/vascular permeability factor receptor)	-1.48	0.027607
ID1	Inhibitor of DNA binding 1, dominant negative helix-loop-helix protein	-4.15	0.000007
JAG1	Jagged 1	-2.09	0.002942
PDGFA	Platelet-derived growth factor alpha polypeptide	-3.59	0.00076
PGF	Placental growth factor	-2.07	0.018385
SERPINE1	Serpin peptidase inhibitor, clade E (nexin, plasminogen activator inhibitor type 1), member 1	-2.28	0.000195
SPHK1	Sphingosine kinase 1	-1.53	0.006278
VEGFA	Vascular endothelial growth factor A	-1.78	0.042835

4.5 IPA core canonical pathways

The most significant pathway related to our study was Hypoxia Inducible Factor **(HIF)** Signaling pathway.

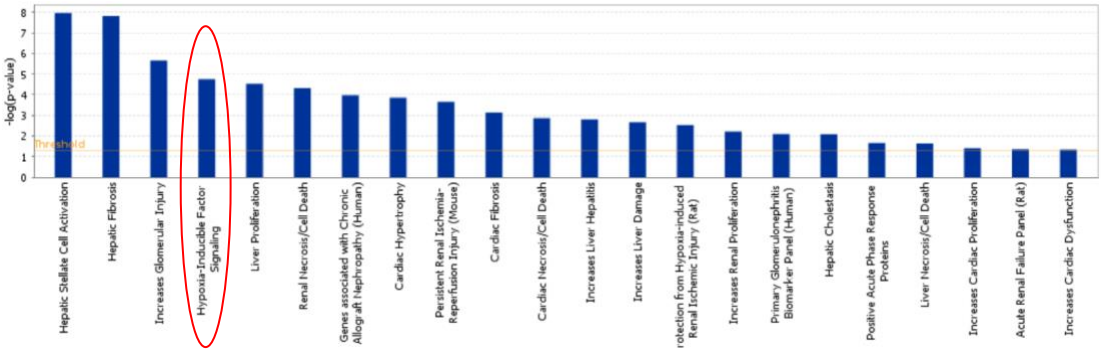

4.5.1 HIF and other signaling pathways

HIF1A signaling interacted with most genes presented by this study (14 genes), either directly or indirectly. These genes were; FLT1, CCL2, CXCL8, VEGF, SERPINE1, SPHK2, EFNB2, PGF, ANGPTL4, CXCL1, PDGFA, S1PR1, TNFSF4, and EPHB4. Figure 19 represents HIF signaling pathways.

The direct and indirect effect by HIF1A is represented as follows:

1- HIF1A has a direct effect on FLT1, CCL2, CXCL8, VEGF, SERPINE1, and SPHK2, and other genes not regulated in this study, such as IL4, ILB, and IL1A.

2- HIF1A has an **i**ndirect effect on EFNB2 and PGF through VEGF-HIF1A pathway, ANGPTL4 through PGF-VEGF pathway, CXCL1, and PDGFA though CCL2-IL1A pathway, S1PR1 though SPHK1-HIF1A, and TNFSF4 and EPHB4 though IL4-HIF1A.

The remaining genes (ID1, EDN1, JAG1, and CTGF/CCN2) interactions are explained in Figure 20. The most significant genes affected were ID1 and EDN1. NOTCH3 (Neurogenic locus notch homolog protein 3) and MYBL2 (Myb-related protein B) signaling pathways interacted directly on ID1 gene. SQSTM1 (sequestosome-1) interacted directly on EDN1 gene. MYBL2 interacted indirectly on both JAG1 and CCN2/CTGF through IFNG- and TGFBR1-MYBL2 pathways. NOTCH3 and MYBL2 interacted indirectly on EDN1 genes through TNF-ID1-NOTCH3 and -MYBL2. SQSTM1 has a direct effect on TNF, which is, in general, has an indirect effect on forth genes EDN1, ID1, JAG1, and CCN2/CTGF.

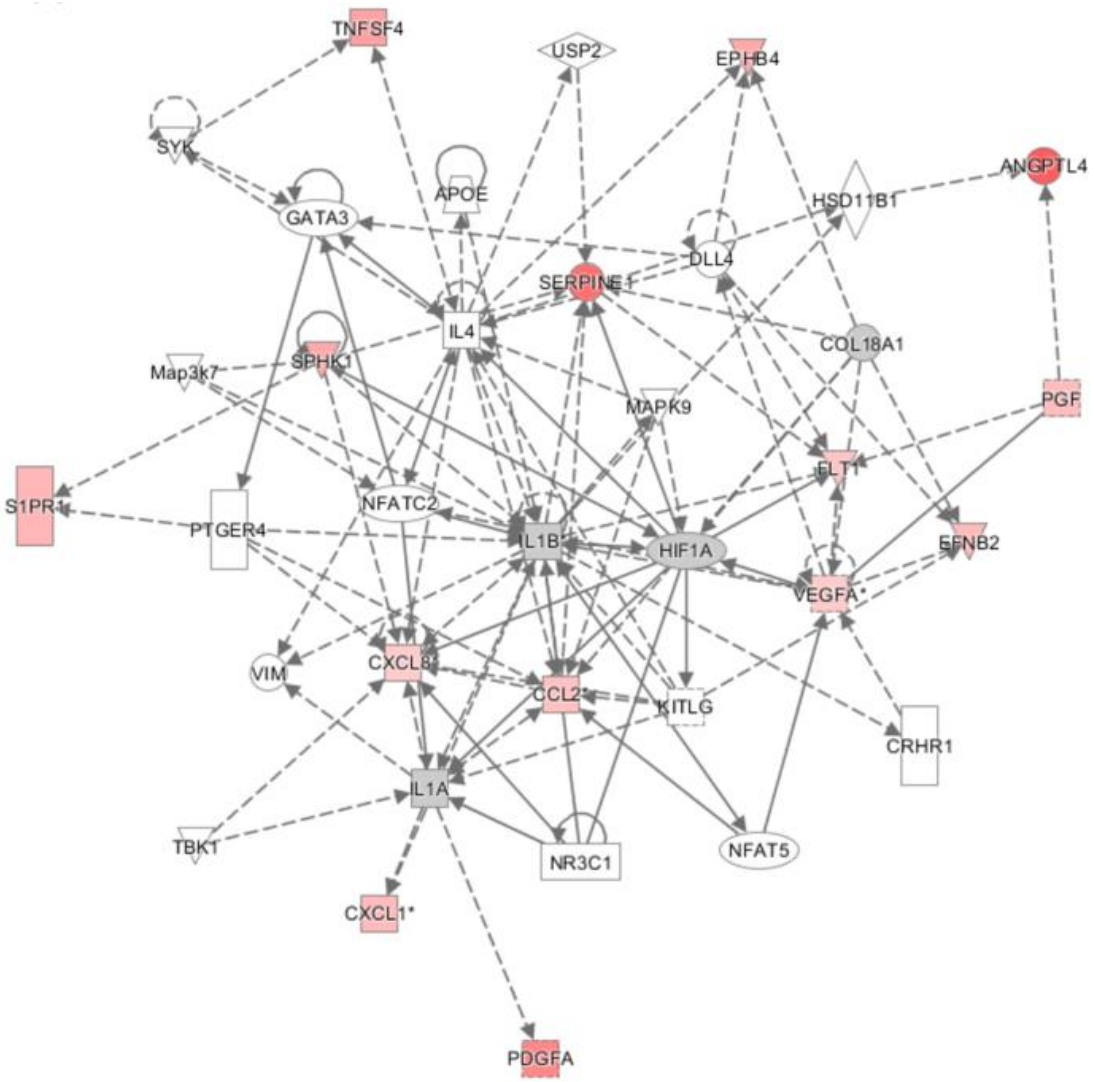

Figure 19. Hypoxia-inducible factor (HIF) singalling pathway.
Arrowhead rigid line represents a direct effect by HIF1A. Arrowhead segmented line represents an indirect effect by HIF1A. Colorful genes are the ones studied. Grey genes are the main effectors of the studied genes.

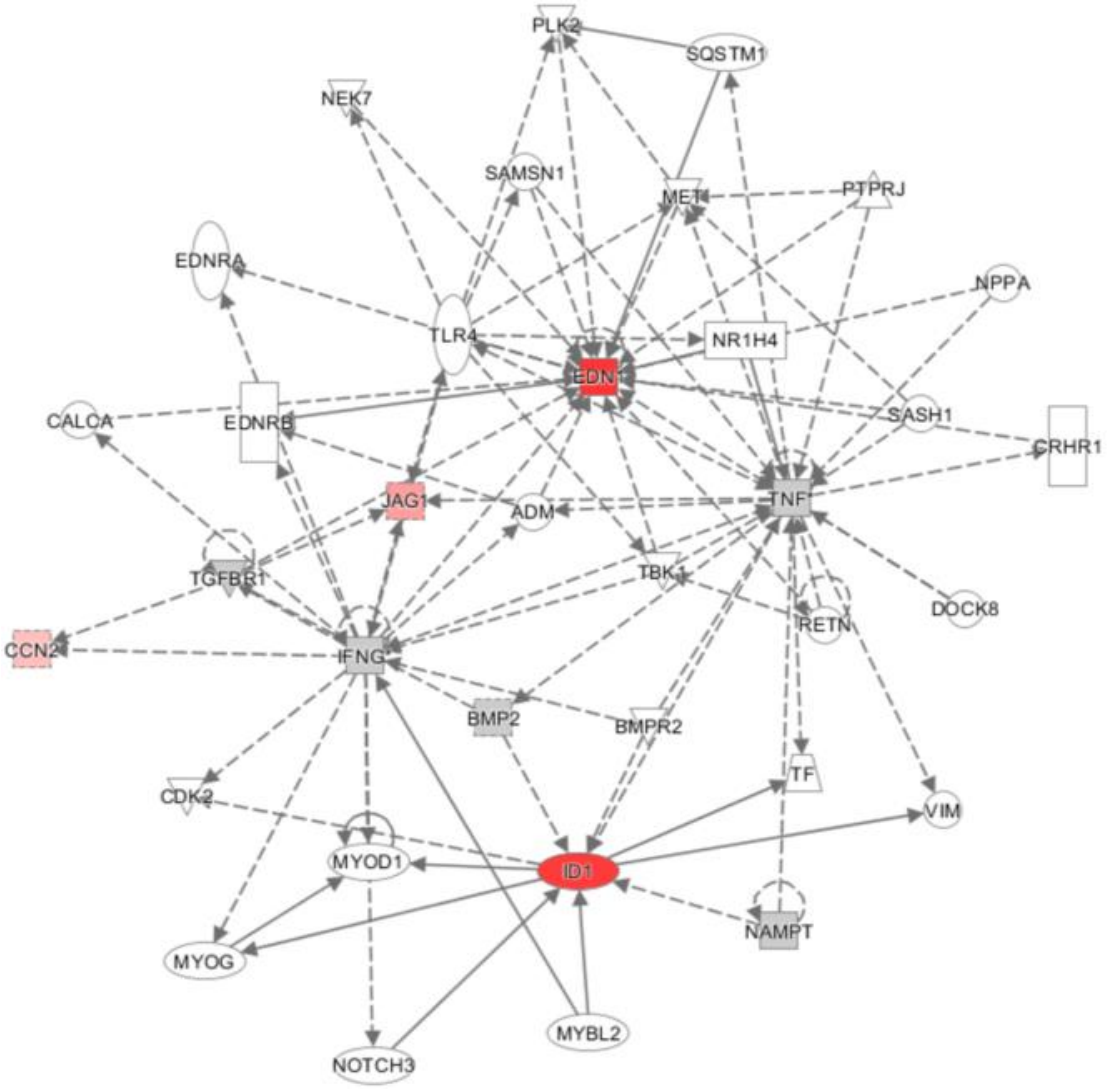

Figure 20. NOTCH3, MYBL2 and SQSTM1 signaling pathway.
Arrowhead rigid line represents a direct effect by HIF1A. Arrowhead segmented line represents an indirect effect by HIF1A. Colorful genes are the ones studied. Grey genes are the main effectors of the studied genes.

Chapter 5: Discussion

Ischemic stroke is an incidental condition of brain neuronal dysfunction due to ischemia with a lack of nutrients and oxygen supply to neuronal cells leading to severe compromise of nervous system functions (The Internet Strokecenter, 2018b) and (Strokecenter; WHO, 2010). Most ischemic stroke models are performed as in-vivo models using animals. However, few studies focused on using in-vitro ischemic stroke model using human cells (Holloway & Gavins, 2016). Although, animal models provide a comprehensive illustration of cellular pathophysiology under ischemic stroke, however, there is 10% difference in the genome between human and animals, which could make different reactions to the same drug tested (Holloway & Gavins, 2016). The advantage of using human cells has been discussed by (Attarwala, 2010), as they illustrated a failure of a clinical trial (TGN1412), where unfortunately, 6 healthy volunteers died, although the drug dose was safe when tested on animal models. However, when it was tested on human cells in-vitro, different reaction was provided by the cells where dramatic release of cytokines was released from the human cells (Attarwala, 2010). Thus, the use of human cells in our study has an advantage of representing the actual biomarker of human.

5.1 Establishment an in-vitro acute ischemic stroke model

5.1.1 Control condition

The control conditions used in our experiments were endothelial cells exposed to 5 mM glucose in normoxia, which could reflect the normal blood level of glucose and oxygen in the human brain. Many studies of OGD experiments utilized media containing high glucose (10 - 25 mM), that is used for growth, to be as control vs. their OGD model (Liao et al., 2016), (Shi et al., 2016), (Niego et al., 2017), (Zhu et al., 2010), and (Li et al., 2016). For more details of these studies, their citations and

others refer to table 3 section 2.4.2.1 in the literature review. Growth media usually have a high level of glucose ranging from (10 – 25 mM), which doesn't represent the normal level of glucose in humans, but to enhance cell proliferation in vitro. The glucose concentration of growth media was discussed earlier by several studies, and they illustrated that glucose level of plasma could range from 2.8 mM (which represents hypoglycemic condition) to 15.2 mM (which represents hyperglycemic/diabetic condition), (Holloway & Gavins, 2016) and (Kleman, Yuan, Aja, Ronnett, & Landree, 2008). Thus, using such growth media (11 – 25 mM) as a control doesn't represent the actual physiological level of normal blood glucose, but it represent a diabetic condition.

In our study, we used classic media that contains (15.76 mM) of glucose to grow our cells to different passages. Thereafter, a human-like pre-conditioning was performed by culturing cells in normal glucose media of 5 mM, followed by incubating cells in different conditions representing the control, OGD or OND.

5.1.2 OGD conditions

Research studies tried to model the ischemic stroke by oxygen glucose deprivation. We tried to use different conditions of OGD using 2 mM glucose media prepared by our lab, glucose-free PBS with or without Ca++ and Mg++ or normal saline with a very low oxygen level for a time duration of 2 hrs. The aim was to induce severe cell injury within this short time to mimic acute ischemic stroke. Up to our knowledge, we are the first to apply the technique of dilution media (2 mM) prepared by our lab. Other studies used a commercially prepared media. Most studies of human cells used glucose-free media or glucose-free balanced salt solutions with absence or very low percentage of oxygen as cited in the following literature (W. Zhang et al., 1999), (Allen et al., 2010), (Liao et al., 2016), and (Shi et al., 2016),

(Niego et al., 2017). The duration of OGD experiments ranged from 1-24 hrs. used in these studies. For more details of these studies, their citations and others refer to table 3 section 2.4.2.1 in the literature review.

Different types of OGD performed in the present study represented with a mild cell injury compared to other studies. Our OGD type of 2 mM glucose represented high viability, around 95%, compared to other studies used nearly similar glucose concentration. The viability of different types of OGD with 2 mM glucose media used in this study are presented in Appendix. Gong, et al. (2019) measured a proliferation of rat brain microvascular cells under OGD with 1.11 mM glucose media for a duration of 4 hrs., where the control or pre-conditioning media was determined for growth (M131 media). Unlike our study, their OGD proliferation decreased to around 45% (Gong et al., 2019). This can be explained by the control/pre-conditioning media used. The control model in terms of glucose concentrations was different between their study and the current study. Gong, et al. (2019) used a growth media (M131) that is known to have high glucose, although normal glucose level in rats are similar to humans; ranging from 3.95 mM to 5.65 mM (Z. Wang et al., 2010), while we used media that contains normal glucose level (5 mM). We believe that the shift of glucose from a high level (11-25 mM) to zero concentration was sharper in their OGD model than ours, where the shift was only from 5 mM to 2 mM; thus, viability results were different between our studies. Furthermore, some studies have reported that the normal brain level of glucose exhibited be lower than the plasma range as represented by 0.16 mM - to 4.5 mM (Kleman et al., 2008) and this could explain why other OGD models of 2 mM we performed in this study could maintain high viability within 2 hrs. of incubation. Additionally, maintaining high viability in

this type of OGD could happen also because of the presence of Ca++ ions that caused delayed cell injury, as will be explained in next section.

5.1.3 OND model

There has been no previous study worldwide that performed our OND-like conditions up to our knowledge. The optimized OND model, manifested the best viability data that are consistent with other OGD results around the world. The model represented a significant increase in number of dead cells (around 43%), while it kept a good number of viable cells (around 45%) that can be used for RNA extraction and gene expression analysis. The absence of glucose, different nutrients; growth factors, amino-acids, and salt ions (Ca++ and Mg++) caused acute and severe cell injury. The reason for the different viability results between normal saline and PBS without Ca++ or Mg++ can be explained by the absence of a buffer system in the saline. NaCl factor itself in the saline could preserve a mechanism for maintaining viability as explained by a study of a hypertonic saline effect on cell viability (S.-L. Chen et al., 2017). Hypertonic saline (which contains NaCl concentration more than the usual 0.9% (154 mM) of isotonic saline) is being used as a therapy for patients who had brain edema, cerebral infarction or trauma. It has the ability to draw fluids back to the intracellular state, thus decreasing the permeability. Also, it decreases the inflammation by suppressing neutrophils activity. Thus, Chen et al. (2017) studied the effect of hypertonic saline on brain endothelial cells, and they found that extra NaCl concentration as 40 mM added over the usual concertation of NaCl found in Balanced Salt Solution (BSS), which is a buffer system that usually contains 137.9 mM, could protect the brain endothelial cells against OGD injury (S.-L. Chen et al., 2017). The final concentration of NaCl assumed to be in their model as 177.9 mM. The authors recorded increased viability and decreased apoptosis with this particular increase in

NaCl concentration compared to other added concentrations of NaCL (10, 20, 80, and 160 mM). Moreover, Chen et al. (2017) studied differentially expressed genes of OGD versus (OGD + 40 mM hypertonic saline), and they detected that genes related to JNK signaling pathway and phosphorylated p38 were significantly upregulated in OGD, whereas, they were down regulated after incubation in hypertonic saline (S.-L. Chen et al., 2017). Thus, as explained previously, this could support our findings that OND model, although using isotonic saline, in hypoxic conditions could cause severe cell injury to model *in-vitro* ischemic stroke, but at the same time keeping a good percentage of cells alive to be analyzed for gene expression and the actin stain.

5.1.3.1 Possible mechanisms of cell injury

One of the possible mechanisms of cell injury that could happen to viable cells under OND model was autophagy. Autophagy is a way that cells try to survive under stress, such as hypoxia, starvation, etc. The cell removes old and damaged proteins and organelles by enclosing them in vesicles fused with the lysosome (phagosome) that have enzymes to degrade the inner materials. This mechanism doesn't evoke an inflammatory response (Kalogeris, Baines, Krenz, & Korthuis, 2012). It was illustrated that most genes of inflammation array were not upregulated, which could support the phenomena of the autophagy mechanism.

5.1.3.2 Biochemical analysis

Incubation of the endothelial cells in OND conditions caused the pH to decrease to an acidic level in contrast to the endothelial cells exposed to normal conditions of glucose and oxygen levels. Saline acidity was studied by (Cheung-Flynn et al., 2019) to investigate if it can be given to patients with serious medical conditions. Cheung-Flynn et al. (2019) used pocrine hemorrhage animal model to study the effect of saline infusion on blood pH. It was found that saline caused

decrease in the blood pH down to 7.3. Additionally, Cheung-Flynn et al. (2019) studied the effect of saline acidity in cell culture conditions different than our conditions. They used human saphenous vain endothelial cells, which are cells found in a superficial vain in human leg, and they exposed cells to saline for 2 hrs. in normoxia, with no effect of hypoxia. Furthermore, viability of cells were not measured by their study. Endothelial dysfunction was recorded to happen in their cells under saline, through the increased measurements of lactate dehydrogenase activity, the ATP release extracellularly, and the activation of p38 MAPK pathway. Furthermore, cells had decreased transendothelial resistance that indicated a loss of membrane integrity. The same study used the actin stain and detected changes in morphology after 2 hrs. of saline treatment (Cheung-Flynn et al., 2019). Thus, the results of such a study by Cheung-Flynn et al. (2019), was in parallel with the current study regarding actin filament changes and biochemical analysis which support the model (OND) used in the current study is causing severe cell injury.

5.1.4 Actin staining of different types of OGD and OND

We observed phenotype changes in response to OND condition used in the present study on the cytoskeleton by staining of the actin filaments (Figures 15 and 16). This observation was based on the abnormal firm attachment of brain endothelial cells to the culture plate with resistance to the proteolytic action of trypsin enzyme compared to the cells exposed to normal conditions. Actin filaments are connected to the tight junctions of the endothelial cells of the blood-brain barrier, and any disruption of these junctions affect the shape of these filaments, with consequent formation of stress fibers (Jiang et al., 2018). Several studies applied the actin staining as an indication of endothelial dysfunction and BBB disruption (Shi et al., 2016), (Abdulkadir et al., 2020) and (Jessick et al., 2013). The results of these studies demonstrated that the presence of thick actin filaments or stress fibers after OGD is indicative of the cell injury.

Cheung-Flynn et al. (2019) studied the actin filaments of human saphenous vain endothelial cells exposed to normal saline under normoxia and it was demonstrated change in cell shape compared to their control, but with a different pattern than our cells under OND conditions (Cheung-Flynn et al., 2019). Furthremore, Abdulkadir et al. (2020) studied the actin filaments of human brain microvascular endothelial cells under of OGD with glucose-free RPMI (Abdulkadir et al., 2020). Compared to our study, their actin filaments represented similar pattern to our OGD types of 2 mM glucose media / PBS with Ca++ and Mg++. Shi et al. (2016) studied the actin filametns and cadherins changes in primary human brain microvascular endothelial cells under OGD condition. They found increase in the actin stress fiber under OGD duration of 1 and 3 hrs. with decrease in cadherins stain

expression. The decrease in cadherins expression and increase in stress fiber indicated BBB disruption and increased permeability (Shi et al., 2016).

In conclusion, the actin stain pattern resulted by our OND model was not similar to any other OGD pattern of other studies explained so far. Therefore, we concluded that the actin staining of OND model represented severe and acute cell injury occurred to the cells compared to other studies and also to other OGD types performed in the present study; either 2 mM glucose media or PBS **with** Ca++ and Mg++.

5.2 Gene expression of the established OND model

Gene function based on information collected from (https://www.uniprot.org) are illustrated in table 10 and 11. It was illustrated that 3 genes related to inflammation were upregulated (CXCL8/IL8, TNFSF4, and CXCL1) that had a function in chemotaxis. They enhance the peripheral immune response to the site of injury, so they attract neutrophils and T-cells mainly.

Moreover, two genes related to actin filaments, S1PR1, and ANGPTL4, were upregulated and down regulated, respectively. S1PR1 gene, which was upregulated, is known to form lamellipodia, which is an actin sheet projection that protrudes from the cell ends and acts like a pod/foot, while on the other hand, ANGPTL4, was downregulation, which is known to inhibit stress fiber in normal condition. This support our findings that OND model could induce severe stress to the cells evidenced by gene expression and by experimental results of actin as shown by Figure 15 and 16 in the results section.

Several genes related to angiogenesis, proliferation, migration, survival, and cell growth were down regulated (EFNB4, SPHK1, EPHB4, FLT1, ID1, JAG1, PDGFA, PGF, SERPINE1, and VEGFA). In contrast to other ischemic stroke studies,

VEGF gene expression was different than our study. Zhang et al. (2017) (H. T. Zhang et al., 2017)performed *in-vivo* ischemic stroke model using the middle cerebral artery occlusion (MCAO) in rats. VEGF was significantly increased in MCAO model with significant decrease in occludin biomarker which indicated BBB disruption. On the other hand, a neutralizing antibody against VEGF was used and it caused a decrease in VEGF and an increase in occludin expression, which indicated recovery of BBB function (H. T. Zhang et al., 2017). In our study, VEGF expression was downregulated, which could indicate increased expression of tight junctions/occludin, and absence of BBB disruption. Thus, it could be concluded that cells had a way of a protective mechanism against this severe ischemia, that they reacted differently to other studies.

Moreover, several genes that inhibit apoptosis were down regulated, such as ID1 and SPHK1. Several genes related to cell adhesions were down regulated, such as (ANGPTL4, EFNB4, EPHB4, and SERPINE1). Several genes related to the regulation of Ca++ mobilization were down regulated, such as CCL2 and JAG1. In contrast to our study, CCL2 was reported to play a role in Ca++ mobilization that causes influx Ca++ into the cells (Kristián & Siesjö, 1998). The influx of Ca++ during stress plays a role in delayed cell injury and thus will increase cell survival (Kristián & Siesjö, 1998) and (Goldberg & Choi, 1993). However, here in our model, Ca++ ion was absent from the extracellular region; thus, influx wasn't applicable, and this could trigger down regulation of CCL2 gene and thus severe cell injury occurred to our model represented by actin stain. As explained previously, removal of Ca++ from the exposure media could cause severe neuronal injury and enhanced death (Goldberg & Choi, 1993).

For more details about each function and gene regulation, adapted from (https://www.uniprot.org), refer to table 10 and 11.

Table 10. Inflammatory genes function.

Gene Symbol	Gene Name and function	Fold regulation	p-value
CXCL8/IL8	**Interleukin 8** Chemotactic factor that attracts neutrophils, basophils, and T-cells but not monocytes. Activates neutrophil.	**+1.85**	0.037547
TNFSF4	**Tumor necrosis factor (ligand) superfamily, member 4** Mediates adhesion of activated T cell antigen presenting cells to endothelial cells. Co-stimulate T-cell proliferation and cytokine production.	**+1.52**	0.003728
CCL2	**Chemokine (C-C motif) ligand 2** Chemotactic factor for monocytes and basophils but not neutrophils or eosinophils. It induces the mobilization of intracellular calcium ions.	-3.6	0.023179

Table 11. Angiogenic genes functions.

Gene Symbol	Gene Name and Function	Fold regulation	p-value
CXCL1	**Chemokine (C-X-C motif) ligand 1 (melanoma growth stimulating activity, alpha) – cytokine** Chemotactic factor for neutrophils. Growth factor that signals through G-protein-coupled receptor – CXC receptor 2	**+1.8**	0.01771
CXCL8/IL8	**Interleukin 8** Chemotactic factor that attracts neutrophils, basophils, and T-cells but not monocytes. Activates neutrophil-potent angiogenic factor.	**+1.8**	0.045896

Gene Symbol	Gene Name and Function	Fold regulation	p-value
S1PR1	**Sphingosine-1-phosphate receptor 1** Highly expressed in endothelial cells. Inhibits sprouting angiogenesis and regulates vascular maturation. Plays a role in cell migration via reorganization of the actin cytoskeleton. It activates Sphingosine kinase SPHK1. It forms **Lamellipodia** which is an **actin** sheet projection on the leading edge if the cells that act like a pod/foot.	**+1.47**	0.013039
ANGPTL4	**Angiopoietin-like 4** **It inhibits adhesion** of endothelial cells to the extracellular matrix. **Inhibits** the formation of **actin stress fibers** and reorganization of the actin cytoskeleton.	**-3.39**	0.000056
CCL2	**Chemokine (C-C motif) ligand 2** Chemotactic factor for monocytes and basophils but not neutrophils or eosinophils. It induces the mobilization of intracellular calcium ions.	-3.43	0.006638
CTGF	**Connective tissue growth factor** Secreted by vascular endothelial cells. It is mitoattractant. **Mediates cells adhesion** by heparin or divalent cation such as Ca++ or Mg++. It induces DNA synthesis.	-2.21	0.021852
EDN1	**Endothelin 1** Vasoconstrictor peptides secreted by Endothelial cells.	-2.27	0.000004
EFNB2	**Ephrin-B2** Cell surface transmembrane ligand for Eph receptor of tyrosine kinases. It plays a role in Angiogenesis and neurogenesis. It **regulates cell adhesion**, differentiation and migration.	-2.1	0.015109
EPHB4	**EPH receptor B4** Transmembrane tyrosine kinase receptor of Ephrin-B. **Regulates adhesion** and migration. Plays a role in angiogenesis, blood vessel remodeling, and permeability.	-1.62	0.005298

Gene Symbol	Gene Name and Function	Fold regulation	p-value
FLT1	**Fms-related tyrosine kinase 1 (vascular endothelial growth factor (VEGF)/vascular permeability factor receptor)** Tyrosine kinase cell surface receptor for VEGF and Placental Growth Factor (PGF). It is a chemotactic factor. Plays a role in cell migration and angiogenesis. Promotes the proliferation and survival of the endothelial cell.	-1.48	0.027607
ID1	**Inhibitor of DNA binding 1, dominant negative helix-loop-helix protein** Negatively regulates transcription activity by forming heterodimer that inhibits the binding of the transcription factor to the DNA—involved in many cell processes such as cell growth, differentiation, angiogenesis, and **apoptosis**.	-4.15	0.000007
JAG1	**Jagged 1** It is a ligand that binds to Notch protein cell surface receptor and to calcium ions. Enhances angiogenesis through fibroblast growth factors in an *in-vitro*.	-2.09	0.002942
PDGFA	**Platelet-derived growth factor alpha polypeptide** Growth factor that regulates cell proliferation, migration, survival, and chemotaxis.	-3.59	0.00076
PGF	**Placental growth factor** Growth factor that bind to FLT1 and VEGF receptors. Stimulates endothelial cell growth, angiogenesis, proliferation and migration.	-2.07	0.018385
SERPINE1	**Serpin peptidase inhibitor, clade E (nexin, plasminogen activator inhibitor type 1), member 1** It inhibits tissue plasminogen activator. Regulates **cell adhesion** and migration. It is responsible for the controlled degradation of blood clots.	-2.28	0.000195

Gene Symbol	Gene Name and Function	Fold regulation	p-value
SPHK1	**Sphingosine kinase 1** Catalyzes the phosphorylation of Sphingosine which forms Sphingosine 1-phosphate (SPP). It enhances cell growth and **inhibits apoptosis**. It regulates the inflammatory response and neuroinflammation.	-1.53	0.006278
VEGFA	**Vascular endothelial growth factor A** Growth factor that binds to FLT1 and VEGF receptors. It regulates angiogenesis and vasculogenesis. It induces proliferation and migration of endothelial cells and permeabilization of blood vessels.	-1.78	0.042835

5.3 Core signaling pathway of the established OND model

The main signaling pathway regulator in our study was HIF1A gene. HIF1 was reported to have an essential function in hypoxic conditions (Ziello, Jovin, & Huang, 2007). HIF1 promotes the survival of cells through increasing vascularization and angiogenesis, maintaining homeostasis, and shifting the metabolism to an anaerobic pathway. HIF1A is known to get inhibited in normoxia and get activated in hypoxia. Prolyl hydroxylase degrades HIF1A in normoxic condition, however in hypoxia, prolyl hydroxylase gets inhibited, thus HIF1A factor keeps activated. Several studies reported an increase of HIF1A factor under OGD condition (Niu et al., 2018) and (Novak, Jones, & Elliott, 2019). Furthermore, an indication of the HIF1A factor activation can be determined by the expression of VEGF gene (Novak et al., 2019). However, in our study, most genes of angiogenesis that were regulated by HIF1A; ANGPTL4, CCL2, EFNB3, EPHB4, FLT1, PDGFA, PGF, SERPINE1, SPHK1, and VEGFA, were down regulated, which indicates an inhibition of HIF1A factor in OND model. The evidence of inhibited HIF1A signaling pathway was represented through the experimental work, where the viability of cells decreased, and

the cellular death increased. HIF1A gene expression in our study was 1.02 with *p-value* > 0.05 which indicated no change in the gene expression in reference to control. Results are represented in table 15 in the Appendix. The inconsistent results between the inhibition of HIF1A factor by the core signaling pathway analysis and with the level of expression in gene array, could be explained by several factors. We assume that during hypoxia, HIF1A was down regulated by some other regulators similar to prolyl hydroxylase, however, once cell culture plate was moved to hood, it was exposed to normoxia, which could make further stress over the cells, thus, these regulators got inhibited and a slight insignificant increase in HIF1A factor could happen. Furthermore, time factor could be the reason for stabilizing HIF1A in hypoxia, other OGD studies has HIF1A factor activated after 5 and 6 hrs. of OGD (Niu et al., 2018) and (Novak et al., 2019). These two assumptions needed to be tested by different ways in the laboratory as available explanations available in the existent literature.

Different studies reported the importance of activation of HIF1A factor as a mechanism for therapy against ischemic injury (Bopp & Lettieri, 2008). An activation of HIF1A factor can be performed to reduce the injury by ischemia through the inhibition of the protein that usually works to degrade HIF1A factor. The inhibition of prolyl hydroxylase (that usually degrades HIF1A) would stabilize the HIF1A protein; thus, the signaling pathway would activate the upregulation of pro-survival genes (such as VEGF) which can increase vascularization and growing of new vessels to reach oxygenated area (Bopp & Lettieri, 2008).

Moreover, NOTCH3 signaling pathways caused downregulation of the expression of angiogenic genes (JAG1, ID1, EDN1, and CCN2/CTGF). NOTCH3 knockout mice with the myocardial ischemic condition were studied by (Tao et al.,

2017), and it was reported that absence of NOTCH3 signaling caused a decrease in the angiogenesis genes expression and an increase in the apoptosis. Moreover, mutation of NOTCH3 gene was reported in several studies to cause an inherited condition of ischemic stroke in the early age of life from (30-50 of age), although with an absence of any other risk factors of stroke (Gallardo et al., 2020) and (Joutel et al., 1996). Activation of NOTCH signaling pathway was reported to be protective against ischemic heart disease (Nistri, Sassoli, & Bani, 2017) as it increases pro-survival signaling, neo-angiogenesis and proliferation decreases apoptosis and oxidative stress. Our OND model represented with inhibition of NOTCH3 signaling as illustrated by the down-regulation genes, which caused severe cell death and decreased survival as illustrated by experimental work; thus, it causes severe cell injury.

Conclusion

The present study aims to explore the pathophysiological changes in signaling pathways underlies such alterations using human brain endothelial cells after exposure to severe stress in a short time in vitro. The aim was to develop an acute severe cell injury under *in-vitro* ischemic stroke conditions. Different OGD types performed in this study represented mild stress that resembles a chronic stroke injury, while OND model resembled an acute stress injury. The major findings of the study were: exposure of the human brain microvascular endothelial cells to severe conditions without glucose and nutrients in the presence of severe hypoxia caused decreased cell vitality parameters associated with marked changes in the cytoskeleton organization with stress change in actin filament fibers. It caused metabolic derangement associated with depletion of lactic acid and marked acidosis. Furthermore, profiling of the gene expression related to the endothelial function biology revealed dysregulation of 20 genes (5 upregulated and 15 down regulated). Major signaling pathways identified were HIF1A and NOTCH3. These signaling pathways mainly affected cell survival, death, angiogenesis, and hemostasis. Gene functions varied from the regulation of cell adhesion, cytoskeleton organization, calcium ion mobilization, and inflammation.

Limitations And Future Prospective

This study has some limitations that can be considered for future studies such as western blot measurements for the tight and adherence junction proteins, trans-endothelial electrical resistance, ATP release measurements, calcium measurements intracellularly and extracellularly, myosin light chain (MLC) phosphorylation, F/G actin ratio measurements.

We believe that conditions of an *in-vitro* ischemic stroke modelling can't be approached to 100% of perfection. However, we can develop our model to contain multiple layers of cells, consisting of different cell types of the brain, such as pericytes, microglial cells, neuronal cells. etc., in order to study cell reaction between each other.

Furthermore, we think about performing our experiments in a developed hypoxia chamber system, where cell culture plates will not be exposed to any oxygen in atmospheric air while transferring them to the hood, to avoid any possible effect on cellular functions.

Moreover, although our control model represented normal blood glucose level (5 mM), however, the level in the brain was investigated to be between 0.16 mM and to 4.5 mM (Holloway & Gavins, 2016). Therefore, we are aiming to optimize our control model to conform to the actual brain glucose level.

We are looking to develop a better way to enhance cell detachment after the experiment of OND model, such as by trying different EDTA-trypsin solutions. Furthermore, we are looking to understand the reason behind the OND cells' reaction to trypsin and MTT and figure out, with test evidence, the explanation behind this behavior. Moreover, we can expand our study to understand the mechanism behind cell viability/death of OGD models we created, and to investigate the role of the PBS

composition, illustrated by table 5, beyond such mechanism.

Finally, we are looking to test a particular drug, such as SGLT2 inhibitors, on our OND model, to investigate if it has a protective effect against acute ischemic stroke. SGLT2 inhibitors are usually used to treat patients with type 2 diabetes. However, several studies are investigating the possibility of using this type of drug to decrease the risk of ischemic stroke in patients (Zinman et al., 2017) and (M. Guo et al., 2018).

REFERENCES

Abdulkadir, R. R., Alwjwaj, M., Othman, O. A., Rakkar, K., & Bayraktutan, U. (2020). Outgrowth endothelial cells form a functional cerebral barrier and restore its integrity after damage. *Neural Regeneration Research, 15*(6), 1071.

Adams Jr, H. P., Bendixen, B. H., Kappelle, L. J., Biller, J., Love, B. B., Gordon, D. L., & Marsh 3rd, E. (1993). Classification of subtype of acute ischemic stroke. Definitions for use in a multicenter clinical trial. TOAST. Trial of Org 10172 in Acute Stroke Treatment. *Stroke, 24*(1), 35-41.

Agouni, A., Parray, A. S., Akhtar, N., Mir, F. A., Bourke, P. J., Joseph, S., . . . Kamran, S. (2019). There is selective increase in pro-thrombotic circulating extracellular vesicles in acute ischemic stroke and transient ischemic attack: a study of patients from the Middle East and Southeast Asia. *Frontiers in neurology, 10*.

Aho, K., Harmsen, P., Hatano, S., Marquardsen, J., Smirnov, V. E., & Strasser, T. (1980). Cerebrovascular disease in the community: results of a WHO collaborative study. *Bulletin of the World Health Organization, 58*(1), 113.

Allen, C., Srivastava, K., & Bayraktutan, U. (2010). Small GTPase RhoA and its effector rho kinase mediate oxygen glucose deprivation-evoked in vitro cerebral barrier dysfunction. *Stroke, 41*(9), 2056-2063.

Alluri, H., Stagg, H. W., Wilson, R. L., Clayton, R. P., Sawant, D. A., Koneru, M., . . . Tharakan, B. (2014). Reactive Oxygen Species-Caspase-3 Relationship in Mediating Blood–Brain Barrier Endothelial Cell Hyperpermeability Following Oxygen–Glucose Deprivation and Reoxygenation. *Microcirculation, 21*(2), 187-195.

Attarwala, H. (2010). TGN1412: from discovery to disaster. *Journal of young*

pharmacists: JYP, *2*(3), 332.

Blann, A. D., Nadar, S. K., & Lip, G. Y. (2003). The adhesion molecule P-selectin and cardiovascular disease. *European heart journal, 24*(24), 2166-2179.

Bonaventura, A., Liberale, L., Vecchié, A., Casula, M., Carbone, F., Dallegri, F., & Montecucco, F. (2016). Update on inflammatory biomarkers and treatments in ischemic stroke. *International journal of molecular sciences, 17*(12), 1967.

Bopp, S. K., & Lettieri, T. (2008). Comparison of four different colorimetric and fluorometric cytotoxicity assays in a zebrafish liver cell line. *BMC pharmacology, 8*(1), 8.

Bowes MP, Z. J., Rothlein R (1993). Monoclonal antibody to the ICAM-1 adhesion site reduces neurological damage in a rabbit cerebral embolism stroke model. *Exp Neurol, 119:215–219*.

Brott, T., & Bogousslavsky, J. (2000). Treatment of acute ischemic stroke. *New England Journal of Medicine, 343*(10), 710-722.

Bustamante, A., López-Cancio, E., Pich, S., Penalba, A., Giralt, D., García-Berrocoso, T., . . . Millan, M. (2017). Blood biomarkers for the early diagnosis of stroke: The stroke-chip study. *Stroke, 48*(9), 2419-2425.

Camós, S., & Mallolas, J. (2010). Experimental models for assaying microvascular endothelial cell pathophysiology in stroke. *Molecules, 15*(12), 9104-9134.

Castellanos, M., Leira, R., Serena, J., Pumar, J. M., Lizasoain, I., Castillo, J., & Dávalos, A. (2003). Plasma metalloproteinase-9 concentration predicts hemorrhagic transformation in acute ischemic stroke. *Stroke, 34*(1), 40-46.

Chen, R.-L., Balami, J. S., Esiri, M. M., Chen, L.-K., & Buchan, A. M. (2010). Ischemic stroke in the elderly: an overview of evidence. *Nature Reviews Neurology, 6*(5), 256.

Chen, S.-L., Deng, Y.-Y., Wang, Q.-S., Han, Y.-L., Jiang, W.-Q., Fang, M., . . . Zeng, H.-K. (2017). Hypertonic saline protects brain endothelial cells against hypoxia correlated to the levels of estimated glomerular filtration rate and interleukin-1β. *Medicine, 96*(1).

Cheung-Flynn, J., Alvis, B. D., Hocking, K. M., Guth, C. M., Luo, W., McCallister, R., . . . Brophy, C. M. (2019). Normal Saline solutions cause endothelial dysfunction through loss of membrane integrity, ATP release, and inflammatory responses mediated by P2X7R/p38 MAPK/MK2 signaling pathways. *PloS one, 14*(8).

Christensen, B. (2014). Modified Rankin Scale Retrieved from https://emedicine.medscape.com/article/2172455-overview

Cowan, K. M., & Easton, A. S. (2010). Neutrophils block permeability increases induced by oxygen glucose deprivation in a culture model of the human blood–brain barrier. *Brain research, 1332*, 20-31.

Cummings, B. S., & Schnellmann, R. G. (2004). Measurement of cell death in mammalian cells. *Current protocols in pharmacology, 25*(1), 12.18. 11-12.18. 22.

Deb, P., Sharma, S., & Hassan, K. (2010). Pathophysiologic mechanisms of acute ischemic stroke: An overview with emphasis on therapeutic significance beyond thrombolysis. *Pathophysiology, 17*(3), 197-218.

El-Hajj, M., Salameh, P., Rachidi, S., & Hosseini, H. (2016). The epidemiology of stroke in the Middle East. *European Stroke Journal, 1*(3), 180-198.

Emsley, H., Smith, C., Georgiou, R., Vail, A., Hopkins, S., Rothwell, N., & Tyrrell, P. (2005). A randomised phase II study of interleukin-1 receptor antagonist in acute stroke patients. *Journal of Neurology, Neurosurgery & Psychiatry,*

76(10), 1366-1372.

Esenwa, C. C., & Elkind, M. S. (2016). Inflammatory risk factors, biomarkers and associated therapy in ischaemic stroke. *Nature Reviews Neurology, 12*(10), 594.

Fisher, C. M. (1958). Intermittent cerebral ischemia. *Cerebral vascular disease. New York: Grune & Stratton*, 81-97.

Foerch, C., Niessner, M., Back, T., Bauerle, M., De Marchis, G. M., Ferbert, A., . . . Kastrup, A. (2011). Diagnostic accuracy of plasma glial fibrillary acidic protein for differentiating intracerebral hemorrhage and cerebral ischemia in patients with symptoms of acute stroke. *Clinical chemistry*, clinchem. 2011.172676.

Foerch, C., Wunderlich, M. T., Dvorak, F., Humpich, M., Kahles, T., Goertler, M., . . . Steinmetz, H. (2007). Elevated serum S100B levels indicate a higher risk of hemorrhagic transformation after thrombolytic therapy in acute stroke. *Stroke, 38*(9), 2491-2495.

Gabay, C. (2006). Interleukin-6 and chronic inflammation. *Arthritis research & therapy, 8*(2), S3.

Gallardo, A., Latapiat, V., Rivera, A., Fonseca, B., Roldan, A., Sandoval, P., . . . Manuel Matamala, J. (2020). NOTCH3 Gene Mutation in a Chilean Cerebral Autosomal Dominant Arteriopathy with Subcortical Infarcts and Leukoencephalopathy Family. In (Vol. 29).

Geng, H.-H., Wang, X.-W., Fu, R.-L., Jing, M.-J., Huang, L.-L., Zhang, Q., . . . Wang, P.-X. (2016). The relationship between C-reactive protein level and discharge outcome in patients with acute ischemic stroke. *International journal of environmental research and public health, 13*(7), 636.

Goldberg, M. P., & Choi, D. W. (1993). Combined oxygen and glucose deprivation in cortical cell culture: calcium-dependent and calcium-independent mechanisms of neuronal injury. *Journal of Neuroscience, 13*(8), 3510-3524.

Gong, P., Li, M., Zou, C., Tian, Q., & Xu, Z. (2019). Tissue Plasminogen Activator Causes Brain Microvascular Endothelial Cell Injury After Oxygen Glucose Deprivation by Inhibiting Sonic Hedgehog Signaling. *Neurochemical research, 44*(2), 441-449.

Group, B. D. W., Atkinson Jr, A. J., Colburn, W. A., DeGruttola, V. G., DeMets, D. L., Downing, G. J., . . . Schooley, R. T. (2001). Biomarkers and surrogate endpoints: preferred definitions and conceptual framework. *Clinical Pharmacology & Therapeutics, 69*(3), 89-95.

Guo, M., Ding, J., Li, J., Wang, J., Zhang, T., Liu, C., . . . Xu, Y. (2018). SGLT2 inhibitors and risk of stroke in patients with type 2 diabetes: A systematic review and meta-analysis. *Diabetes, Obesity and Metabolism, 20*(8), 1977-1982.

Guo, S., Stins, M., Ning, M., & Lo, E. H. (2010). Amelioration of inflammation and cytotoxicity by dipyridamole in brain endothelial cells. *Cerebrovascular diseases, 30*(3), 290-296.

Hamad, A., Hamad, A., Sokrab, T. E. O., Momeni, S., Mesraoua, B., & Lingren, A. (2001). Stroke in Qatar: a one-year, hospital-based study. *Journal of Stroke and Cerebrovascular Diseases, 10*(5), 236-241.

Harrington, E. O., Stefanec, T., Newton, J., & Rounds, S. (2006). Release of soluble E-selectin from activated endothelial cells upon apoptosis. *Lung, 184*(5), 259-266.

Hasan, N., McColgan, P., Bentley, P., Edwards, R. J., & Sharma, P. (2012). Towards

the identification of blood biomarkers for acute stroke in humans: a comprehensive systematic review. *British journal of clinical pharmacology, 74*(2), 230-240.

Hess, J., Angel, P., & Schorpp-Kistner, M. (2004). AP-1 subunits: quarrel and harmony among siblings. *Journal of cell science, 117*(25), 5965-5973.

Hirano, T. (2010). Interleukin 6 in autoimmune and inflammatory diseases: a personal memoir. *Proceedings of the Japan Academy, Series B, 86*(7), 717-730.

Holloway, P. M., & Gavins, F. N. (2016). Modeling ischemic stroke in vitro: status quo and future perspectives. *Stroke, 47*(2), 561-569.

Jessick, V. J., Xie, M., Pearson, A. N., Torrey, D. J., Ashley, M. D., Thompson, S., & Meller, R. (2013). Investigating the role of the actin regulating complex ARP2/3 in rapid ischemic tolerance induced neuro-protection. *International journal of physiology, pathophysiology and pharmacology, 5*(4), 216.

Jiang, X., Andjelkovic, A. V., Zhu, L., Yang, T., Bennett, M. V., Chen, J., . . . Shi, Y. (2018). Blood-brain barrier dysfunction and recovery after ischemic stroke. *Progress in neurobiology, 163*, 144-171.

Jickling, G. C., Ander, B. P., Zhan, X., Noblett, D., Stamova, B., & Liu, D. (2014). microRNA expression in peripheral blood cells following acute ischemic stroke and their predicted gene targets. *PloS one, 9*(6), e99283.

Jickling, G. C., & Sharp, F. R. (2015). Biomarker panels in ischemic stroke. *Stroke, 46*(3), 915-920.

Johnson, W., Onuma, O., Owolabi, M., & Sachdev, S. (2016). Stroke: a global response is needed. *Bulletin of the World Health Organization, 94*(9), 634.

Joutel, A., Corpechot, C., Ducros, A., Vahedi, K., Chabriat, H., Mouton, P., . . . Tournier-Lasserve, E. (1996). Notch3 mutations in CADASIL, a hereditary

adult-onset condition causing stroke and dementia. *Nature, 383*(6602), 707-710. doi:10.1038/383707a0

Kalmarova, K., Kurca, E., Nosal, V., Dluha, J., Ballova, J., Sokol, J., . . . Vadelova, L. (2018). Measurement of platelet p-selectin expression by flow cytometry in patients with acute ischemic stroke. *Acta Medica Martiniana, 18*(1), 14-20.

Kalogeris, T., Baines, C. P., Krenz, M., & Korthuis, R. J. (2012). Cell biology of ischemia/reperfusion injury. In *International review of cell and molecular biology* (Vol. 298, pp. 229-317): Elsevier.

Kaneko, Y., Tajiri, N., Shojo, H., & Borlongan, C. V. (2014). Oxygen–Glucose-Deprived Rat Primary Neural Cells Exhibit DJ-1 Translocation into Healthy Mitochondria: A Potent Stroke Therapeutic Target. *CNS neuroscience & therapeutics, 20*(3), 275-281.

Katan, M., & Elkind, M. S. (2018). The potential role of blood biomarkers in patients with ischemic stroke: An expert opinion. *Clinical and Translational Neuroscience, 2*(1), 2514183X18768050.

Katan, M., Fluri, F., Morgenthaler, N. G., Schuetz, P., Zweifel, C., Bingisser, R., . . . Kappos, L. (2009). Copeptin: a novel, independent prognostic marker in patients with ischemic stroke. *Annals of neurology: official journal of the American Neurological Association and the Child Neurology Society, 66*(6), 799-808.

Katsanos, A. H., Makris, K., Stefani, D., Koniari, K., Gialouri, E., Lelekis, M., . . . Rizos, I. (2017). Plasma glial fibrillary acidic protein in the differential diagnosis of intracerebral hemorrhage. *Stroke, 48*(9), 2586-2588.

Khan, F. Y. (2007). Risk factors of young ischemic stroke in Qatar. *Clin Neurol Neurosurg, 109*(9), 770-773. doi:10.1016/j.clineuro.2007.07.006

Khan, F. Y., Yasin, M., Abu-Khattab, M., El Hiday, A. H., Errayes, M., Lotf, A. K., . . . Alhail, H. (2008). Stroke in Qatar: a first prospective hospital-based study of acute stroke. *J Stroke Cerebrovasc Dis, 17*(2), 69-78. doi:10.1016/j.jstrokecerebrovasdis.2007.11.004

Khoshnam, S. E., Winlow, W., Farbood, Y., Moghaddam, H. F., & Farzaneh, M. (2017). Emerging roles of microRNAs in ischemic stroke: as possible therapeutic agents. *Journal of stroke, 19*(2), 166.

Kleman, A. M., Yuan, J. Y., Aja, S., Ronnett, G. V., & Landree, L. E. (2008). Physiological glucose is critical for optimized neuronal viability and AMPK responsiveness in vitro. *Journal of neuroscience methods, 167*(2), 292-301.

KOCAMAN, G., Dürüyen, H., Kocer, A., & Asil, T. (2015). Recurrent ischemic stroke characteristics and assessment of sufficiency of secondary stroke prevention. *Nöro Psikiyatri Arşivi, 52*(2), 139.

Kristián, T., & Siesjö, B. K. (1998). Calcium in ischemic cell death. *Stroke, 29*(3), 705-718.

Kurzepa, J., Kurzepa, J., Golab, P., Czerska, S., & Bielewicz, J. (2014). The significance of matrix metalloproteinase (MMP)-2 and MMP-9 in the ischemic stroke. *International Journal of Neuroscience, 124*(10), 707-716.

Kwan, J., Horsfield, G., Bryant, T., Gawne-Cain, M., Durward, G., Byrne, C. D., & Englyst, N. A. (2013). IL-6 is a predictive biomarker for stroke associated infection and future mortality in the elderly after an ischemic stroke. *Experimental gerontology, 48*(9), 960-965.

Lachin, J. M., Orchard, T. J., Nathan, D. M., & Group, D. E. R. (2014). Update on cardiovascular outcomes at 30 years of the diabetes control and complications trial/epidemiology of diabetes interventions and complications study. *Diabetes*

care, 37(1), 39-43.

Lagente, V., & Boichot, E. (2008). *Matrix metalloproteinases in tissue remodelling and inflammation*: Springer Science & Business Media.

Langhorne, P., Stott, D., Robertson, L., MacDonald, J., Jones, L., McAlpine, C., . . . Murray, G. (2000). Medical complications after stroke. *Stroke*.

Laskowitz, D. T., Kasner, S. E., Saver, J., Remmel, K. S., Jauch, E. C., & Group, B. S. (2009). Clinical usefulness of a biomarker-based diagnostic test for acute stroke: the Biomarker Rapid Assessment in Ischemic Injury (BRAIN) study. *Stroke, 40*(1), 77-85.

Ley, K. (2003). The role of selectins in inflammation and disease. *Trends in molecular medicine, 9*(6), 263-268.

Li, W., Chen, Z., Yan, M., He, P., Chen, Z., & Dai, H. (2016). The protective role of isorhamnetin on human brain microvascular endothelial cells from cytotoxicity induced by methylglyoxal and oxygen–glucose deprivation. *Journal of neurochemistry, 136*(3), 651-659.

Liao, L.-X., Zhao, M.-B., Dong, X., Jiang, Y., Zeng, K.-W., & Tu, P.-F. (2016). TDB protects vascular endothelial cells against oxygen-glucose deprivation/reperfusion-induced injury by targeting miR-34a to increase Bcl-2 expression. *Scientific reports, 6*, 37959.

Linton, M. F., Yancey, P. G., Davies, S. S., Jerome, W. G. J., Linton, E. F., & Vickers, K. C. (2015). The role of lipids and lipoproteins in atherosclerosis.

Liu, Y., Song, X. D., Liu, W., Zhang, T. Y., & Zuo, J. (2003). Glucose deprivation induces mitochondrial dysfunction and oxidative stress in PC12 cell line. *Journal of cellular and molecular medicine, 7*(1), 49-56.

Lorente, L., Martín, M. M., Abreu-González, P., Ramos, L., Argueso, M., Solé-

Violán, J., . . . Jiménez, A. (2015). Serum malondialdehyde levels in patients with malignant middle cerebral artery infarction are associated with mortality. *PloS one, 10*(5), e0125893.

Lusis, A. J. (2000). Atherosclerosis. *Nature, 407*(6801), 233-241. doi:10.1038/35025203

Maas, M. B., & Furie, K. L. (2009). Molecular biomarkers in stroke diagnosis and prognosis. *Biomarkers in medicine, 3*(4), 363-383.

Marousi, S. G., Theodorou, G. L., Karakantza, M., Zampakis, P., Papathanasopoulos, P., & Ellul, J. (2010). Acute post-stroke adiponectin in relation to stroke severity, progression and 6 month functional outcome. *Neurological research, 32*(8), 841-844.

Miao, Y., & Liao, J. K. (2014). Potential serum biomarkers in the pathophysiological processes of stroke. *Expert review of neurotherapeutics, 14*(2), 173-185.

Milner, R., Hung, S., Wang, X., Berg, G. I., Spatz, M., & del Zoppo, G. J. (2008). Responses of endothelial cell and astrocyte matrix-integrin receptors to ischemia mimic those observed in the neurovascular unit. *Stroke, 39*(1), 191-197.

Molnar, T., Pusch, G., Nagy, L., Keki, S., Berki, T., & Illes, Z. (2016). Correlation of the L-Arginine Pathway with Thrombo-Inflammation May Contribute to the Outcome of Acute Ischemic Stroke. *Journal of Stroke and Cerebrovascular Diseases, 25*(8), 2055-2060.

Montaner, J., Perea-Gainza, M., Delgado, P., Ribó, M., Chacón, P., Rosell, A., . . . Alvarez-Sabín, J. (2008). Etiologic diagnosis of ischemic stroke subtypes with plasma biomarkers. *Stroke, 39*(8), 2280-2287.

Mracsko, E., & Veltkamp, R. (2014). Neuroinflammation after intracerebral

hemorrhage. *Frontiers in cellular neuroscience, 8*, 388.

Mushlin, A. I., Christos, P. J., Abu-Raddad, L., Chemaitelly, H., Deleu, D., & Gehani, A. R. (2012). The importance of diabetes mellitus in the global epidemic of cardiovascular disease: the case of the state of Qatar. *Transactions of the American Clinical and Climatological Association, 123*, 193.

Musuka, T. D., Wilton, S. B., Traboulsi, M., & Hill, M. D. (2015). Diagnosis and management of acute ischemic stroke: speed is critical. *Canadian Medical Association Journal, 187*(12), 887-893.

Narasimhan, P., Liu, J., Song, Y. S., Massengale, J. L., & Chan, P. H. (2009). VEGF Stimulates the ERK 1/2 signaling pathway and apoptosis in cerebral endothelial cells after ischemic conditions. *Stroke, 40*(4), 1467-1473.

National Institute of Health. (2018). Stroke. Retrieved from https://www.nhlbi.nih.gov/health-topics/stroke

Niego, B. e., Lee, N., Larsson, P., De Silva, T. M., Au, A. E.-L., McCutcheon, F., & Medcalf, R. L. (2017). Selective inhibition of brain endothelial Rho-kinase-2 provides optimal protection of an in vitro blood-brain barrier from tissue-type plasminogen activator and plasmin. *PloS one, 12*(5).

NIH. Stroke. *Retrieved on 16/07/2018 from:, https://www.nhlbi.nih.gov/health-topics/stroke*.

Nistri, S., Sassoli, C., & Bani, D. (2017). Notch signaling in ischemic damage and fibrosis: Evidence and clues from the heart. *Frontiers in pharmacology, 8*, 187.

Niu, G., Zhu, D., Zhang, X., Wang, J., Zhao, Y., & Wang, X. (2018). Role of hypoxia-inducible factors 1α (HIF1α) in SH-SY5Y cell autophagy induced by oxygen-glucose deprivation. *Medical science monitor: international medical*

journal of experimental and clinical research, *24*, 2758.

Novak, A. E., Jones, S. M., & Elliott, J. P. (2019). Induction of the HIF pathway: Differential regulation by chemical hypoxia and oxygen glucose deprivation. *bioRxiv*, 525006.

Oza, R., Rundell, K., & Garcellano, M. (2017). Recurrent Ischemic Stroke: Strategies for Prevention. *American family physician*, *96*(7).

Pan, R., Yu, K., Weatherwax, T., Zheng, H., Liu, W., & Liu, K. J. (2017). Blood Occludin Level as a Potential Biomarker for Early Blood Brain Barrier Damage Following Ischemic Stroke. *Sci Rep*, *7*, 40331. doi:10.1038/srep40331

Reynolds, M. A., Kirchick, H. J., Dahlen, J. R., Anderberg, J. M., McPherson, P. H., Nakamura, K. K., . . . Buechler, K. F. (2003). Early biomarkers of stroke. *Clinical chemistry*, *49*(10), 1733-1739.

Richard, S., Lagerstedt, L., Burkhard, P. R., Debouverie, M., Turck, N., & Sanchez, J.-C. (2015). E-selectin and vascular cell adhesion molecule-1 as biomarkers of 3-month outcome in cerebrovascular diseases. *Journal of Inflammation*, *12*(1), 61.

Riss, T. (2017). Is your MTT assay really the best choice. *Promega Corporation website http://www. promega. in/resources/pubhub/is-your-mtt-assay-really-the-best-choice/(Accessed March 19 2018)*.

S Pandya, R., Mao, L., Zhou, H., Zhou, S., Zeng, J., John Popp, A., & Wang, X. (2011). Central nervous system agents for ischemic stroke: neuroprotection mechanisms. *Central Nervous System Agents in Medicinal Chemistry (Formerly Current Medicinal Chemistry-Central Nervous System Agents)*, *11*(2), 81-97.

Sacco, R. L., Kasner, S. E., Broderick, J. P., Caplan, L. R., Culebras, A., Elkind, M. S., . . . Hoh, B. L. (2013). An updated definition of stroke for the 21st century: a statement for healthcare professionals from the American Heart Association/American Stroke Association. *Stroke*, STR. 0b013e318296aeca.

Shaafi, S., Sharifipour, E., Rahmanifar, R., Hejazi, S., Andalib, S., Nikanfar, M., . . . Mehdizadeh, R. (2014). Interleukin-6, a reliable prognostic factor for ischemic stroke. *Iranian journal of neurology, 13*(2), 70.

Shalia, K. K., Mashru, M. R., Vasvani, J. B., Mokal, R. A., Mithbawkar, S. M., & Thakur, P. K. (2009). Circulating levels of cell adhesion molecules in hypertension. *Indian Journal of Clinical Biochemistry, 24*(4), 388.

Shi, Y., Zhang, L., Pu, H., Mao, L., Hu, X., Jiang, X., . . . Liu, X. (2016). Rapid endothelial cytoskeletal reorganization enables early blood–brain barrier disruption and long-term ischaemic reperfusion brain injury. *Nature communications, 7*(1), 1-18.

Shoamanesh, A., Preis, S. R., Beiser, A. S., Kase, C. S., Wolf, P. A., Vasan, R. S., . . . Romero, J. R. (2016). Circulating biomarkers and incident ischemic stroke in the Framingham Offspring Study. *Neurology, 87*(12), 1206-1211.

Simats, A., García-Berrocoso, T., & Montaner, J. (2016). Neuroinflammatory biomarkers: from stroke diagnosis and prognosis to therapy. *Biochimica et Biophysica Acta (BBA)-Molecular Basis of Disease, 1862*(3), 411-424.

Singh, G., Siddiqui, M., Khanna, V., Kashyap, M., Yadav, S., Gupta, Y., . . . Pant, A. (2009). Oxygen glucose deprivation model of cerebral stroke in PC-12 cells: glucose as a limiting factor. *Toxicology mechanisms and methods, 19*(2), 154-160.

Slevin, M., Krupinski, J., Rovira, N., Turu, M., Luque, A., Baldellou, M., . . .

Badimon, L. (2009). Identification of pro-angiogenic markers in blood vessels from stroked-affected brain tissue using laser-capture microdissection. *BMC genomics, 10*(1), 113.

Song, J., Kang, S. M., Lee, W. T., Park, K. A., Lee, K. M., & Lee, J. E. (2014). The beneficial effect of melatonin in brain endothelial cells against oxygen-glucose deprivation followed by reperfusion-induced injury. *Oxidative medicine and cellular longevity, 2014*.

Stanimirovic, D., Shapiro, A., Wong, J., Hutchison, J., & Durkin, J. (1997). The induction of ICAM-1 in human cerebromicrovascular endothelial cells (HCEC) by ischemia-like conditions promotes enhanced neutrophil/HCEC adhesion. *Journal of neuroimmunology, 76*(1-2), 193-205.

Strokecenter. What is a Stroke. *http://www.strokecenter.org/patients/about-stroke/what-is-a-stroke/*.

Sun, Z.-Y., Wang, F.-J., Guo, H., Chen, L., Chai, L.-J., Li, R.-L., . . . Wang, S.-X. (2019). Shuxuetong injection protects cerebral microvascular endothelial cells against oxygen-glucose deprivation reperfusion. *Neural Regeneration Research, 14*(5), 783.

Tao, Y.-K., Zeng, H., Zhang, G.-Q., Chen, S. T., Xie, X.-J., He, X., . . . Chen, J.-X. (2017). Notch3 deficiency impairs coronary microvascular maturation and reduces cardiac recovery after myocardial ischemia. *International journal of cardiology, 236*, 413-422.

Tedder, T., Steeber, D., Chen, A., & Engel, P. (1995). The selectins: vascular adhesion molecules. *The FASEB Journal, 9*(10), 866-873.

The Internet Strokecenter. (2018a). Acute infarction. Retrieved from http://www.strokecenter.org/professionals/stroke-diagnosis/neuropathology-

image-library/acute-infarction/

The Internet Strokecenter. (2018b). What is a stroke. Retrieved from http://www.strokecenter.org/patients/about-stroke/what-is-a-stroke/

Thrift, A. G., Thayabaranathan, T., Howard, G., Howard, V. J., Rothwell, P. M., Feigin, V. L., . . . Cadilhac, D. A. (2017). Global stroke statistics. *International Journal of Stroke, 12*(1), 13-32.

Tiedt, S., Prestel, M., Malik, R., Schieferdecker, N., Duering, M., Kautzky, V., . . . Klein, M. (2017). RNA-Seq identifies circulating miR-125a-5p, miR-125b-5p, and miR-143-3p as potential biomarkers for acute ischemic stroke. *Circulation research, 121*(8), 970-980.

Tornabene, E., Helms, H. C. C., Pedersen, S. F., & Brodin, B. (2019). Effects of oxygen-glucose deprivation (OGD) on barrier properties and mRNA transcript levels of selected marker proteins in brain endothelial cells/astrocyte co-cultures. *PloS one, 14*(8).

Turner, R. J., & Sharp, F. R. (2016). Implications of MMP9 for blood brain barrier disruption and hemorrhagic transformation following ischemic stroke. *Frontiers in cellular neuroscience, 10*, 56.

Vaillant, A. A. J., & Qurie, A. (2018). Interleukin. In *StatPearls [Internet]*: StatPearls Publishing.

Wang, Q., Zhao, W., & Bai, S. (2013). Association between plasma soluble P-selectin elements and progressive ischemic stroke. *Experimental and therapeutic medicine, 5*(5), 1427-1433.

Wang, Z., Yang, Y., Xiang, X., Zhu, Y., Men, J., & He, M. (2010). Estimation of the normal range of blood glucose in rats. *Wei sheng yan jiu= Journal of hygiene research, 39*(2), 133-137, 142.

Whiteley, W., Wardlaw, J., Dennis, M., Lowe, G., Rumley, A., Sattar, N., . . . Sandercock, P. (2012). The use of blood biomarkers to predict poor outcome after acute transient ischemic attack or ischemic stroke. *Stroke, 43*(1), 86-91.

WHO. (2010). Stroke, cerebrovascular accident. *http://www.who.int/topics/cerebrovascular_accident/en/ (last checked 3 August 2010)*.

Woltmann, G., McNulty, C. A., Dewson, G., Symon, F. A., & Wardlaw, A. J. (2000). Interleukin-13 induces PSGL-1/P–selectin–dependent adhesion of eosinophils, but not neutrophils, to human umbilical vein endothelial cells under flow. *Blood, 95*(10), 3146-3152.

Woodruff, T. M., Thundyil, J., Tang, S.-C., Sobey, C. G., Taylor, S. M., & Arumugam, T. V. (2011). Pathophysiology, treatment, and animal and cellular models of human ischemic stroke. *Molecular neurodegeneration, 6*(1), 11.

Xiang, W., Tian, C., Peng, S., Zhou, L., Pan, S., & Deng, Z. (2017). Let-7i attenuates human brain microvascular endothelial cell damage in oxygen glucose deprivation model by decreasing toll-like receptor 4 expression. *Biochemical and biophysical research communications, 493*(1), 788-793.

Xin, J. W., & Jiang, Y. G. (2017). Long noncoding RNA MALAT1 inhibits apoptosis induced by oxygen-glucose deprivation and reoxygenation in human brain microvascular endothelial cells. *Experimental and therapeutic medicine, 13*(4), 1225-1234.

Xu, J., He, L., Ahmed, S. H., Chen, S.-W., Goldberg, M. P., Beckman, J. S., & Hsu, C. Y. (2000). Oxygen-glucose deprivation induces inducible nitric oxide synthase and nitrotyrosine expression in cerebral endothelial cells. *Stroke, 31*(7), 1744-1751.

Xu, T., Zuo, P., Wang, Y., Gao, Z., & Ke, K. (2018). Serum omentin-1 is a novel biomarker for predicting the functional outcome of acute ischemic stroke patients. *Clinical Chemistry and Laboratory Medicine (CCLM), 56*(2), 350-355.

Yang, X., He, X.-Q., Li, G.-D., & Xu, Y.-Q. (2017). AntagomiR-451 inhibits oxygen glucose deprivation (OGD)-induced HUVEC necrosis via activating AMPK signaling. *PloS one, 12*(4).

Yang, X.-y., Gao, S., Ding, J., Chen, Y., Zhou, X.-s., & Wang, J.-E. (2014). Plasma D-dimer predicts short-term poor outcome after acute ischemic stroke. *PloS one, 9*(2), e89756.

Yilmaz, G., & Granger, D. N. (2008). Cell adhesion molecules and ischemic stroke. *Neurological research, 30*(8), 783-793.

Yin, K.-J., Deng, Z., Hamblin, M., Xiang, Y., Huang, H., Zhang, J., . . . Chen, Y. E. (2010). Peroxisome proliferator-activated receptor δ regulation of miR-15a in ischemia-induced cerebral vascular endothelial injury. *Journal of Neuroscience, 30*(18), 6398-6408.

Zafar, A., Al-Khamis, F. A., Al-Bakr, A. I., Alsulaiman, A. A., & Msmar, A. H. (2016). Risk factors and subtypes of acute ischemic stroke: A study at King Fahd Hospital of the University. *Neurosciences, 21*(3), 246.

Zaheer, S., Beg, M., Rizvi, I., Islam, N., Ullah, E., & Akhtar, N. (2013). Correlation between serum neuron specific enolase and functional neurological outcome in patients of acute ischemic stroke. *Annals of Indian Academy of Neurology, 16*(4), 504.

Zhang, H. T., Zhang, P., Gao, Y., Li, C. L., Wang, H. J., Chen, L. C., . . . Jiang, C. L. (2017). Early VEGF inhibition attenuates blood-brain barrier disruption in

ischemic rat brains by regulating the expression of MMPs. *Molecular medicine reports, 15*(1), 57-64.

Zhang, R., Chopp, M., Zhang, Z., Jiang, N., & Powers, C. (1998). The expression of P-and E-selectins in three models of middle cerebral artery occlusion. *Brain research, 785*(2), 207-214.

Zhang, W., Smith, C., Shapiro, A., Monette, R., Hutchison, J., & Stanimirovic, D. (1999). Increased expression of bioactive chemokines in human cerebromicrovascular endothelial cells and astrocytes subjected to simulated ischemia in vitro. *Journal of neuroimmunology, 101*(2), 148-160.

Zhang, Y., Park, T. S., & Gidday, J. M. (2007). Hypoxic preconditioning protects human brain endothelium from ischemic apoptosis by Akt-dependent survivin activation. *American Journal of Physiology-Heart and Circulatory Physiology, 292*(6), H2573-H2581.

Zhang, Y., Wang, T., Yang, K., Xu, J., Ren, L., Li, W., & Liu, W. (2016). Cerebral microvascular endothelial cell apoptosis after ischemia: role of enolase-phosphatase 1 activation and aci-reductone dioxygenase 1 translocation. *Frontiers in molecular neuroscience, 9*, 79.

Zhong, C., Bu, X., Xu, T., Guo, L., Wang, X., Zhang, J., . . . Ju, Z. (2018). Serum Matrix Metalloproteinase-9 and Cognitive Impairment After Acute Ischemic Stroke. *Journal of the American Heart Association, 7*(1), e007776.

Zhong, C., Yang, J., Xu, T., Xu, T., Peng, Y., Wang, A., . . . Ju, Z. (2017). Serum matrix metalloproteinase-9 levels and prognosis of acute ischemic stroke. *Neurology*, 10.1212/WNL. 0000000000004257.

Zhu, D., Wang, Y., Singh, I., Bell, R. D., Deane, R., Zhong, Z., . . . Zlokovic, B. V. (2010). Protein S controls hypoxic/ischemic blood-brain barrier disruption

through the TAM receptor Tyro3 and sphingosine 1-phosphate receptor. *Blood, The Journal of the American Society of Hematology, 115*(23), 4963-4972.

Ziello, J. E., Jovin, I. S., & Huang, Y. (2007). Hypoxia-Inducible Factor (HIF)-1 regulatory pathway and its potential for therapeutic intervention in malignancy and ischemia. *The Yale journal of biology and medicine, 80*(2), 51.

Zinman, B., Inzucchi, S. E., Lachin, J. M., Wanner, C., Fitchett, D., Kohler, S., . . . Johansen, O. E. (2017). Empagliflozin and cerebrovascular events in patients with type 2 diabetes mellitus at high cardiovascular risk. *Stroke, 48*(5), 1218-1225.

APPENDIX

A.1 Experimental work

A.1.1 Viability

A.1.1.1 Live/Dead staining

This technique was not recommended to be used for optimization of OGD models as it is time consuming and needed cell count. Furthermore, cells must be alive while being under the stain and fixation wasn't applicable. Fixation is good for cells who have been under stress, as they will not be under further stress while they are at room temperature, under stain, while investigating by microscope. Cells tend to detach after sometimes while being investigated under microscope. Figure 22 illustrates live dead staining for type of OGD with 2 mM glucose media in PBS with Ca++ and Mg++. Although the technique wasn't applicable, the figure represents nearly similar results of viability between control and OGD.

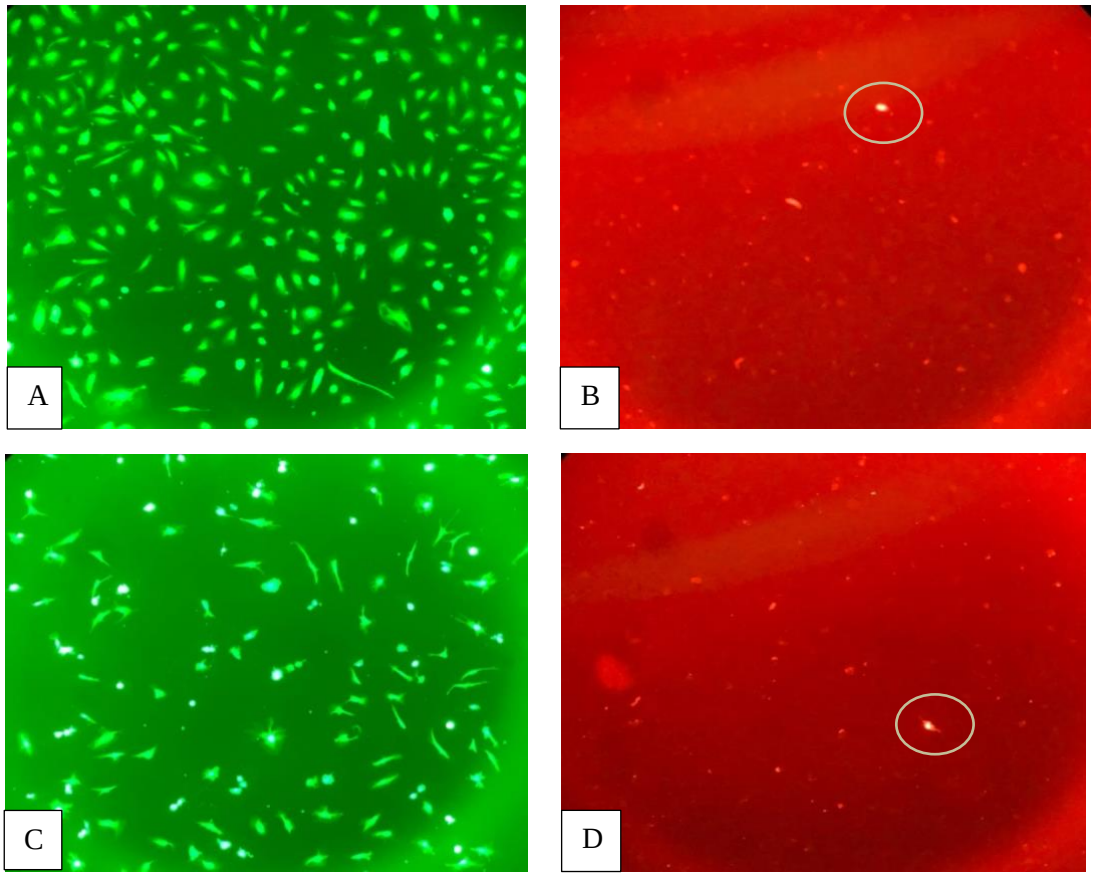

Figure 21. Live/dead staining.
A and B represent control cells. C and D represent OGD exposed cells. Live cells are in green color. Dead cells are in red color.

A.1.1.2 Apoptosis

The results of following types of OGD are represented in Figure 23.

- OGD 1: 2 mM glucose media in PBS **with** Ca++ and Mg++, and hypoxia for 2 hrs. (this type was performed in triplicates and it was illustrated in results section).
- OGD 2: 2 mM glucose media in PBS **without** Ca++ or Mg++, and hypoxia for 2 hrs.
- OGD3: 2 mM glucose media in **saline**, and hypoxia for 2 hrs.
- OGD 4: PBS **with** Ca++ and Mg++, and hypoxia for 2 hrs.
- OGD 5: PBS **without** Ca++ or Mg++, and hypoxia for 2 hrs.
- OGD 6: RPMI media **without** growth factors, and hypoxia for 2 hrs.

All cells incubated under OGD conditions had viability similar to control except cells incubated under PBS without Ca++ or Mg++ where it represents 100% dead cells. Our aim was to induce cell injury, but not to use a model with 100% cell death, as RNA extraction and actin staining wouldn't not be applicable.

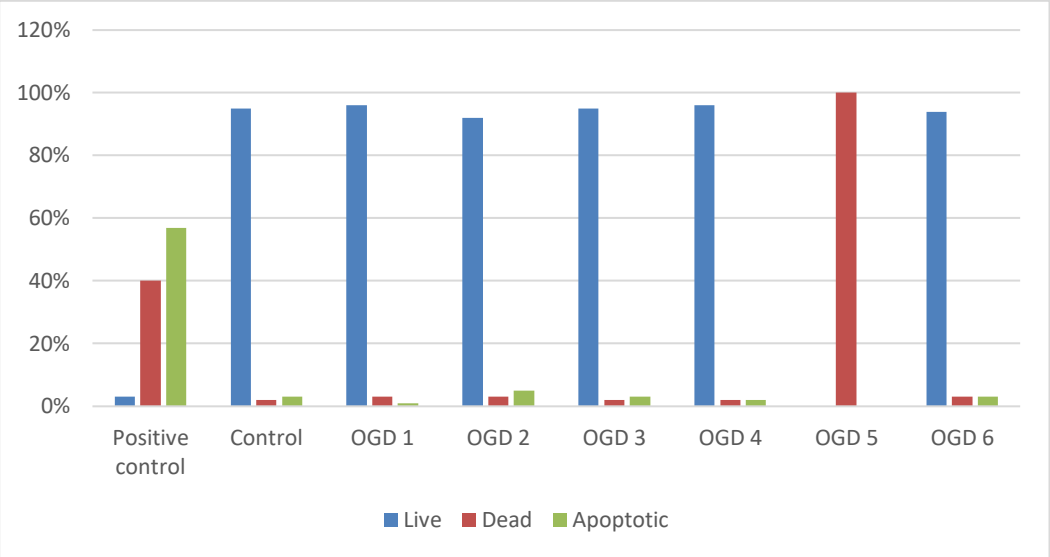

Figure 22. Apoptosis anlaysis with different types of OGD.
Positive control (DMSO treated cells), n1, represented with high dead and apoptotic cells (40% and 57%) respectively. Control (n3), has high viability around 95%. OGD type 1 (n3), type 2 (n1), type 3 (n1), type 4 (n1), and type 6 (n1) represented with similar viability to control. Control and OGD type 1 were performed in triplicates as mentioned previously, and their bar chart is added to results section. OGD type 5 had 100% dead cells and it wasn't applicable to be used for actin staining.

A.1.1.3 MTT test

This technique wasn't recommended to measure viability of OND model as cells were kept intact and were not absorbing MTT stain as illustrated by Figure 24. The viability measurement was not applicable as OND exposed cells readings were similar to the negative control used (which was: media + no cells). OND cells were still firmly attached as indicated by figure below, which concludes that cells still were viable, but possible changes could happen to the cell membrane, that made them resistant to absorb this type of stain. Table 12 illustrates absorption values.

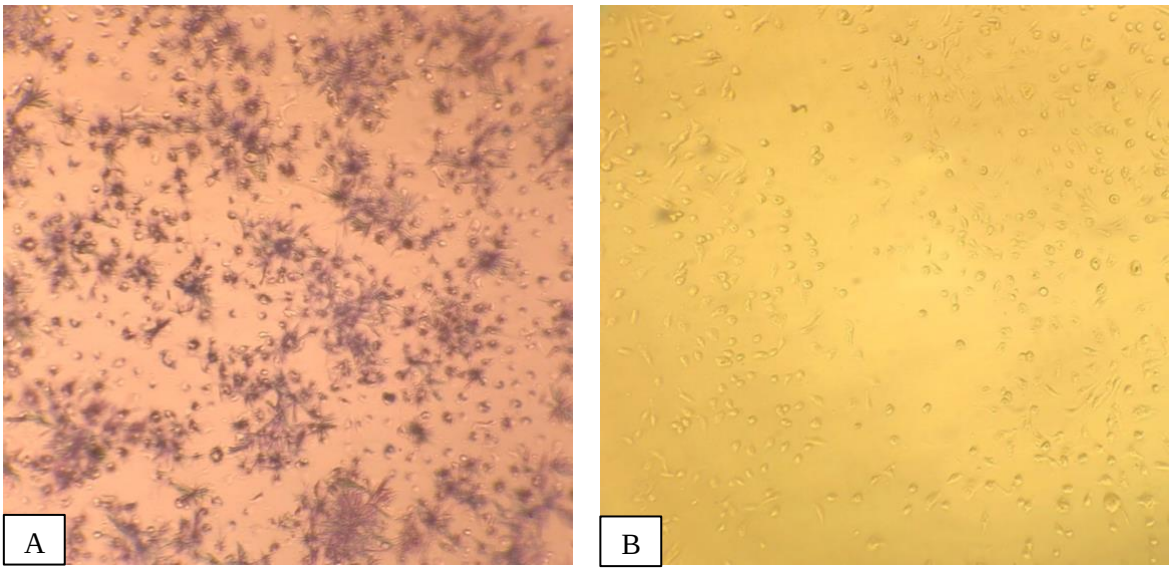

Figure 23. MTT viability test.
A. Control. B. OND exposed cells. Control cells could absorb the stain, in contrast to OND cells which kept intact and didn't absorb the stain.

Absorption values shows no difference between negative control and OND sample (0.115 and 0.114 respectively). Negative control in OND was used as saline only with no cells. OND sample which was cells exposed to saline under hypoxia for 2 hrs. On the other hand, control sample (cells exposed to 5 mM glucose media under normoxia for 2 hrs.) had high absorption (0.417) compared to its negative control (0.145) which represented (5 mM glucose media + No cells).

Table 12. Aborption of MTT for OND model.

Conditions	Control	OND
Negative control (media + no cells)	0.145	0.115
Sample (media + cells)	0.417	0.114

Optimization of MTT using triton couldn't help in increasing absorbance. Furthermore, control exposed to triton had low viability compared to control without trition. Therefore, optimization failed to increase absorption of OND cells to MTT. Figure 25 represents results of control with triton. Figure 26 represents results of OND with triton.

Further optimization was performed. OND exposed cells were incubated in MTT solution with either:

- 2 mM glucose media in saline
- PBS with Ca++ and Mg++
- 2 mM glucose media in PBS without Ca++ or Mg++

Viability of this optimization type wasn't considered as well. Results of cells asportation were not consistent between each type of solution, thus, it was concluded that the method was not valid to use with this type of model. Figure 27 represents the

result. Possible interpretations for such reaction of OND cells under MTT are explained in section A.1.1.3.1.

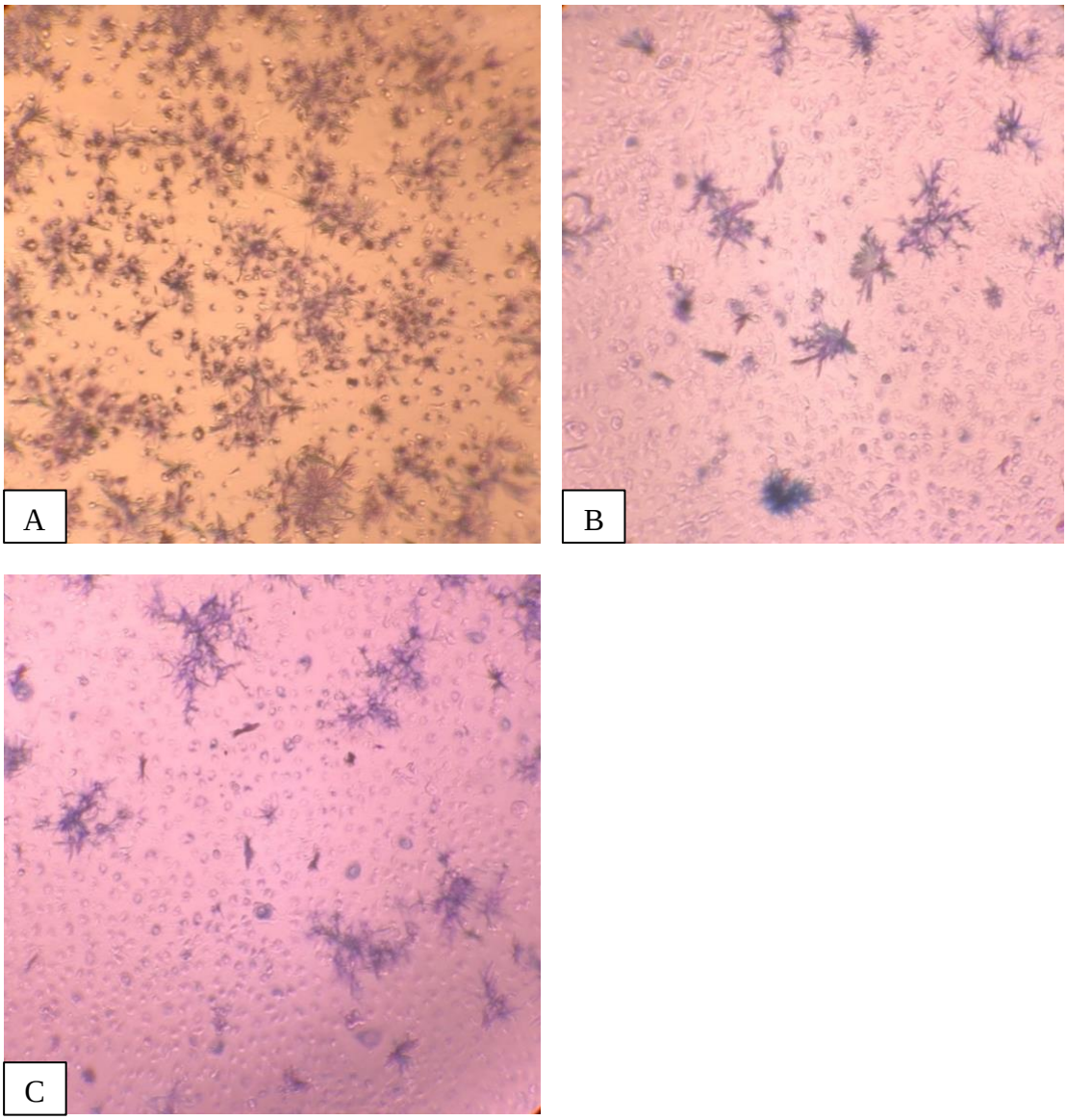

Figure 24. MTT control with triton.
A.Control without triton. B.Control with 0.01% triton. C.Control with 0.001% triton. As illustrated, cells of control with triton has decreased absorption compared to control without triton. Thus, this technique is not valid as triton could kill control cells.

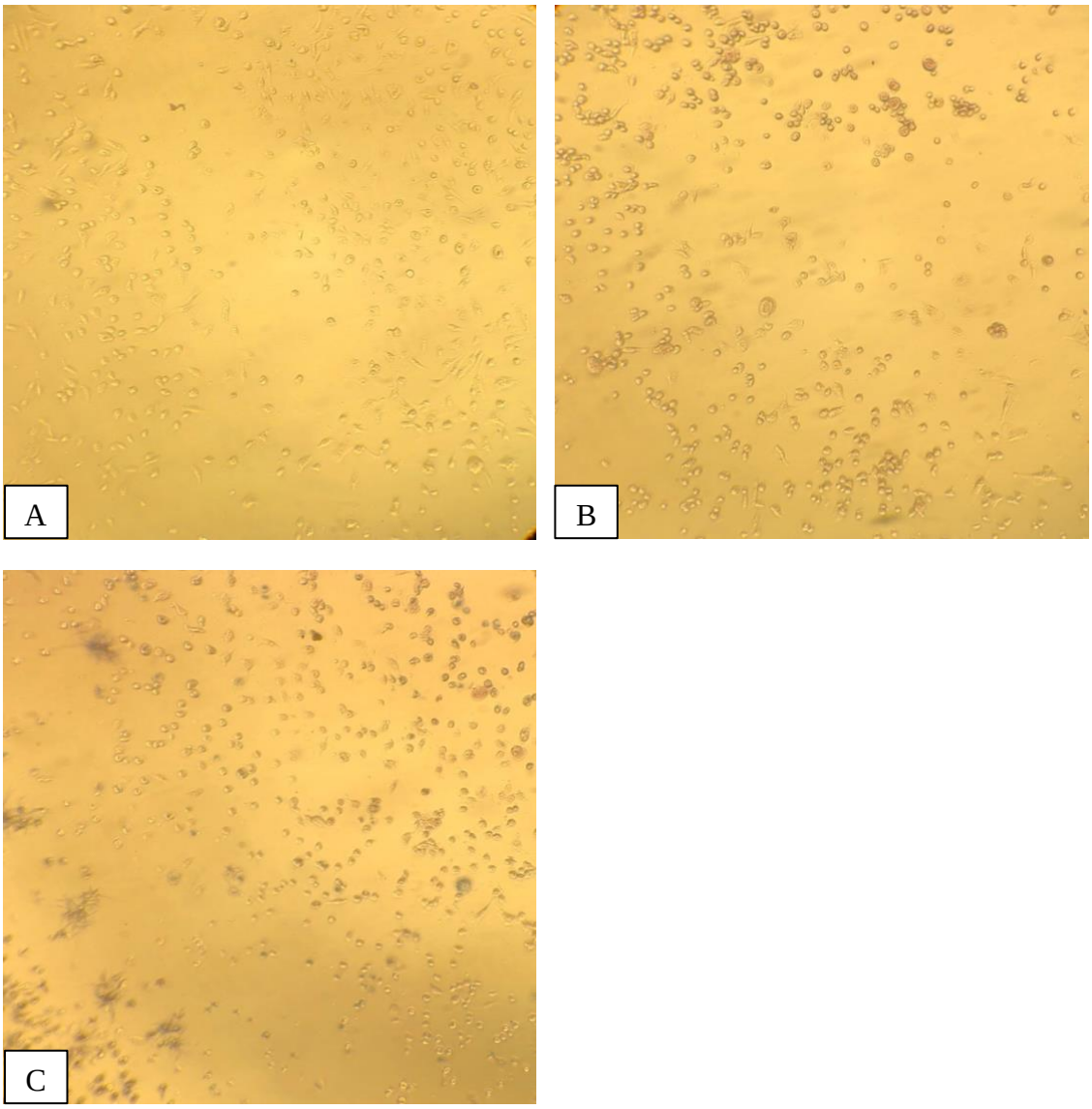

Figure 25. MTT of OND with triton.
A.OND without triton. B. OND with 0.01% triton. C. OND with 0.001% triton. As illustrated, triton didn't help OND cells to absorb MTT, thus viability testing wasn't applicable.

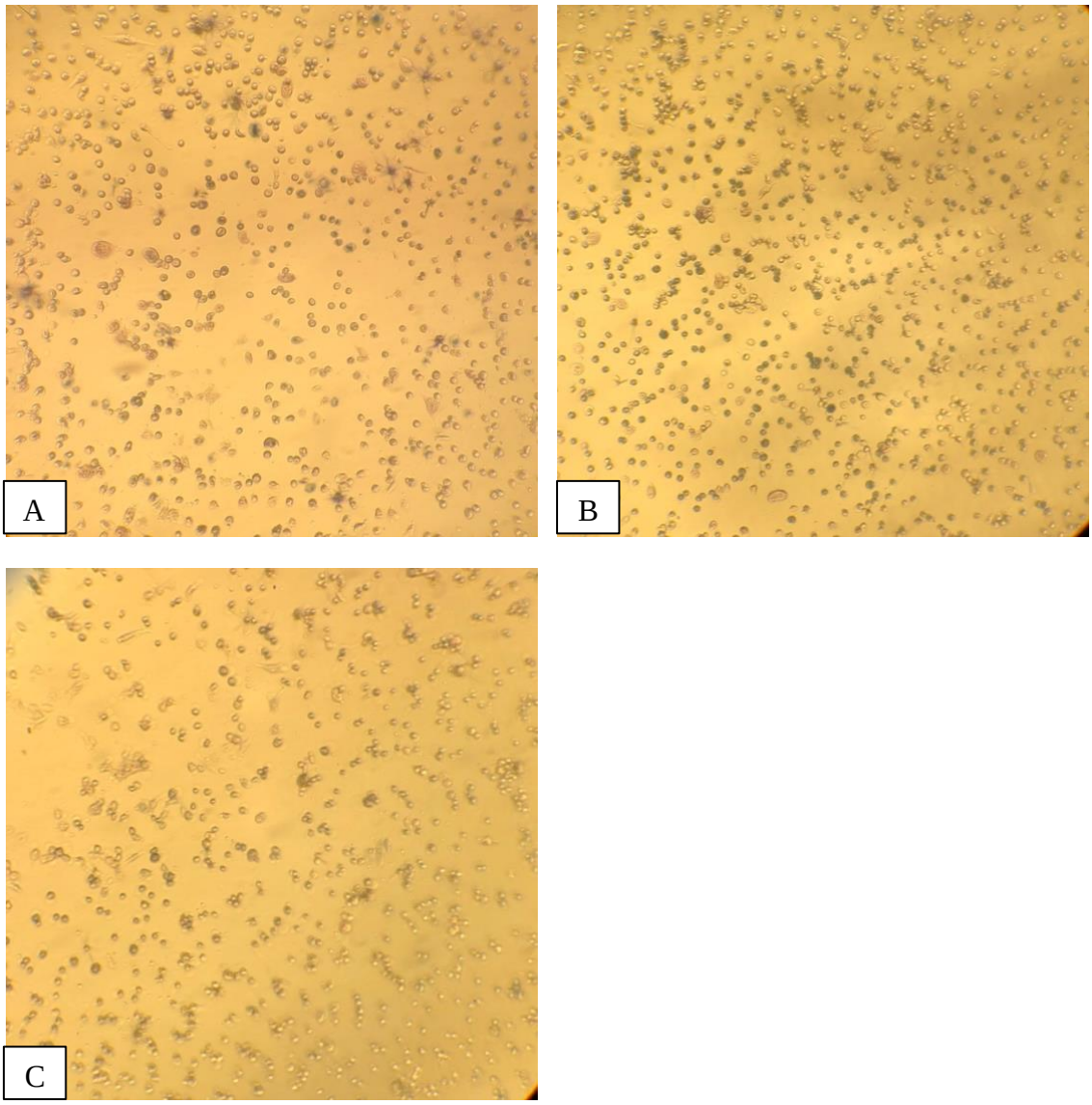

Figure 26. MTT of OND with PBS/media.
A.OND with 2 mM glucose media in saline. B. OND with PBS with Ca++ and Mg++. C. OND 2 mM glucose media in PBS without Ca++ or Mg++. Figures illustrated increased response to MTT in presence of media/buffer solution. However, this method wasn't valid to be used for measuring viability, as results were not consistent, possible interpretation is in next section.

A.1.1.3.1 Possible interpretation of OND cells reactions in MTT

The reason behind the behavior of OND exposed cells to MTT could be explained by the following citations. MTT mechanism was reported by (Bopp & Lettieri, 2008) that it works on the destruction of cells so that the yellow tetrazolium salt by MTT would be reduced by cytosolic and mitochondrial fractions into blue formazan crystals. It was clarified that this technique might not be suitable for different kinds of cell investigations (Bopp & Lettieri, 2008).

Our OND model showed the presence of attached cells under a microscope. This indicates that cells were still alive; however, the MTT mechanism couldn't work properly on this model type. Riss (2017) illustrated that the MTT mechanism reflects cell metabolism and not the number of viable cells. Thus, MTT reduction can be affected by several factors of the culture conditions such as **pH, glucose**, and the physiological condition of the cells (Riss, 2017). Thus, in our reported OND model, the culture condition was acidic, and it lacks glucose, these could affect MTT reduction, and it could cause inhibition of its mechanism. In contrast to OND, MTT could work well on our **control** that had normal pH and normal glucose. Furthermore, our optimization technique using media/PBS conditions along with MTT incubation caused an increase in cell absorption, although wasn't consistent, but it indicated the power of pH to help in MTT reduction, as media/PBS have nearly normal pH.

Riss, (2017) added further, that MTT reduction is not associated only with mitochondria and cytoplasm only, but also with other cell membranes such as endosome/lysosome and plasma membrane. This could explain possible changes in cell membranes that made cells not responding, and other factors affecting MTT mechanism such acidic pH and absence of glucose that could make MTT technique not applicable method to measure viable cells in OND model.

Therefore, we conclude that we do not recommend MTT to measure viability for OND model, we may suggest performing MTT for other types of OGD models, as different studies used this test to measure viability such as (J. Xu et al., 2000) and (Singh et al., 2009).

On the other hand, a question may be raised regarding the mechanism of Annexin V and PI to measure apoptotic and dead cells in OND model. These cell stain mechanisms were successful, and questions may be raised about the reason for their success. First, the apoptosis mechanism could explain such effects. In live cells, phosphatidylserine, a type of phospholipid, is usually translocated in the plasma membrane internally, however in apoptosis, this phosphatidylserine will be translocated extracellularly so membrane structure would change, and it signals for phagocytic cells. Annexin V mechanism relies on the detection of this phosphatidylserine in the presence of calcium and thus can be detected by fluorescent microscope or flow cytometry. Secondly, live, and apoptotic cells membranes are not permeable to a fluorescent dye, like PI which binds to DNA; however, dead cells membrane integrity is lost; thus, the PI stain can reach DNA, and it can be detected by fluorescent microscope or flowcytometry (Cummings & Schnellmann, 2004).

We conclude from this that, in contrast to MTT, apoptosis technique was successful as no need to stain live cells, live cells were detected based on cells that don’t have either PI or Annexin V stain. Furthermore, apoptotic cells, although still having an intact membrane and not permeable, could be stained based on signals that were expressed extracellularly on the cell membrane. It was easy for dead cells to attain PI stain as they lost their membrane integrity and are permeable to such fluorescent reagents.

A.1.2 RNA quality and concentration

Extracted RNA quality was high with a ratio greater than 1.80. The concentration range was from 237 ng/μL to 762 ng/μL. Table 13 shows details of ratio and concentration.

Table 13. RNA quality and concertation.

Sample	260/280 ratio	Concentration (ng/μL)
Control - 1	2	762.9
OGD - 1	2.01	616.5
Control - 2	2.03	508.7
OGD - 2	1.96	245.5
Control - 3	2.01	429
OGD - 3	2	323.4
Control - 4	1.84	238.3
OGD - 4	1.89	237.2

A.2 Data analysis

A.2.1 list of genes

A.2.1.1 List of up- and down regulated genes of inflammation

Genes of inflammation with their fold regulation, p-value and their position on the array are illustration in table 14. The rows of significant genes are highlighted in grey color.

Table 14. Significant and insignificant genes of inflammation.

Position	Symbol	Gene Name	Fold Regulation	p-value
A01	AIMP1	Aminoacyl tRNA synthetase complex-interacting multifunctional protein 1	-1.06	0.512570
A02	BMP2	Bone morphogenetic protein 2	-1.00	0.991343
A03	C5	Complement component 5	1.00	0.951730
A04	CCL1	Chemokine (C-C motif) ligand 1	-2.73	0.550010
A05	CCL11	Chemokine (C-C motif) ligand 11	-1.77	0.818543
A06	CCL13	Chemokine (C-C motif) ligand 13	-1.68	0.622517
A07	CCL15	Chemokine (C-C motif) ligand 15	-2.65	0.624969
A08	CCL16	Chemokine (C-C motif) ligand 16	-1.54	0.479037
A09	CCL17	Chemokine (C-C motif) ligand 17	-1.42	0.473896
A10	CCL2	Chemokine (C-C motif) ligand 2	-3.60	0.022667
A11	CCL20	Chemokine (C-C motif) ligand 20	-1.20	0.916564
A12	CCL22	Chemokine (C-C motif) ligand 22	-1.78	0.564592
B01	CCL23	Chemokine (C-C motif) ligand 23	-1.66	0.704665
B02	CCL24	Chemokine (C-C motif) ligand 24	-2.61	0.492876
B03	CCL26	Chemokine (C-C motif) ligand 26	-1.27	0.651237
B04	CCL3	Chemokine (C-C motif) ligand 3	-2.68	0.530826
B05	CCL4	Chemokine (C-C motif) ligand 4	-1.99	0.649045
B06	CCL5	Chemokine (C-C motif) ligand 5	-1.79	0.748571
B07	CCL7	Chemokine (C-C motif) ligand 7	-1.57	0.725009
B08	CCL8	Chemokine (C-C motif) ligand 8	-1.87	0.760226
B09	CCR1	Chemokine (C-C motif) receptor 1	-1.88	0.786753
B10	CCR2	Chemokine (C-C motif) receptor 2	-1.85	0.480124
B11	CCR3	Chemokine (C-C motif) receptor 3	-1.48	0.757344
B12	CCR4	Chemokine (C-C motif) receptor 4	-1.12	0.786319
C01	CCR5	Chemokine (C-C motif) receptor 5	-1.33	0.720683
C02	CCR6	Chemokine (C-C motif) receptor 6	-1.37	0.726781
C03	CCR8	Chemokine (C-C motif) receptor 8	-1.71	0.833583
C04	CD40LG	CD40 ligand	-1.24	0.727499
C05	CSF1	Colony stimulating factor 1 (macrophage)	-1.06	0.682983
C06	CSF2	Colony stimulating factor 2 (granulocyte-macrophage)	-1.36	0.622245

Position	Symbol	Gene Name	Fold Regulation	p-value
C07	CSF3	Colony stimulating factor 3 (granulocyte)	-2.51	0.224521
C08	CX3CL1	Chemokine (C-X3-C motif) ligand 1	-2.52	0.357882
C09	CX3CR1	Chemokine (C-X3-C motif) receptor 1	-1.58	0.585095
C10	CXCL1	Chemokine (C-X-C motif) ligand 1 (melanoma growth stimulating activity, alpha)	1.49	0.065270
C11	CXCL10	Chemokine (C-X-C motif) ligand 10	-1.79	0.950750
C12	CXCL11	Chemokine (C-X-C motif) ligand 11	-1.40	0.906024
D01	CXCL12	Chemokine (C-X-C motif) ligand 12	-4.02	0.412602
D02	CXCL13	Chemokine (C-X-C motif) ligand 13	-1.65	0.922905
D03	CXCL2	Chemokine (C-X-C motif) ligand 2	1.54	0.072094
D04	CXCL3	Chemokine (C-X-C motif) ligand 3	-1.28	0.984424
D05	CXCL5	Chemokine (C-X-C motif) ligand 5	-1.01	0.804131
D06	CXCL6	Chemokine (C-X-C motif) ligand 6 (granulocyte chemotactic protein 2)	1.01	0.800511
D07	CXCL9	Chemokine (C-X-C motif) ligand 9	-1.48	0.931030
D08	CXCR1	Chemokine (C-X-C motif) receptor 1	-1.55	0.598660
D09	CXCR2	Chemokine (C-X-C motif) receptor 2	-1.51	0.722710
D10	FASLG	Fas ligand (TNF superfamily, member 6)	-2.67	0.818001
D11	IFNA2	Interferon, alpha 2	-2.09	0.956103
D12	IFNG	Interferon, gamma	1.57	0.853230
E01	IL10RA	Interleukin 10 receptor, alpha	-1.56	0.596889
E02	IL10RB	Interleukin 10 receptor, beta	1.05	0.710093
E03	IL13	Interleukin 13	-1.39	0.706204
E04	IL15	Interleukin 15	1.26	0.556158
E05	IL16	Interleukin 16	-1.69	0.663109
E06	IL17A	Interleukin 17A	-2.59	0.940554
E07	IL17C	Interleukin 17C	-1.66	0.397623
E08	IL17F	Interleukin 17F	-1.31	0.906137
E09	IL1A	Interleukin 1, alpha	-1.24	0.495431
E10	IL1B	Interleukin 1, beta	-1.54	0.791133
E11	IL1R1	Interleukin 1 receptor, type I	-1.41	0.373175
E12	IL1RN	Interleukin 1 receptor antagonist	-3.55	0.584177
F01	IL21	Interleukin 21	1.11	0.996279
F02	IL27	Interleukin 27	-2.17	0.148188
F03	IL3	Interleukin 3 (colony-stimulating factor, multiple)	-1.45	0.640308
F04	IL33	Interleukin 33	-1.57	0.668051
F05	IL5	Interleukin 5 (colony-stimulating factor, eosinophil)	-2.21	0.846770

Position	Symbol	Gene Name	Fold Regulation	p-value
F06	IL5RA	Interleukin 5 receptor, alpha	-1.86	0.835818
F07	IL7	Interleukin 7	-1.31	0.920123
F08	CXCL8	Interleukin 8	1.85	0.039416
F09	IL9	Interleukin 9	-2.51	0.574837
F10	IL9R	Interleukin 9 receptor	-1.49	0.775234
F11	LTA	Lymphotoxin alpha (TNF superfamily, member 1)	-1.42	0.539716
F12	LTB	Lymphotoxin beta (TNF superfamily, member 3)	-1.26	0.540534
G01	MIF	Macrophage migration inhibitory factor (glycosylation-inhibiting factor)	1.04	0.694099
G02	NAMPT	Nicotinamide phosphoribosyltransferase	1.13	0.203257
G03	OSM	Oncostatin M	-1.16	0.362248
G04	SPP1	Secreted phosphoprotein 1	-1.08	0.989762
G05	TNF	Tumor necrosis factor	-1.39	0.490385
G06	TNFRSF11B	Tumor necrosis factor receptor superfamily, member 11b	-1.50	0.728671
G07	TNFSF10	Tumor necrosis factor (ligand) superfamily, member 10	1.05	0.792837
G08	TNFSF11	Tumor necrosis factor (ligand) superfamily, member 11	-1.66	0.782264
G09	TNFSF13	Tumor necrosis factor (ligand) superfamily, member 13	-1.27	0.495623
G10	TNFSF13B	Tumor necrosis factor (ligand) superfamily, member 13b	-1.47	0.936008
G11	TNFSF4	Tumor necrosis factor (ligand) superfamily, member 4	1.52	0.004192
G12	VEGFA	Vascular endothelial growth factor A	-1.51	0.101627
H01	ACTB	Actin, beta	-1.06	0.514803
H02	B2M	Beta-2-microglobulin	1.08	0.399438
H03	GAPDH	Glyceraldehyde-3-phosphate dehydrogenase	1.06	0.210562
H04	HPRT1	Hypoxanthine phosphoribosyltransferase 1	-1.08	0.354458
H05	RPLP0	Ribosomal protein, large, P0	-1.00	0.991444

A.2.1.2 List of up- and down regulated genes of angiogenesis

Genes of angiogenesis with their fold regulation, p-value and their position on the array are illustration in table 15. The rows of significant genes are highlighted in grey color.

Table 15. Significant and insignificant genes of Angiogenesis.

Position	Symbol	Description	Fold Regulation	p-value
A01	AKT1	V-akt murine thymoma viral oncogene homolog 1	-1.01	0.851467
A02	ANG	Angiogenin, ribonuclease, RNase A family, 5	-1.13	0.743912
A03	ANGPT1	Angiopoietin 1	1.05	0.811243
A04	ANGPT2	Angiopoietin 2	1.07	0.632287
A05	ANGPTL4	Angiopoietin-like 4	-3.41	0.000040
A06	ANPEP	Alanyl (membrane) aminopeptidase	1.10	0.525001
A07	ADGRB1	Brain-specific angiogenesis inhibitor 1	-2.65	0.286595
A08	CCL11	Chemokine (C-C motif) ligand 11	-1.04	0.410852
A09	CCL2	Chemokine (C-C motif) ligand 2	-3.45	0.006038
A10	CDH5	Cadherin 5, type 2 (vascular endothelium)	-1.28	0.080182
A11	COL18A1	Collagen, type XVIII, alpha 1	-1.19	0.318816
A12	COL4A3	Collagen, type IV, alpha 3 (Goodpasture antigen)	-1.86	0.876882
B01	CTGF	Connective tissue growth factor	-2.22	0.020772
B02	CXCL1	Chemokine (C-X-C motif) ligand 1 (melanoma growth stimulating activity, alpha)	1.79	0.017659
B03	CXCL10	Chemokine (C-X-C motif) ligand 10	-1.26	0.917876
B04	CXCL5	Chemokine (C-X-C motif) ligand 5	-1.05	0.903459
B05	CXCL6	Chemokine (C-X-C motif) ligand 6 (granulocyte chemotactic protein 2)	1.22	0.743874
B06	CXCL9	Chemokine (C-X-C motif) ligand 9	1.24	0.979524
B07	EDN1	Endothelin 1	-2.79	0.000004
B08	EFNA1	Ephrin-A1	1.04	0.827962
B09	EFNB2	Ephrin-B2	-2.12	0.013579
B10	EGF	Epidermal growth factor	-1.13	0.999652
B11	ENG	Endoglin	-1.19	0.316602
B12	EPHB4	EPH receptor B4	-1.63	0.004605
C01	ERBB2	V-erb-b2 erythroblastic leukemia viral oncogene homolog 2, neuro/glioblastoma derived oncogene homolog (avian)	-1.08	0.574684
C02	F3	Coagulation factor III (thromboplastin, tissue factor)	-1.04	0.910626
C03	FGF1	Fibroblast growth factor 1 (acidic)	-1.50	0.719577
C04	FGF2	Fibroblast growth factor 2 (basic)	1.03	0.779340
C05	FGFR3	Fibroblast growth factor receptor 3	-2.34	0.063143
C06	FIGF	C-fos induced growth factor (vascular endothelial growth factor D)	-1.32	0.929128
C07	FLT1	Fms-related tyrosine kinase 1 (vascular endothelial growth factor/vascular permeability factor receptor)	-1.49	0.024350
C08	FN1	Fibronectin 1	-1.27	0.303534
C09	HGF	Hepatocyte growth factor (hepapoietin A; scatter factor)	-1.41	0.946449

Position	Symbol	Description	Fold Regulation	p-value
C10	HIF1A	Hypoxia inducible factor 1, alpha subunit (basic helix-loop-helix transcription factor)	1.02	0.858535
C11	HPSE	Heparanase	-1.19	0.356001
C12	ID1	Inhibitor of DNA binding 1, dominant negative helix-loop-helix protein	-4.18	0.000007
D01	IFNA1	Interferon, alpha 1	-1.64	0.946681
D02	IFNG	Interferon, gamma	-1.45	0.937265
D03	IGF1	Insulin-like growth factor 1 (somatomedin C)	-1.45	0.880184
D04	IL1B	Interleukin 1, beta	-1.48	0.910705
D05	IL6	Interleukin 6 (interferon, beta 2)	-1.07	0.964307
D06	CXCL8	Interleukin 8	1.79	0.046894
D07	ITGAV	Integrin, alpha V (vitronectin receptor, alpha polypeptide, antigen CD51)	-1.39	0.109321
D08	ITGB3	Integrin, beta 3 (platelet glycoprotein IIIa, antigen CD61)	-1.09	0.907878
D09	JAG1	Jagged 1	-2.10	0.002682
D10	KDR	Kinase insert domain receptor (a type III receptor tyrosine kinase)	-1.04	0.786346
D11	LECT1	Leukocyte cell derived chemotaxin 1	-1.66	0.909180
D12	LEP	Leptin	-1.56	0.773405
E01	MDK	Midkine (neurite growth-promoting factor 2)	1.08	0.697797
E02	MMP14	Matrix metallopeptidase 14 (membrane-inserted)	-1.09	0.747109
E03	MMP2	Matrix metallopeptidase 2 (gelatinase A, 72kDa gelatinase, 72kDa type IV collagenase)	-1.20	0.240580
E04	MMP9	Matrix metallopeptidase 9 (gelatinase B, 92kDa gelatinase, 92kDa type IV collagenase)	-1.19	0.630428
E05	NOS3	Nitric oxide synthase 3 (endothelial cell)	1.10	0.329214
E06	NOTCH4	Notch 4	-1.34	0.455605
E07	NRP1	Neuropilin 1	1.08	0.607965
E08	NRP2	Neuropilin 2	-1.12	0.470622
E09	PDGFA	Platelet-derived growth factor alpha polypeptide	-3.61	0.000645
E10	PECAM1	Platelet/endothelial cell adhesion molecule	1.07	0.550291
E11	PF4	Platelet factor 4	-1.15	0.900827
E12	PGF	Placental growth factor	-2.09	0.017824
F01	PLAU	Plasminogen activator, urokinase	1.03	0.874273
F02	PLG	Plasminogen	-2.37	0.824571
F03	PROK2	Prokineticin 2	-1.37	0.842931
F04	PTGS1	Prostaglandin-endoperoxide synthase 1 (prostaglandin G/H synthase and cyclooxygenase)	-1.07	0.471331
F05	S1PR1	Sphingosine-1-phosphate receptor 1	1.46	0.014163

Position	Symbol	Description	Fold Regulation	p-value
F06	SERPINE1	Serpin peptidase inhibitor, clade E (nexin, plasminogen activator inhibitor type 1), member 1	-2.29	0.000141
F07	SERPINF1	Serpin peptidase inhibitor, clade F (alpha-2 antiplasmin, pigment epithelium derived factor), member 1	-1.29	0.444331
F08	SPHK1	Sphingosine kinase 1	-1.54	0.005866
F09	TEK	TEK tyrosine kinase, endothelial	-1.05	0.653262
F10	TGFA	Transforming growth factor, alpha	-2.45	0.601201
F11	TGFB1	Transforming growth factor, beta 1	-1.28	0.127613
F12	TGFB2	Transforming growth factor, beta 2	-1.29	0.700756
G01	TGFBR1	Transforming growth factor, beta receptor 1	-1.28	0.278116
G02	THBS1	Thrombospondin 1	-1.35	0.166199
G03	THBS2	Thrombospondin 2	-1.60	0.642770
G04	TIE1	Tyrosine kinase with immunoglobulin-like and EGF-like domains 1	-1.11	0.314422
G05	TIMP1	TIMP metallopeptidase inhibitor 1	-1.08	0.431641
G06	TIMP2	TIMP metallopeptidase inhibitor 2	1.03	0.776841
G07	TIMP3	TIMP metallopeptidase inhibitor 3	1.17	0.949999
G08	TNF	Tumor necrosis factor	-2.52	0.603276
G09	TYMP	Thymidine phosphorylase	-1.37	0.495211
G10	VEGFA	Vascular endothelial growth factor A	-1.79	0.039941
G11	VEGFB	Vascular endothelial growth factor B	1.09	0.436351
G12	VEGFC	Vascular endothelial growth factor C	-1.29	0.108604

B.1 Copyrights permission

My Orders

Orders | Billing History | Payable Invoices

SEARCH

Order Number:

Date Range: From 1-Jan-2018 To 11-Apr-2020 Go

View: All On Hold Response Required Pending Completed Canceled Denied Credited

Results: 1-3 of 3

Order Date	Article Title	Publication	Type Of Use	Price	Order Status	Expiration Date	Order Number
11-Apr-2020	Blood-brain barrier dysfunction and recovery after ischemic stroke	Progress in Neurobiology	reuse in a thesis/dissertation	0.00 $	Completed		4806041020001
21-May-2018	Inflammatory risk factors, biomarkers and associated therapy in ischaemic stroke	Nature Reviews Neurology	Thesis/Dissertation	0.00 $	Completed		4353881439863
19-Apr-2018	Improving Modified Rankin Scale Assessment With a Simplified Questionnaire	Stroke	Dissertation/Thesis	0.00 $	Completed		4332531479361

Figure 27. Copyright permision 1

Copyright Clearance Center RightsLink® Home Help Email Support Fatima Alzahra Al Hamed

Treatment of Acute Ischemic Stroke

Author: Thomas Brott, Julien Bogousslavsky

Publication: The New England Journal of Medicine

Publisher: Massachusetts Medical Society

Date: Sep 7, 2000

Copyright © 2000, Massachusetts Medical Society

This type of reuse is available outside of RightsLink

For permission for this type of reuse, please visit
http://www.nejm.org/page/about-nejm/permissions

BACK CLOSE

Figure 28. Copyright permission 2

Reuse of Content Within a Thesis or Dissertation

Content (full-text or portions thereof) may be used in print and electronic versions of a dissertation or thesis without formal permission from the Massachusetts Medical Society (MMS), Publisher of the *New England Journal of Medicine*.

The following credit line must be printed along with the copyrighted material:

> Reproduced with permission from (scientific reference citation), Copyright Massachusetts Medical Society.

Figure 29. Copyright permission 3

Update on Inflammatory Biomarkers and Treatments in Ischemic Stroke

© This is an open access article distributed under the **Creative Commons Attribution License** which permits unrestricted use, distribution, and reproduction in any medium, provided the original work is properly cited

Figure 30. Copyright permission 4

B.2 iThenticate similarity index report

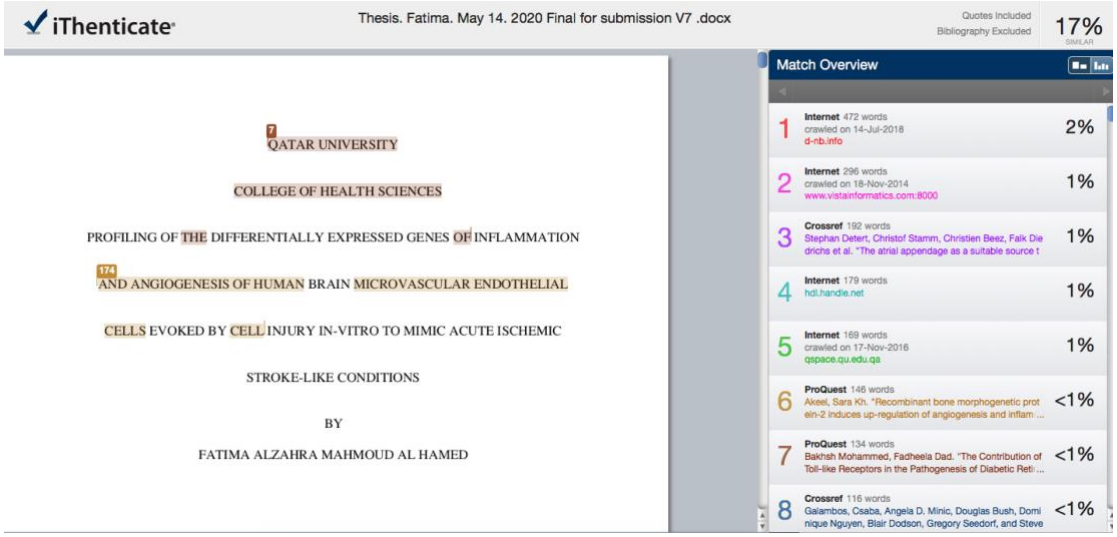

Figure 31. iThenticate Report.